Republic of Iraq
Ministry of Higher Education & Scientific Research
University of Kerbala
College of Engineering
Department of Civil Engineering

Assessment of Modulus of Subgrade Reaction of Different Soils Using Light Weight Deflectometer

A Thesis Submitted to the Department of Civil Engineering, University of Kerbala in Partial Fulfillment of the Requirements for the Degree of Master of Science in Civil Engineering (Infrastructure Engineering)

By

Ahelah Alaa Jawad

BSc. in Civil Eng. / University of Kerbala (2016)

Supervised by

Dr. Raid R. A. Almuhanna

Dr. Alaa M. Shaban

September 2019 Muharram 1441

بِسْمِ اللَّهِ الرَّحْمَٰنِ الرَّحِيمِ

يَرْفَعِ اللَّهُ الَّذِينَ آمَنُوا مِنكُمْ وَالَّذِينَ أُوتُوا الْعِلْمَ دَرَجَاتٍ

صدق الله العلي العظيم

(المجادلة: من الآية 11)

LINGUISTIC CERTIFICATE

I certify that this thesis entitled “Assessment of Modulus of Subgrade Reaction of Stabilized Soil Using Light Weight Deflectometer” which is prepared by "Ahelah Alaa Jawad”, under my linguistic supervision. It was amended to meet the English style.

Supervisor

Signature:

Name: ……

Date…... /….. / 2019

DEDICATION

This thesis is dedicated to:

My parents, my family, brothers, sisters and friends for their love and continuous support

ACKNOWLEDGMENTS

Above all and beyond, I would like to thank God, who gave me the desire and ability to complete this work in spite of the constrains along the way.

I would like to express my deepest gratitude to my supervisors (Dr. Raid R. A. Almuhanna, and Dr. Alaa M. Shaban), who play a great role in introducing the basis of this research and take over the supervision of this thesis, for their guidance's, advices and encouragements.

My deep and special thanks to (Asst. Prof. Dr. Shakir Al-Busaltan) for his kind advices and scientific guidance.

The author wish to thank the staff of highway materials and soil materials laboratories/ College of Engineering in University of Kerbala (especially, Eng. Sinaa Jaber, Eng. Mannar) and Department of project management and direct implementation of Karbala city for raw materials supplementation.

Thanks are also extended to my colleagues (Rawq Mohammad, and Narjis Basil) for their help and support during thesis experiment works.

Great thanks to my mother, father, brothers, and sisters who supported me and encouraged me to complete this work.

ABSTRACT

The subgrade is a soil layer on which a pavement and unbound soil layers are placed. Thus, it works as a foundation to support the pavement's structure. The important geotechnical design parameter that describes the relationship between stress and the associated settlement of subgrades is the modulus of subgrade reaction (Ks). The modulus of subgrade reaction is an essential parameter in the design and analysis of rigid pavements. It has a significant effect on the required thickness of pavements surface, and gives an estimation of the supporting of the layers under pavement surface. The Ks is typically obtained from the plate load test, PLT. The PLT test has a several limitations; difficult to carry out, costly, and time-consuming. To overcome some of these limitations, it is requisite to find an alternative testing technique which can rapidly and simply predict this parameter.

This study aims to evaluate the effectiveness of using a light weight deflectometer (LWD) in predicting subgrade reaction modulus of subgrade soils. LWD is a portable non-destructive testing device also known as the dynamic plate load test that is utilized to measure the properties of soil layers under the effect of dynamic loads. To achieve the aim of this study, a series of tests were carried out on three types of subgrade soils. The subgrade soils were collected from different site projects in Karbala city (Al-Meelad, Al-Faris, and Al-Rofae), the soils collected and tested into two phase; [1] in the laboratory to identify the type and classification of soils, and to identify its basic properties. [2] in a laboratory setup model which is designed and manufactured to simulate the field conditions. The collected soils were prepared and compacted in the laboratory setup, three degree of compaction were achieved and tested the soil under each degree of compaction using the dynamic light weight deflectometer (LWD) in conjunction with the static plate load test (PLT).

On the other hand, the experimental results were statistically modeled to predict the subgrade reaction. The statistical analysis was carried into to phase; granular subgrade soils, and fine subgrade soil.

For granular subgrade soils, three groups of regression models were developed based on independent variables; [1] LWD measurements data, [2] basic soil properties, [3] both the LWD measurements and basic soil properties. In this phase the higher value of R^2

was 0.93 for subgrade reaction modulus – LWD degree of compatibility model (KS –Dc) model.

For fine subgrade soil, two groups of regression models were conducted based on independent variables; [1] LWD measurements data and [2] basic soil properties. The results showed that there is a good correlation between Ks and LWD measured data (Ed, δd, and Dc). Also, a strongly correlation was identified between the dry density of the subgrade soil and Ks. The results also showed acceptable relation between Ks and water content.

Additionally, the results of experimental work were verified using the finite element software PLAXIS 3D. Two types of models were used to simulate the soil behavior. The linear elastic model was used to represent the behavior of subgrades under the effect of LWD dynamic loads. And the Mohr-Coulomb was used to represent the behavior of subgrade under the effect of static PLT load.

The FE results were compared with those obtained from experimental work, and the T-Tests were carried out to examine the variance between the results.

In the term of LWD surface deflection the mean deference between predicted and measured value ranged from 0.003 to 0.242 mm. And in the term of PLT surface deflection the mean deference ranged from 0.105 to 0.15 mm, and for the subgrade reaction modulus the mean deference ranged from 3.088, and 25.125 kPa/mm.

Finally, the results of this study showed the efficiency and possibility of using the LWD device rapidly and easily to predict the subgrade reaction modulus of pavements materials.

Table of Contents

List Of Figures

List Of Figures - Continue

List Of Figures – Continue

List Of Figures - Continue

List Of Figures - Continue

List Of Figures - Continue

List Of Plates

List Of Tables

List Of Tables - Continue

List of Symbols

σ_o: Applied dynamic stress
$\emptyset_o$: Initial phase angle
a: Radius of the loading plate (mm)
C: Cohesion
C_c: coefficient of curvature
C_u: coefficient of uniformity
D_{10}: diameter corresponding to percent passing of 10 %
D_{30}: diameter corresponding to percent passing of 30 %
D_{60}: diameter corresponding to percent passing of 60 %
Dc: degree of compatibility obtained from LWD
E_d: dynamic modulus in (MPa) obtained from LWD
EI: flexural rigidity of footing.
Es: Young's modulus of soil
F: Shape factor depending on stress distribution under a plate
h_c: Thickness of pavement slab
h_e: Equivalent thickness
IS ,IF: Influence factors depend on the shape of footing.
Ks: Subgrade Reaction Modulus
K_o: coefficient of lateral earth pressure.
Ḿ: Amplitude multiplier
Mr: Resilient modulus
N_{60}: a measured SPT below counts for the 60% energy level.
P_{max}: maximum contact pressure in (kPa)
q_{alt}: Ultimate bearing capacity
w: slab deflection
γ : Unit weight of the soil
δ: Soil surface deflection (mm)
δ_d: Dynamic surface deflection in (mm) obtained from LWD
v: Poisson's ratio
ϕ: Friction angle
ψ: Dilatancy angle

List of Abbreviations

AASHTO:	American Association of State Highway and Transportation Official
ANOVA:	Analysis of Variance
ASTM	American Society for Testing and Materials
CBR:	California Bearing Ratio
CIT:	Clegg Impact Test
DCP:	Dynamic Cone Penetration
FDD:	Field Dry Density
FEM:	Finite Element Method
FWD:	Falling Weight Deflectometer
LVDT:	Linear Variable Differential Transformers
LWD:	Light Weight Deflectometer
MAE;	Mean Absolute Error
MS_E:	Mean Square of Residual or Error
MS_R:	Mean Square of Regression
PLAXIS:	Plaxis– Plasticity Axi-Symmetry
PLT:	Plate Load Test
QC/QA:	Quality Control and Quality Assurance
RMSE:	Root Mean Square Error
rPLT:	Repetitive Static Plate Load Tests
SASW:	Spectral Analysis of Surface Waves
SPSS:	Statistical Package for Social Science
SPT:	Standard Penetration Test
SS_E:	Error or Residual Sum of Squares
SS_R:	Regression sum of Squares
SS_T:	Total of Sum Squares
uPLT:	Unrepetitive Plate Loading Test
USCS:	Unified Soil Classification System

Chapter One

Introduction

1.1: Background

The subgrade is a soil layer of natural formation which can bear wheel loads transporting from vehicles as well as from pavement layers. The subgrade soil works as the foundation that supports the road. The success or failure of any pavement system is more often dependent upon the strength of the underlying subgrade upon which the pavement structure is built. The main functions of subgrade soils are principally based on several parameters, such as load-bearing capacity, and moisture content. These necessary parameters are typically characterized by resistance to deformation under wheel load actions, which can be either a measure of strength or a measure of stiffness **(Marradi et al, 2014).**

In the rigid pavement, the modulus of subgrade reaction (Ks) is an essential parameter which needs to be considered in the design procedure, and it estimates the supporting of layers under the surface of pavement **(Ping and Sheng, 2011).** The modulus of subgrade reaction depends on various factors including: elastic properties of soil, dimensions of the area acted upon the subgrade soil, and other parameters like soil type, shape particle, embedment depth and type of foundation. The subgrade reaction (Ks) can be obtained from the field plate load test according to (**AASHTO T 222, 2007)** and (**ASTM D 1196, 2004).** However, this test has several limitations as itis difficult and expensive …etc. Therefore, many studies investigated the possibility of unitizing alternative methods to predict the subgrade reaction modulus. Several researchers developed empirical and theoretical relationships between the modulus of subgrade reaction of the pavement layer and other soil properties that can be determined from field or laboratory tests.

Pavement design methodologies depend increasingly on non-destructive tests to predict the dynamic pavement response to traffic loadings. Non-destructive deflectometer testing techniques including falling weight deflectometer (FWD) and light weight deflectometer (LWD) are the most common devices for assessing the structural performance of pavement systems (**Alavi, and Lecates, 2002)**.

1.2: Research Problem

One of the most important engineering parameters that needs to be considered in the design of pavements underlying soils is the reaction modulus of soil in contact with pavements structure. The modulus of subgrade reaction (Ks) describes the relationship between the applied pressure and the vertical deflection of soils. The Ks is typically determined from the standard plate loading test according to (**AASHTO T 222, 2007)** and (**ASTM D 1196, 2004)**. The nonrepetitive static plate load test is the most popular test that performed on pavement components and subgrade soils in either compacted conditions or in its natural state, to determine the modulus of subgrade reaction and bearing capacity of soils. However, there are several limitations associated with performing the plate load test including:

1. It is exceedingly time-consuming and expensive.
2. Test's results may be evaluated only for the specific conditions under which the tests are performed.
3. There is a difficulty in selecting a proper critical deflection value.
4. It is difficult to conduct this test in narrow trenches and exploration pits because there is insufficient space.

In order to overcome some of these problems, many studies examine the possibility of using alternative methods to predict the subgrade reaction modulus. It is necessary to develop a simple and reliable testing procedure for predicting pavement moduli based on dynamic measurements obtained from non-destructive deflectometer testing techniques including falling weight deflectometer (FWD) and light weight deflectometer (LWD). The lightweight deflectometer (LWD) is a non-destructive testing device which provides a reliable and fast tool to measure the field soil properties under the effect of dynamic loads. The dynamic measurements obtained from the LWD are utilized to identify structural integrity and estimate the remaining service life of the pavement systems (**Vennapusa and White, 2013)**. A very limited number of researches conducted an investigation to compare between the light weight deflectometer and the loading plate to assess the pavement moduli of airfield and highway pavements based on deflection measurements of the deflectometer tests.

1.3: Research Aim and Objectives

1.3.1: Aim

This study aims to develop simple and reliable statistical models to predict the subgrade reaction modulus based on dynamic measurements obtained from performing the light weight deflectometer test.

1.3.2: Objectives of the Study

To achieve the aim of this research, the subgrade materials were examined in the laboratory testing setup under both the static and dynamic load. Figure (1.1) is a flow chart that explains research activities which were conducted to achieve the following objectives:

1. Develop a portable of laboratory testing setup which was designed and manufactured to simulate the actual subgrade layers.
2. Soil samples from different roadway projects were collected and tested in the laboratory. Different laboratory tests were carried out including; CBR test, Atterberg limits, grain size distribution, direct shear test…etc., to identify basic physical properties of the subgrade soils.
3. Three degree of compaction were obtained depends on number of passes of compacting device for each type of soil. And two test methods; Light Weight Deflectometer (LWD), and Plate Load Test (PLT) were carried out to obtain strength characteristics of subgrade layers. Three dynamic measurements were obtained from LWD: surface deflection, degree of compatibility, and dynamic modules. Also, three parameters were obtained from PLT tests: maximum settlement, modulus of subgrade reaction, and Young's elastic modulus.
4. The testing measurements of each soil type were recorded and analyzed using statistical analyses software called SPSS [Statistical Package for Social Science]to determine any possible correlations equation to compute the modulus of subgrade reaction.
5. Developing finite element models using Plaxis 3D to simulate the LWD surface deflection and the plate load-deformation curve. Then, the finite element results were compared with those obtained from the laboratory experiments.

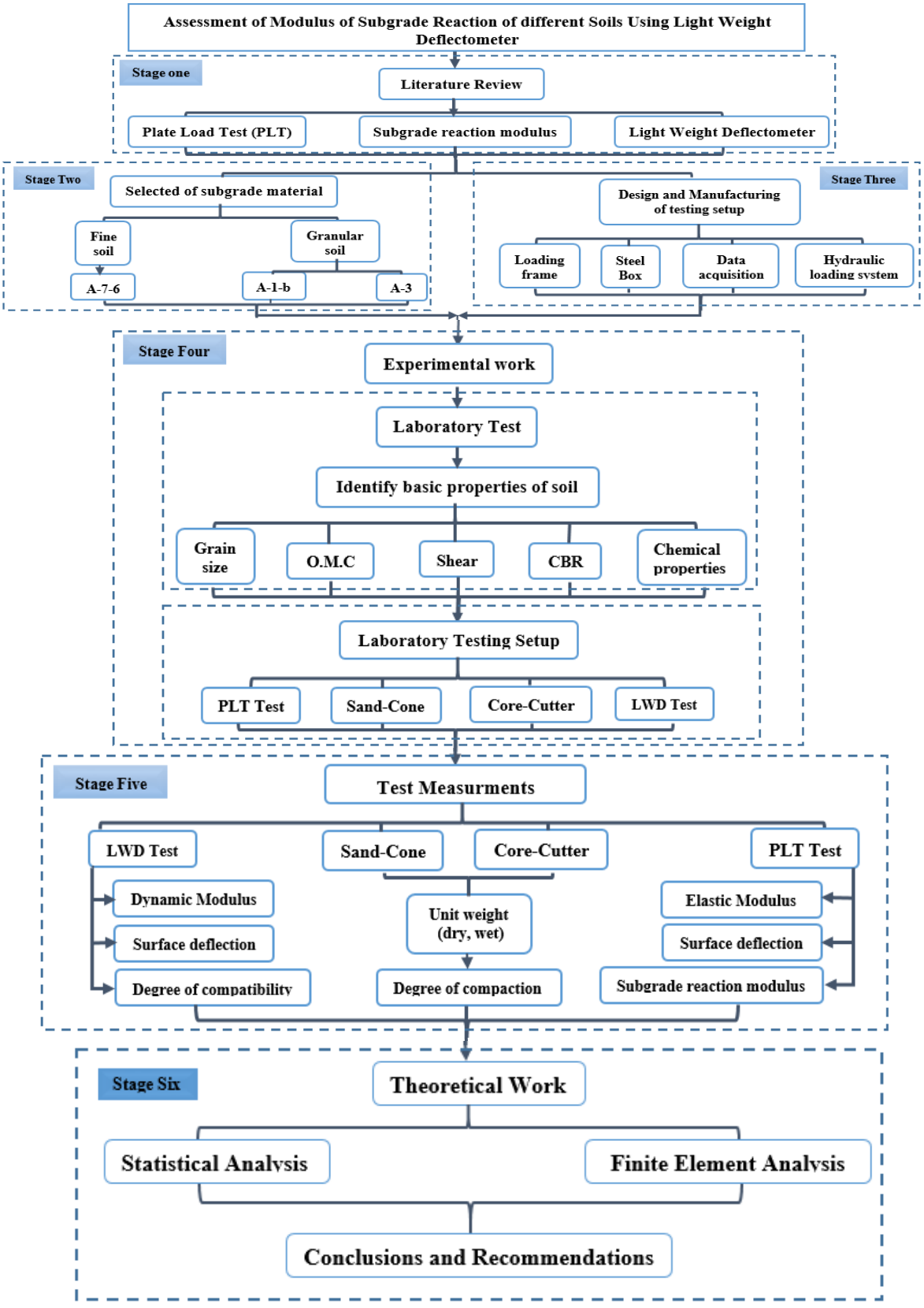

Figure (1.1): Research Activities

1.4: Thesis Layout

This research is presented in seven chapters, which are outlined as follows:

1. Chapter One gives a brief introduction about the importance of the subgrade layer in pavement systems and how to evaluate its modulus of subgrade reaction. Also, this chapter presents the research problem, and explains the aim and principal objectives of this research, and finally summarize thesis layout.
2. Chapter Two provides an overview on the subgrade reaction modulus and theories to explain it. Also, presents previous studies that are related with the Light Weight Deflectometer test and Plate load test. It also presents a short review of existing correlation studies between PLT and other tests.
3. Chapter Three presents the methodologies of the experimental work, which includes description of: soil samples collected and identification of their basic characteristics, manufacturing the laboratory testing setup for the model tests, testing procedures of LWD and PLT.
4. Chapter Four displays and discusses the results of the experimental work.
5. Chapter Five illustrates the statistical analyses of the results, and a theoretical model developed by using SPSS software.
6. Chapter Six explains the numerical modeling to simulate the experiments work using the finite element software known as Plaxis 3D. Then presents and discusses the output of numerical modeling
7. Chapter Seven summarizes the conclusions that obtained from the experimental and theoretical works, and gives recommendations for future studies.

Chapter Two

Literature Review

2.1: Introduction

Highway and airport pavements are complex structures supported by foundations of soil layers. During the service life of pavement systems, soil layers beneath a pavement surface course are subjected to different intensities of loads by the wheels of moving vehicles. The weight of this traffic is finally transmitted and carried by the subgrade itself, which in turn provides support to the pavement structure. The behavior of subgrades under different loading conditions must be thoroughly investigated before a rational pavement design or analysis is conducted.

In the pavement design process, the strength characteristics of the subgrade on which the pavement is placed are essential design parameters that need to be considered and determined. Subgrades are typically characterized by their resistance to deformation under various loading conditions **(Ping & Sheng, 2011).**

2.2: Subgrade Reaction Modulus

Structural elements such as concrete pavements are commonly supported by underlying soils. In the pavement design process, it is suitable to assume that the intensity of the continuously distributed reaction at each point is proportional to the deflection at that point. This reaction can be represented as modulus of subgrade reaction.

The modulus of subgrade reaction (Ks) is a required parameter for the design of rigid pavements. It estimates the support of the layers below a rigid pavement surface course. The modulus of subgrade reaction is determined from the plate bearing load test **(Naeini & Taherabadi, 2015).**

The value of (Ks) depends on several factors including:

1. Elastic properties (elastic modulus, Poisson's ratio…etc.) of a subgrade soil.
2. Dimensions of the area acted upon by the subgrade reaction.
3. Other parameters like soil type, embedment depth and type of foundation (Flexible or Rigid).

Soil medium has very complex mechanical behavior, thus subgrade is often represented by a much simpler system in theoretical analyses. Many theoretical subgrade models such as: Winkler foundation model, Pasternak foundation model, elastic isotropic half-space model … etc. were developed. The following subsections discuss most common theoretical models utilized to represent structural behavior of subgrades:

2.2.1: Winkler Foundation Model

One of the oldest and most popular models in determining the modulus of subgrade reaction is the one - parameter Winkler model. Winkler in 1867 assumed that a soil medium could be represented by a system of identical but mutually independent, closely spaced, discrete and linearly elastic springs. The ratio between contact pressure (P) at any given point, and settlement (δ) produced by load application at that point is named the modulus of subgrade reaction, Ks:

$$K_s = \frac{P}{\delta} \qquad (2.1)$$

In this model, a subsoil is replaced by fictitious springs whose stiffness is equal to K_S, as shown in Figure (2.1)

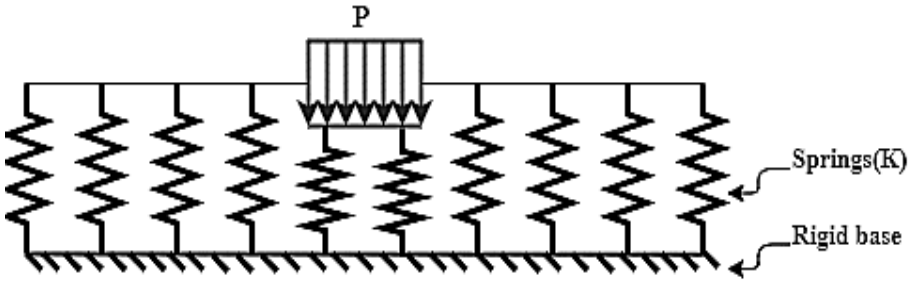

Figure (2.1): One- Parameter Winkler model **(Bhatia, 2016)**

One of the basic limitations of Winkler model lies in the fact that this model cannot transmit the shear stresses which are derived from the lack of spring coupling. Also, this model cannot account for the dispersion of the load over a gradually increasing influence area with an increase in depth. Moreover, it considers the linear stress–strain behavior of soil **(Dutta & Roy, 2002).**

2.2.2: Elastic Continuum Model:

In this model, the continuous behavior of a soil is idealized as three-dimensional continuous elastics solid. The origin of this model is from the research work of Boussinesq

in 1885. Boussinesq found a solution for the stress caused by a single point load applied on a homogeneous, elastic, isotropic and semi-infinite medium, as shown in Figure (2.2), with the aid of the mathematical theory of elasticity.**(Dalili et al, 2013)**

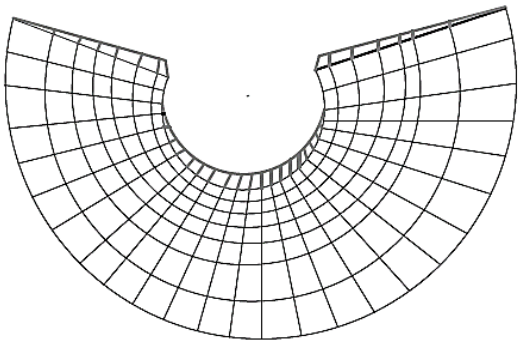

Figure (2.2): Boussinesq's analysis of a point load on an elastic half space (**Ferretti, 2013)**

In the derivation of Boussinesq theory, it was assumed that the soil medium extends infinitely in all directions from a level surface, obeys to the Hooke's law, the soil is initially unstressed, and the self-weight of the soil is ignored.

In this model the soil characteristics which influence the stresses in the pavements are the modulus of elasticity (E), and Poisson's ratio (*v*) **(Siddiqi, and Hudson, 1970) .**To find the modulus of subgrade reaction Ks, and the deflection w, due to a pressure (p), uniformly distributed over a rigid surface plate of diameter (D), Boussinesq developed this expression **(Teodoru and Toma, 2009).** In the derivation of Boussinesq theory, it was assumed that the soil medium extends infinitely in all directions from a level surface, obeys to the Hooke's law, the soil is initially unstressed, and the self-weight of the soil is ignored

$$w = \frac{\pi}{4}\frac{pD(1-\boldsymbol{v}^2)}{E_S} \qquad (2.2)$$

Where

- **P:** Contact pressure (MPa).
- **w:** Slab deflection (mm)
- ***v* :** Poison's ratio..
- **Es :** Young's modulus of soil (MPa).
- **D:** Diameter of plate (mm)

$$K_s = \frac{4E_S}{\pi D(1-v^2)} \qquad (2.3)$$

The advantages of this model are listed as follow:**(Dutta & Roy, 2002):**

1. This approach provides much more information on the stresses and deformations within soil mass than Winkler model.
2. It has the simplicity of input the parameters, Young's modulus and Poisson's ratio.
3. Solutions for some practical problems, idealizing the soil media as an elastic continuum, are available for a few limited cases.

The major drawbacks of the elastic continuum model are listed as follow:**(Dutta & Roy, 2002):**

1. Inaccuracy in calculating the reactions at the peripheries of the foundation.
2. The surface displacements away from the loaded area decrease more rapidly than what is predicted by this approach.
3. Idealization of this model fails to represent the physical behavior of soil very closely.

2.3: Types of Field Tests:

There are different test methods for the structural evaluation of the pavement layers:

1. Destructive tests: these test methods cause a damage to the pavement when coring and preparing a sample to the laboratory testing. These methods are very costly and time consuming due to coring process. Some popular destructive test methods include tests of mechanical properties (bending, impact tests, tensile).**(Akbariyeh, 2015).**
2. Non-destructive tests: these in situ tests are most popular and preferred in the geotechnical engineering and evaluation the highway and airfield pavements during the construction or after the construction. These tests require less time and cost to conduct. Non-destructive tests can be divided into two categories:
    - Deflection basin test: are those in which the deflections are recorded along the surface of a pavement subjected to a static state load like a transient dynamic impact like (Clegg impact test (CIT), Falling Weight Deflectometer (FWD), and Light Weight Deflectometer (LWD)) **(Roesset, 1998).**

- Wave propagation tests: The spectral analysis of surface waves (SASW) is the characteristic of the nondestructive tests method that widely used for determining moduli and thicknesses of paved surface systems. By means of a traveler impact hammer, a falling weight, or a hydraulic shaker on the surface of pavement system (or soil deposit), a group of waves with different frequencies is transmitted to the medium. The resulting wave field is recorded by a number of sensors at the medium surface and used to determine dispersion and attenuation curve, stress wave, electromagnetic method etc. **(Nazarian et al, 1983)**, and **(Roesset, 1998)**.

2.4: Static Plate Load Test (PLT):

The static plate load test (PLT) is a useful site investigation tool in obtaining the necessary information about the soil to design the shallow foundation or rigid pavement structure. Figure (2.3) displays a schematic illustration of the static plate load test.

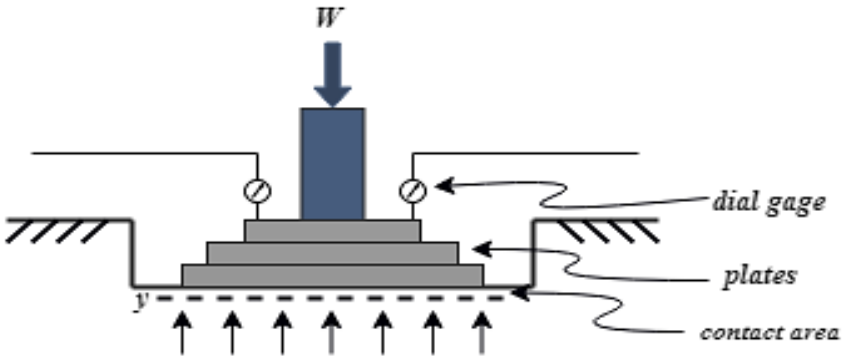

Figure (2.3): Plate Bearing Test **(Bowles, 1998)**

The plate load test is the most reliable method early developed for obtaining various geotechnical design parameters such as bearing capacity, subgrade reaction (Ks) and modulus of deformation of a soil, compacted subgrade, and compacted subbase. In many European countries it has been used for proof testing of pavement layers. Currently, it is used for rigid pavements. Over the last 15 years **(Tuse et al, 2016)** conducted many of field and laboratory tests for different problems relating to bearing capacity or design of foundation. The plate bearing test was used in their work, for this test, there are three types: gravity loading, truss and anchoring, and reaction load. According to their experience, the test procedure of both first and second type is not convenient and the results are not realistic **(Tuse et al, 2016).**

The interpretation of plate bearing test results requires full information on the subgrades condition. Hence, the results of PLT are affected by several factors:

1. **Water content:** the PLT is performed on unsaturated soil layers, where ground water table is at great depth. Several researchers showed that the behavior of soils under applied load from in-situ PLTs is significantly influenced when pore water pressure is negative with respect to the atmospheric pressure.**(Oh and Vanapalli, 2013)** .

   In the saturated condition, there is a correction for the difference in the subgrade moisture content at the time of testing. Studies conducted at **(US Army Engineer Waterways Experiment Station, 1945),** and **(CRD-C 655, 1995)** recommended the method for obtaining the modulus of subgrade reaction at a saturated condition empirically by the following relation:

$$Ks = K_u \cdot \frac{p_s}{p_d} \qquad (2.4)$$

   where

   Ks: Modulus of subgrade reaction for the saturated soil
   K_u: Modulus of soil reaction for the soil at natural moisture as found by a field-bearing test.
   p_s: The unit pressure in psi used to determine the value of K_u
   p_d: The unit pressure in psi used in a saturated consolidation test.

   In this equation the reference of stress is that for 0.05 in of plate deformation. While **(AASHTO T222, 2007)** recommended the corrected equation below taking into account the thickness of base, and in the applied stress 10 psi, that the value was expected typical vertical stress under a rigid pavement.

$$Ks = K_u \cdot \left[\frac{d}{d_s} + \frac{b}{75} \cdot \left(1 - \frac{d}{d_s}\right)\right] \qquad (2.5)$$

where

Ks: Corrected modulus of subgrade reaction for the saturated soil, psi/in
K_u: Modulus of soil reaction uncorrected for saturation, psi/in.
d: Deformation of consolidometer specimen at in situ moisture content under a unit load of 10 psi
d_s: Formation of a saturated consolidometer specimen under a unit load of 10 psi
b: thickness of base course material, in.

2. **Size of plate:** the influence of plate size on the soil behaviors under the load should be taken in to account. A series of tests made by **(Ohio River Division, 1943)** and **(U.S.**

Army Engineer Waterways Experiment Station, 1945) laboratories indicated that as the plate size increases, the measured value of (K) approaches a constant value.

As summarized in Table (2.1), different shapes and sizes of the plate load test can be used in determining the modulus of subgrade reaction (Ks).

Table (2.1): Some different methods to calculate (Ks) by using plate load test

No.	Investigator	Shape	Dimensions
1	Terzaghi (1955)	Square	L = 305 mm
2	ASTM D1195 and D 1196 (2004)	Circular	D: 305 to 762 mm
3	British standards code (B.S 5930) (1999)	Circular or square of equivalent area	D: 300 to 1000 mm
4	Peck et al. (1997)	Square	L=305 mm
5	Ping and Yang. (1998)	Circular	D: 705, 950 and 1050 mm
6	Egyptian code (2001)	Circular or square of equivalent area	D: 300, 450 and 706 mm
7	Reza. and Masoud (2008)	Circular or square of equivalent area	D: 300 and 1000 mm

Also, another factors effect on the plate bearing test results like:

1. The amount and effect of temperature.
2. The amount and effect of frost action and thawing.
3. Stress transfer devices.

2.4.1: Types of static PLT:

The static PLT are classified according to the testing procedure performed in determining subgrade modulus as follows:

1. **Repetitive Static Plate Load Tests (rPLT):**

   The rPLT was introduced from Europe to obtain moduli of the soil based on the loading and deformation, to evaluate whether sufficient compaction has occurred. It also used to evaluate the bearing capacity during railroad construction. According to **(ASTM D 1195 – 93, 2004)**, and **(AASHTO, 2007),** this test is performed on soils, unbound base, and subbase. **(Kim and Park, 2011).**

2. **Unrepetitive Plate Loading Test (uPLT):**

The uPLT is performed on soils, unbound base, and subbase to determine the modulus of subgrade reaction (Ks) and the shear strength of pavement components **(AASHTO, 2007) and (ASTM D 1196 – 93, 2004).** This test is widely utilized in various geotechnical applications in Asia, the modulus of subgrade reaction (Ks) can be calculated based on the relationship between the average normal stress and the settlement of the plate, see Equation (2.1). As shown in Figure (2.4), the depth of influence of this test is assumed to be equal to 2B, where B is the diameter of loading plate.

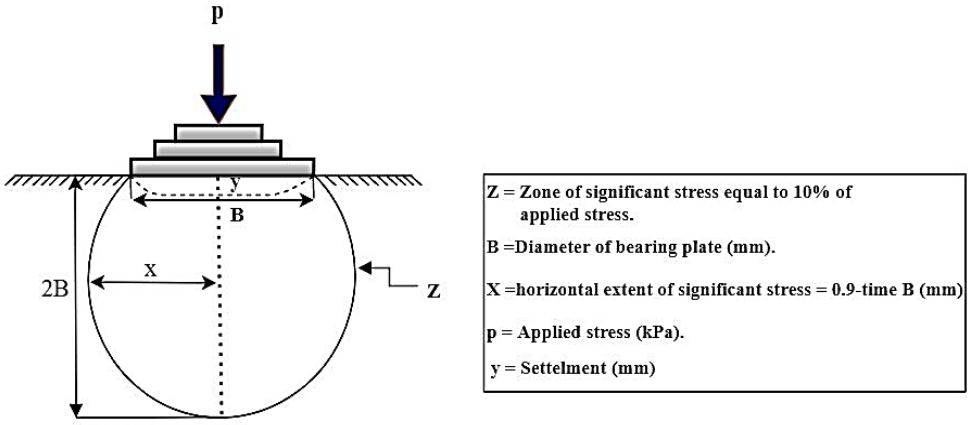

Figure (2.4): The influence of the total deformation in PLT

2.4.2: Disadvantage of Plate Load Tests:

According **(Adam et al, 2009)** there are several limitations associated with performing the plate load test including**:**

1. PLT test is costly and quite time consuming, so its application restricted to a control point of compacted subsoil.
2. Very difficult to use this test in narrow trenches and in different depths because there is no enough space for the testing equipment.
3. There is difficulty in selecting a proper critical deflection value.

In order to overcome these limitations, many studies investigated the possibility of unitizing alternative methods to predict the subgrade reaction modulus. Several researchers developed empirical and theoretical relationships between the modulus of subgrade reaction of the pavement layer and other soil properties that can be determined from field or laboratory tests; these relationships are presented in the Table (2.2).

Table (2.2): Some of Ks- Soil properties relationships

	Authors.	Suggested formula
K–CBR Relationships	Packard (1986)	$Ks = 53.438\ CBR^{0.5719}$
	Federal Aviation Administration(FAA) (2009)	$Ks = \left[\frac{1500CBR}{26}\right]^{0.7788}$
	Tuleubekov and Brill (2014)	$Ks = 28.6926\ CBR^{0.7788}$
K–Mr Relationships	UFC (2001)	$Ks = \left[\frac{M_r}{26}\right]^{-1.284}$
	Ping and Sheng (2011)	$Ks = 2.25\ M_r$
	Barker and Alexander (2012)	$Ks = 0.74\left[\frac{M_r}{E}\right]^{-0.284}$
K-E Relationships	Vesic and Saxena (1974)	$Ks = 0.42\left(\frac{E}{E_c}\right)^{1/3}\left(\frac{E}{(1-\mu^2)h_c}\right)$
	AASHTO (1986)	$Ks = \frac{E}{0.492}$
	Ullidtz (1987)	$Ks = 0.54\left(\frac{E}{h_e}\right)$
	Khazanovich et al (2001)	$Ks = 0.296\ E$
	Setiadji and Fwa (2008)	$Ks = 0.259\ E - 6.512$

Where

E : Elastic modulus of subgrade (MPa)
E_c : Elastic modulus of pavement slab (MPa)
μ : Poison's ratio..
h_c : Thickness of pavement slab (mm).
h_e : Equivalent thickness (mm).
Ks: Modulus of subgrade reaction (in MPa/m^3).
Mr: Resilient modulus is (psi)
CBR: California bearing ratio

These empirical correlations between modulus of subgrade reaction (Ks) and soil properties are approximate and applicable only under the conditions when they were derived. For this reason, other researchers, studied the correlation between the (PLT) and other tests to determine the soil moduli. These correlations are presented in the following subsections:

1. **Correlation Between SPT and PLT:(Moayed and Naeini, 2006)** studied the correlation between (PLT) and (SPT) to determine the modulus of subgrade reaction for dense gravely soils, the result of the statistical analysis with R^2 of 0.915 shown:

$$\mathrm{Ks} = 3.143(\mathrm{N})_{60}{}^{0.489} \tag{2.6}$$

Where:

Ks: Modulus of subgrade reaction for the saturated soil (MPa/mm).

N_{60}: Is a measured SPT below counts for the 60% energy level.

Another empirical relationships are derived by **(Mohamed and Vanapalli, 2012)** to estimate the bearing capacity of saturated and unsaturated sand soils

$$q_{alt(sat)} = \frac{0.15}{B^{.63}}\left[0.37(N_{SPT(sat)})^{0.73}\right] * 1000 \tag{2.7}$$

$$q_{alt(unsat)} = \frac{0.19}{B^{.68}}\left[0.45(N_{SPT(unsat)})^{0.83}\right] * 1000 \tag{2.8}$$

Where:

q_{alt}: Ultimate bearing capacity, kN/m^2

N: Is a measured SPT

B: Footing width (m),

2. **Correlation Between DCP and PLT**

Table (2.3) summaries the theoretical model that obtained from field and laboratory data between the DCP-PR (mm) and PLT initial [$E_{PLT(i)}$ (MPa)] and reloading moduli [$E_{PLT(R2)}$ (MPa)] produced by **(Abu-Farsakh et al, 2005)**

Table (2.3): Summary of correlations between DCP and PLT

Proposed Relationship	Descriptions	R^2
$\mathrm{E_{PLT(i)}} = \frac{7000}{(6.1 + \mathrm{PR}^{1.5})}$	From laboratory data	R^2=0.62
$\mathrm{E_{PLT(R2)}} = \frac{2460}{\mathrm{PR}^{-1.285}}$	From laboratory data	R^2=0.77
$\mathrm{E_{PLT(i)}} = \frac{17421.2}{(\mathrm{PR}^{2.05} + 62.53)} - 5.71$	From field data	R^2=0.94

Table (2.3): Summary of correlations between DCP and PLT - continue

Proposed Relationship	Descriptions	R^2
$E_{PLT(R2)} = \frac{5142.61}{(PR^{1.57} - 14.7)} - 3.49$	From field data	R^2=0.95
$E_{PLT(i)} = \frac{9770}{(PR^{1.6} + 36.9)} - 0.75$	From field and laboratory data	R^2=0.67
$E_{PLT(R2)} = \frac{4374.5}{(PR^{1.4} + 14.9)} - 2.16$	From field and laboratory data	R^2=0.78

3. Correlation Between Geogauge and PLT

The results of the statistical regression analysis between the Geogauge stiffness modulus (EG in (MPa)) and the back-calculated PLT initial [$E_{PLT(i)}$ (MPa)] and reloading moduli [$E_{PLT(R2)}$ (MPa)] are summarized in the table below:**(Abu-Farsakh et al, 2004).**

Table (2.4): Summary of correlation between Geogauge and PLT

Proposed Relationship	Descriptions	R^2
$E_{PLT(i)} = -15.5e^{.013(E_G)}$	From laboratory data	R^2=0.83
$E_{PLT(R2)} = 15.8e^{.011(E_G)}$	From laboratory data	R^2=0.69
$E_{PLT(i)} = -75.58 + 1.62(E_G)$	From field data	R^2=0.87
$E_{PLT(R2)} = -65.37 + 1.50(E_G)$	From field data	R^2=0.90
$E_{PLT(i)} = 1.168(E_G) - 37.42$	From field and laboratory data	R^2=0.72
$E_{PLT(R2)} = 10^{(1.2(\log(E_G))-1.39)}$	From field and laboratory data	R^2=0.59

4. Correlation Between LWD and PLT

Several research conducted a comparison investigation between the light weight deflectometer and the loading plate to evaluate the initial and reload elastic modulus of pavement foundations at different highways projects. The results showed a promising regression between the LWD stiffness and the plate load modulus that summarized in Table (2.5).

Table (2.5): Summary of correlation between LWD and PLT

Reference.	Suggested formula	Descriptions	R^2
Abu-Farsakh et al., (2004)	$E_{PLT(i)}(MPa) = 0.907 * (E_{LWD}(MPa)) - 1.8$	From laboratory data	0.62
	$E_{PLT(R2)}(MPa) = 28.25e^{.006(E_{LWD}(MPa))}$		0.77
	$E_{PLT(i)}(MPa) = 22 + 0.7(E_{LWD}(MPa))$	From field data	0.94
	$E_{PLT(R2)}(MPa) = 20.9 + 0.69(E_{LWD}(MPa))$		0.95
	$E_{PLT(i)}(MPa) = 0.71(E_{LWD})(MPa) + 18.63$	From field and laboratory data	0.67
	$E_{PLT(R2)}(MPa) = 0.65(E_{LWD})(MPa) + 13.8$		0.78
Nazzal et al., 2007	$E_{PLT(i)}(MPa) = 1.041E_{LWD}(MPa)$	From field data	0.92
	$E_{PLT(R2)}(MPa) = 0.875E_{LWD}(MPa)$		0.97
Vennapusa and White, 2013	$E_{PLT(i)}(MPa) = \frac{E_{LWD}(MPa)}{1.58}$	From field data	0.66
	$E_{PLT(R2)}(MPa) = \frac{E_{LWD}(MPa)}{0.47}$		0.64

several authors proposed another formula to calculate the modulus of subgrade reaction using plate load test. Table (2.6) summarizes most common formulas.

Table (2.6): Some different formula to calculate the subgrade reaction, Ks

No.	Authors.	Suggested formula
1	Biot (1937)	$K_s = \frac{0.95E_s}{B(1-v_s^2)}\left[\frac{B^4E_s}{(1-v_s^2)EI}\right]^{0.108}$
2	Terzaghi (1955)	For square footing with dimensions (B*B) $K_{sf} = K_{sp}\left[\frac{B+0.305}{2B}\right]^2$ For rectangular footing with dimensions (B*L) $K_{sfr} = \frac{K_{sf}\left(1+\frac{B}{L}\right)}{1.50}$
3	Vesic (1961)	$K_s = \frac{0.65E_s}{B(1-v_s^2)}\sqrt[12]{\frac{E_sB^4}{EI}}$
4	Meyerhof (1965)	$K_s = \frac{E_s}{B(1-v_s^2)}$
5	Selvadurai (1984)	$K_s = \frac{0.65}{B}.\frac{E_s}{(1-v_s^2)}$
6	Bowles (1998)	$K_s = \frac{E_s}{B_1(1-v_s^2)mI_sI_F}$

Where

- **B:** Width of footing (m)
- **Es:** Modulus of elasticity (MPa)
- **EI:** flexural rigidity of footing.
- **IS ,IF** Influence factors depend on the shape of footing.
- **Ks:** Modulus of subgrade reaction.
- **K_{SP}:** The value of subgrade reaction for 0.3×0.3 m (1 ft. wide) bearing plate
- **K_{sf} :** Value of modulus of subgrade reaction for the full-size foundation.

2.5 Light Weight Deflectometer (LWD):

The Light Weight Deflectometer (LWD) is a portable and non-destructive device, first appeared in Germany in 1980s. The LWD which is used to measure the in-situ elastic modulus of unbound pavement layers was developed as an alternative field test to many other tests such as Plate Load test (PLT), Field Dry Density (FDD), and California Bearing Ratio (CBR). LWD considered by State and Federal agencies in the United State as an evaluation tool in the quality control and quality assurance (QC/QA) process for earth work construction, geotechnical applications, and pavement management.**(Akbariyeh, 2015).**

The benefits of using the LWD are: It is a non-destructive testing equipment, the deflection measurements are repeatable and accurate, **t**he equipment is durable and inexpensive comparted to other complicated testing systems, small and Easy to operate any place.

The LWD device provides a time-deflection curve which is utilized to measure the in-situ maximum vertical surface deflection and elastic modulus of pavement layers. The maximum vertical deflections are measured by integrating the geophone (velocity transducer) signal. This has two important divisions; the peak deflection may not occur instantaneous under the peak load due to dynamic effects, and the peak deflection may include both plastic and elastic deflection that depends on the strength of testing materials and proper contact between material and geophone. **(Fleming et al., 2007).**

The peak deflection is a measure either to degree of compaction or stiffness of soil, or both together with the peak force. to calculate the elastic modulus based on the well – known Boussinesq elastic half – space theory by the following expression:

$$E_{LWD} = \frac{(1 - v^2)\,\sigma_o a}{\delta} \,.\, f \qquad (2.18)$$

Where

E_{LWD}: Dynamic LWD soil Modulus

σ_o: Applied dynamic stress (MPa)

δ: Soil surface deflection (mm)

a: Radius of the loading plate (mm)

v **:** Poison's ratio in range 0.3-0.45 depending on the type of test material

f: Shape factor depending on stress distribution under a plate as shown in Table (2.7). The stress distribution depends on soil type and rigidity of the loading plate.

Table (2.7): Summary of shape factors in E_{LWD} estimation **(Vennapusa and White, 2013)**

.

Plate type	Soil type	Stress distribution (Shape)		Shape factor (f)
Rigid	Clay (elastic material)	Parabolic	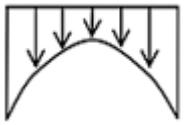	$\pi/2$
Rigid	Cohesion less Sand	Parabolic	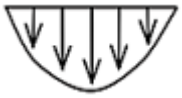	8/3
Rigid	Material with intermediate characteristics	Inverse Parabolic to uniform	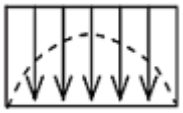	$\pi/2\ to\ 2$
Flexible	Clay (elastic material)	Uniform	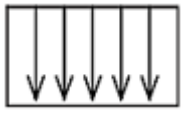	2
Flexible	Cohesion less Sand	Parabolic	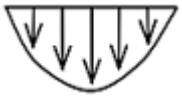	8/3

2.5.1 Type of Light Weight Deflectometer (LWD):

There are different types of LWD that have many similarities in their mechanics of operation, although there are differences in their style and diameter of plate, sensor type, dropping weight and height, impulse time, and contact pressure. Table (2.8) shows the physical characteristics of different types of LWD .**(Burhani, 2016)**

Table (2.8): Characteristics of typical LWD devices **(Burhani, 2016)**

Manufacture	CSM	Zorn	Prima	Load man	TFT
Plate style	Solid	Solid	Annulus	Solid	Annulus
Plate diameter (mm)	200 , 300	150, 200 300	100, 200 300	130, 200 300	100, 150 200, 300
Plate thickness (mm)	Unknown	124, 45 28, 20	20	Unknown	Unknown
Plate mass (Kg)	6.8, 8.3	15.0	12.0	6.0	Variable
Drop mass (Kg)	10.0	10.0	10,15,20	10.0	10,15,20
Drop height (m)	Variable	0.72	Variable	0.8	Variable
Maximum applied Force (KN)	8.8	7.07	15.0	17.6	8.5
Force measured	Yes	No	Yes	Yes	Yes
Impulse time (ms)	15-20	18 ± 2	15-20	25-30	15-25
Type of Buffer	Urethane	Steel spring	Rubber (conical shape)	Rubber	Rubber
Plate response Sensor	Geophone	Accelerometer	Geophone	Accelerometer	Geophone
Contact stress	User def.	Uniform	User def.	Rigid	User def.
Poisson's ratio	User def.	0.50	User def.	0.50	User def.

2.5.2 Factors Influencing the LWD Results:

The measurements of LWD test are influenced by several factors including:

1. **Bearing plate size:** the size of loading plate is the most significant factor that change the LWD test condition. The diameter of plate effects on the amount of pressure, the pressure reduces as it transfers from top down through pavement layers. The test conducted by **(lin et al, 2006)** on natural sandy soil found that the elastic modulus

(E_{LWD}) for a 100 mm plate was 1.5 to 1.6 times higher than for a 300 mm plate at similar loads.

2. **Types and location of deflection sensor:** the type and position of deflection sensors are different with various manufacturers, for example, the Zorn LWD reads the vertical surface deflection using an accelerometer built into the solid plate, as shown in Figure (2.5 c). The other types like Prima, TFT, Keros /Dynatest LWD devices estimate vertical surface deflection using a spring-loading geophone in direct contact with the ground surface through a (40 mm) diameter hole in the center of plate as shown in Figure (2.5 a and b) **(Dived, and Mooney, 2013)**

   The number of sensors used in LWD testing setup have an effect on LWD results. **(Akbariyeh, 2015),** indicated that the elastic modulus estimated by using LWD with a single sensor would be true only if the layer consists of a homogeneous and uniform materials, like a subgrade or compacted soil at the maximum depth of 1 to 1.5 times the plate diameter. But for layered structure like an asphalt pavement, it is difficult to estimate the modulus. The maximum number of geophones used in LWD is three.

3. **Plate contact stress:** the effect of this factor depends on the type of layers underneath, **(Vennapusa and White, 2013)** explained that for dense and granular materials the increasing contact stress lead to increase the elastic modulus. While the materials with cementitious properties will not influenced by changes in contact stress.

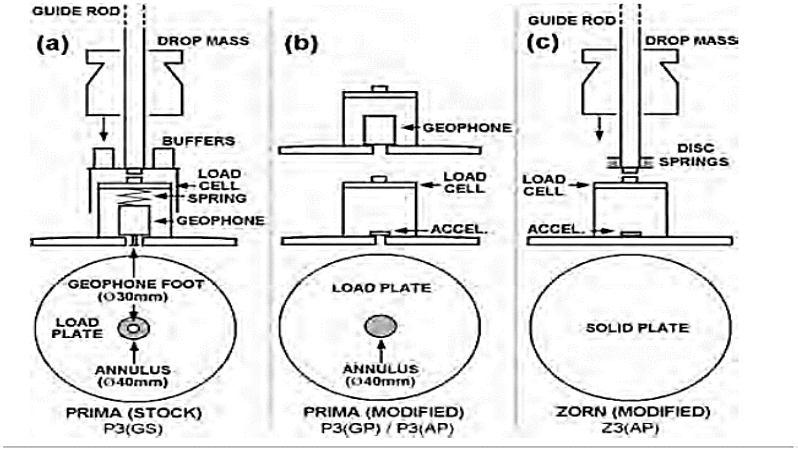

Figure (2.5): (a) Stock Prima 100 LWD, (b) modified configurations of Prima LWD with geophone (top) or accelerometer (bottom) fixed rigidly to the load plate, and (c) Zorn LWD showing modification to include load cell. **(Vennapusa and White, 2013)**

4. **Plate Rigidity:** this factor is important for estimating the distribution of stress under the plate and for selecting the shape factor (f) as explained in Table (2.7).
5. **Loading rate and buffer stiffness:** the elastic modulus (E_{LWD}) that measured by using elastic half – space theory influences by the rate of loading which can be controlled by changing the stiffness of buffer placed between the contact plate and drop weight.**(Vennapusa and White, 2013)**
6. **Proper contact between the loading plate and the surface of being tested:** The **(ASTM E 2835, 2011)** recommended that the test surface should be clean and smooth to obtained a uniform contact between the surface and load plate, so it recommended to place a thin layer of fine sand over the test point for a gravel surface.

2.5.3 Existing Correlation between LWD Moduli and Other In-Situ Test

A number of comparative work were carried out by several research to correlate the LWD with other field tests, to evaluate in-situ elastic modulus of pavement foundations at different highways projects. These correlations are summarized in the Table below:

Table (2.9): Summary of correlation between LWD moduli and other in-situ Test.

Reference.	Suggested formula	R^2
Rao et al, 2008.	$E_{LWD} = \frac{CBR + 2.754}{0.2867}$	0.90
Louay et al, 2009	$E_{LWD} = \left[\frac{M_r}{27.75}\right]^{-0.18}$	0.54
	$E_{LWD} = \left[\frac{M_r - 11.23 - 242.32(1/w)}{12.64}\right]^{-0.2}$	0.70
Zhang, 2010	$E_{LWD} = \frac{E_{FWD} - 8.1}{0.4}$	0.35
	$E_{LWD} = \frac{E_{BCD} - 29}{0.3}$	0.11
Nazzal et al., 2016	$E_{LWD} = \frac{CBR + 14}{0.66}$	0.83
Shaban, 2016	For subgrade coarse $E_{LWD} = 4.22 + 3.36E_{i\,(MPMT)} + 0.04\,E_{i(MPMT)}{}^2$	0.84
	For subgrade coarse $E_{LWD} = 7.07 + 0.66E_{r\,(MPMT)} - 0.001\,E_{r(MPMT)}{}^2$	0.79
	For base coarse $E_{LWD} = 34.48 + 3.34E_{i\,(MPMT)} - 0.01\,E_{i(MPMT)}{}^2$	0.94
	For base coarse $E_{LWD} = 50.93 + 0.34E_{r\,(MPMT)} - 4.2 \times 10^{-4}\,E_{r(MPMT)}{}^2$	0.77

Where

E_{LWD}: Dynamic LWD soil Modulus (MPa).

Mr: Resilient modulus of pavement materials

E_{FWD}: Dynamic FED soil Modulus (MPa)

E_{BCD}: Modulus of the compacted material obtained from Briaud Compaction Device (BCD) (MPa)

$E_{i(MPMT)}$ Initial Elastic Modulus (MPa**)** obtained from the MPMT tests

$E_{r(MPMT)}$ Reload Elastic Modulus (MPa) obtained from the MPMT tests

2.6 Summary:

As explained in the literature review, the plate load test is an important famous site test, it's necessary in various geotechnical engineering application. Plate load test (PLT) estimates bearing capacity of soil, subgrade reaction modulus, and modulus of deformation. Because of this test is difficult and time consuming many research tend to correlate the PLT with other tests like; standard penetration test (SPT), cone penetration test (CPT), failing weight deflectometer (FWD), and light weight deflectometer (LWD). These correlations were carried out to identify the initial and reload elastic modulus of pavement foundation. In this research, correlates the static plate load test(PLT) with the light weight deflectometer(LWD) to evaluate the possibility of using dynamic measurements obtained from (LWD) to predict the modulus of subgrade reaction.

Chapter Three

Experimental Work

3.1 General

In order to achieve the aim and objective of this work, a series of laboratory testing methods were carried out on different types of subgrade soils. The subgrade soils were excavated from different sites in Kerbala city and tested in the laboratory testing setup, which were designed and manufactured to simulate the actual field conditions.

The experimental work consists of 219 sets of laboratory tests, 126 of them were carried out in the laboratory setup, the remaining were divided into two parts; 69 tests to determine the physical properties, and 24 tests were carried out to identify the chemical characteristics. Tables (3.1) summarize the types of materials that have been investigated as well as the total number of laboratory tests.

Table (3.1): Summary of Number of laboratory Tests

Type of Tests			Type of Soils			Total Number of Tests		
			A-1-b	A-3	A-7-6			
Laboratory testing Setup		PLT	9	9	9	27	Σ = 126	Σ = 219
		LWD	18	18	18	54		
		Sand-Cone	9	9	0	18		
		Core-Cutter	9	9	9	27		
Physical Tests	CBR	Soaked	9	9	9	27	Σ = 93	
		Un soaked	9	9	9	27		
	Proctor	Standard	1	1	1	3		
		Modified	2	2	2	6		
	Direct shear		3	3	0	6		
Chemical test			8	8	8	24		

For determining basic soil properties, the following tests were conducted; specific gravity **(ASTM D854, 2014)**, particle size distribution **(ASTM D2487, 2005)** to classify the soil samples and modified proctor test **(ASTM D 1557, 2012)** was conducted to determine the maximum dry density and optimum moisture content. These tests are necessary for determining how the sample will be prepared later in the testing setup.

In the laboratory testing setup; the following tests were implemented [1] Plate Load Test (PLT) measured data, [2] Light Weight Deflectometer (LWD) measured data. In addition, the density and water content of compacted soils are determined by Sand-Cone Method **(ASTM D2011, 2011),** and Core Cutter method **(ASTM D2937, 2004).**

3.2 Laboratory Testing Setup:

The laboratory testing apparatus were designed and manufactured to simulate soil conditions as close as possible to those occurring in the field. Also, it provided the following advantages; facilitating the use of in-situ testing devices to determine the deflection of subgrade materials under the influence of static and dynamic loads, facilitating the change of water content and degree of compaction so as to simulate different materials of a pavement layers, moisture and compaction conditions in practical situation. Plate (3.1) shows the general view of the laboratory testing setup, which consists of the following components:

1. Loading steel frame.
2. Steel box.
3. Hydraulic loading system.
4. Data acquisition system.

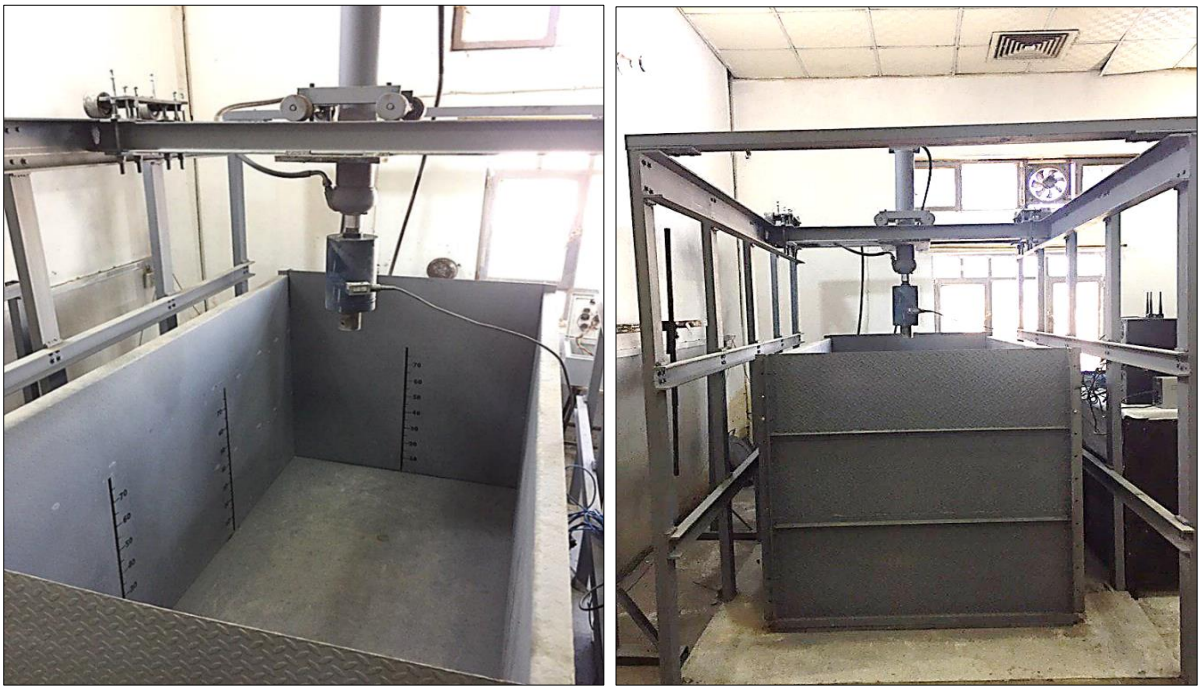

Plate (3.1): Laboratory Testing Setup.

3.2.1 Loading frame:

The steel loading frame was manufactured with the dimension (1.75 m width, 2.82 m length, and 2.65 m height) to support and ensure the verticality of the hydraulic jack. Figure (3.1) illustrates a schematic diagram of the steel structure of the loading frame.

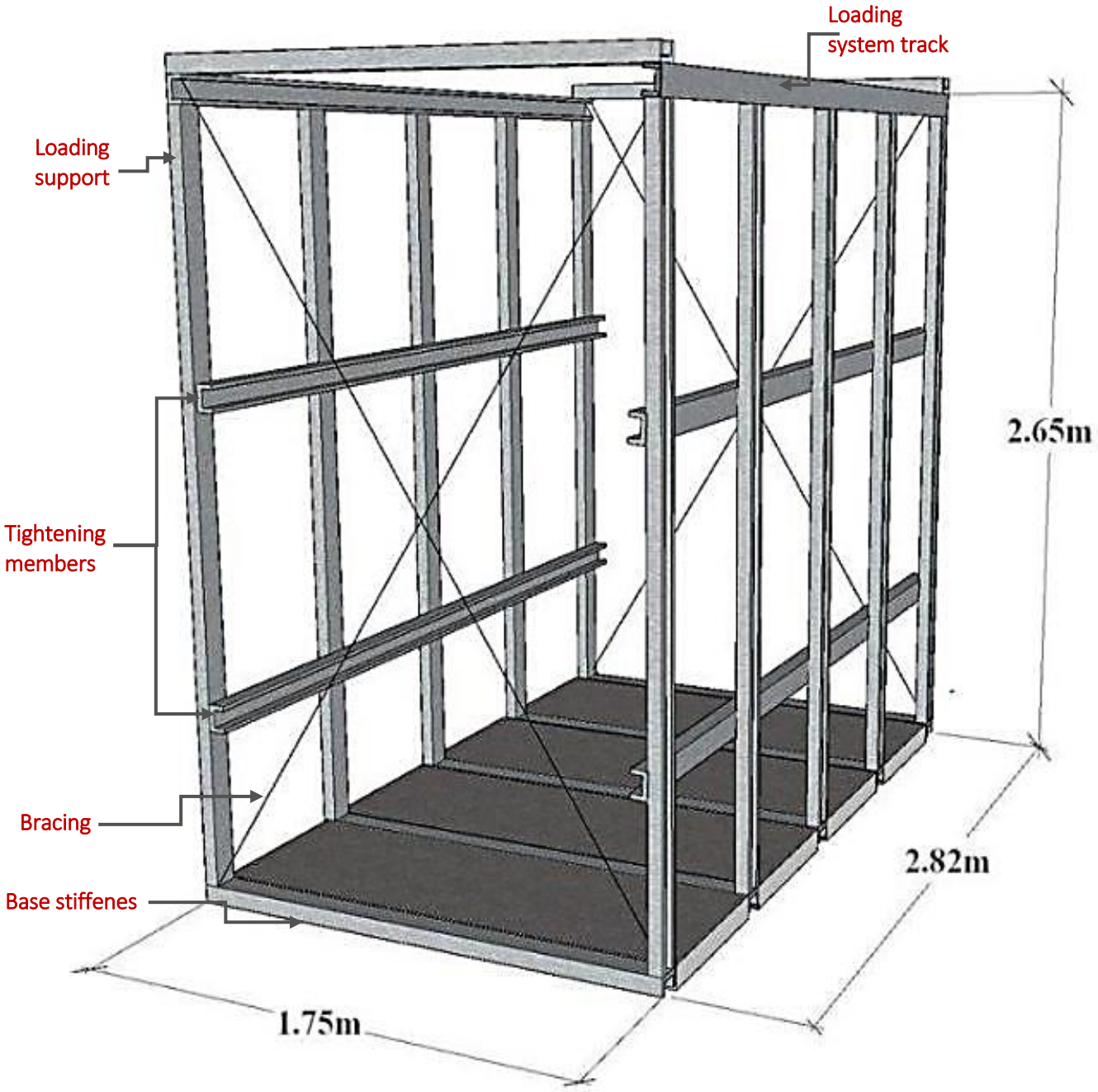

Figure (3.1): Steel loading frame

3.2.2 Steel box.

A large steel box in which the sample of subgrade material was compacted and tested shown in Figure (3.2), was manufactured with dimensions (1.2 m width ×2.4m length ×1.25m depth). These dimensions are large enough to allow the use of in-situ devices such as PLT and LWD, and to eliminate the effect of boundary conditions on failure zone, because both PLT and LWD devices create a bulb shape zone of stress under the plates of test. The diameter of significant stress zone extends approximately (0.9 times the diameter of the plate) horizontally from the center line of (300 mm) diameter bearing plate, and (1.5 to 2 times the diameter) vertically. So the box must be larger than (0.60 m) wide and (0.5 m) deep, and its length is large enough for taking more than one point for testing. The steel box was strengthened by L-section steel member to enhance the rigidity to minimize lateral deformation during soil compacting and testing.

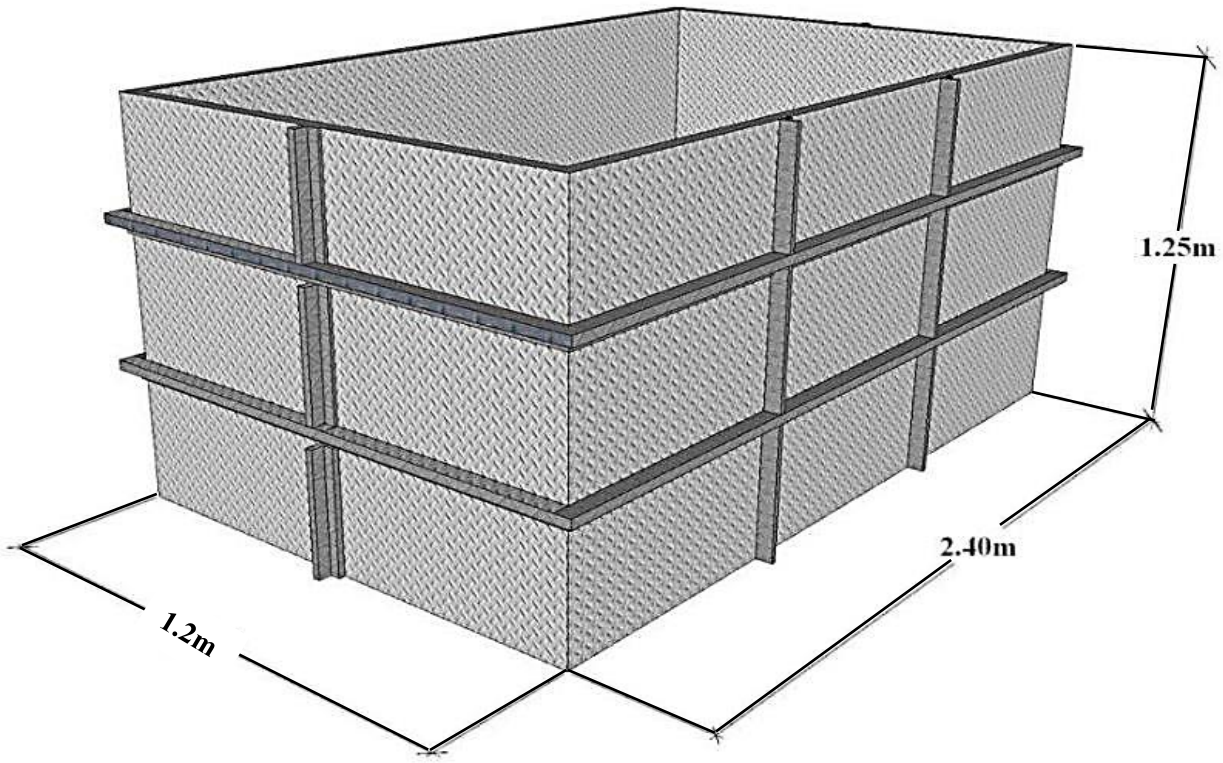

Figure (3.2): Steel box

3.2.3 Hydraulics loading system:

Hydraulics loading system consists of the following parts:

- Hydraulic pump.
- Hydraulic jack with capacity of 20 tonnes to apply compression load. The jack supported by a thin steel plate with dimensions (30 cm × 55 cm), the plate attached to an over-hanging of two I-section beams [3in. (7.5 cm) web × 3 in. (7.5 cm) flanges] which facilitated the transvers movement of the loading devices. While the two I- section beams itself travelled longitudinally above the steel box. Thus, it provided a two-dimensional selection loading location, this part was explained in Plate (3.2).

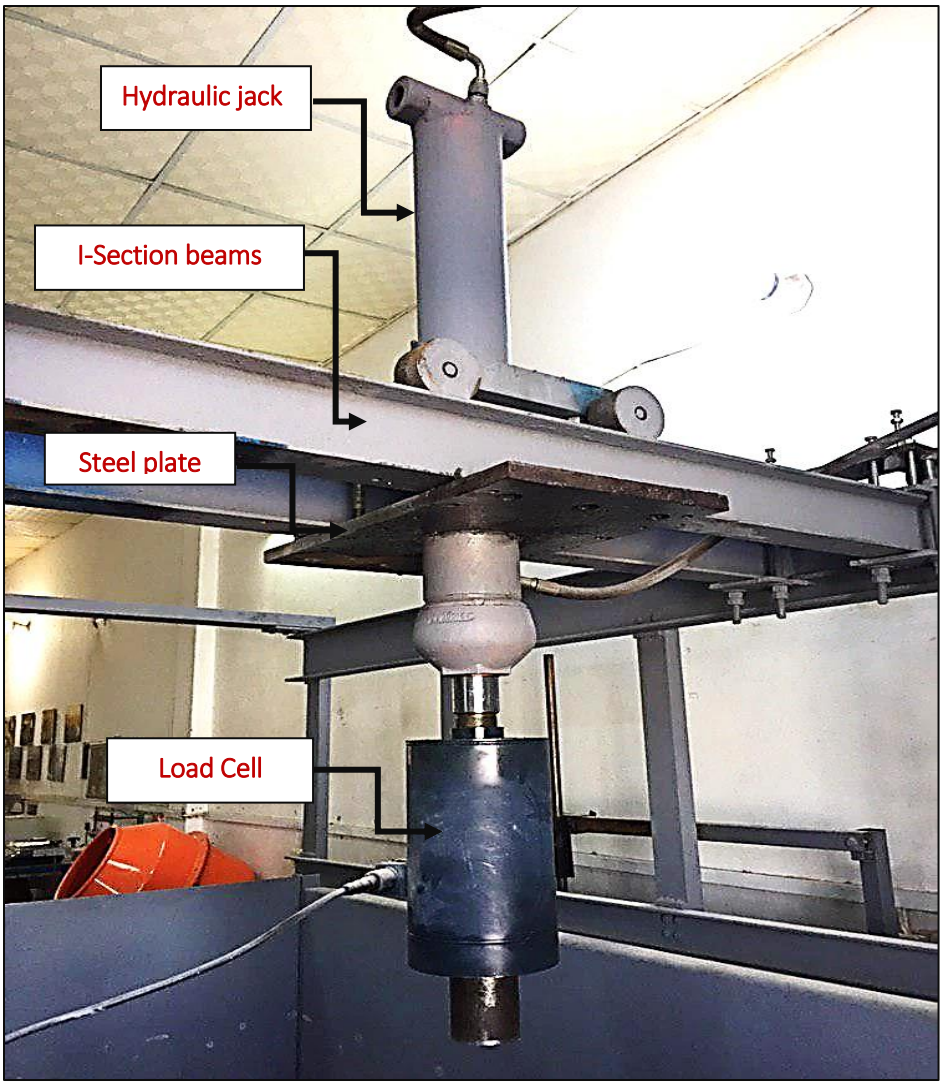

Plate (3.2): Loading assembly parts

- Hydraulic control system: which is reasonable for moving the piston into up and down, and applying the required load. The movement of piston was controlled electrically, either manually by press the suitable key in the control unit explained in Plate (3.3), or controlled automatically by a LabVIEW program as illustrates in Figure (3.3).

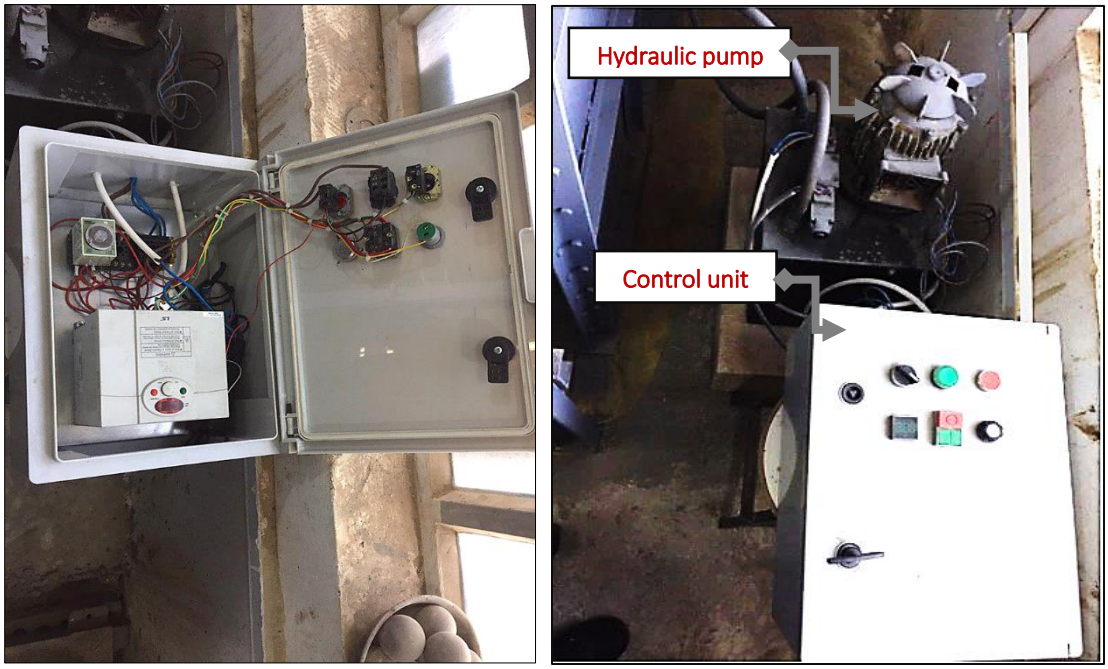

Plate (3.3): Hydraulics loading system.

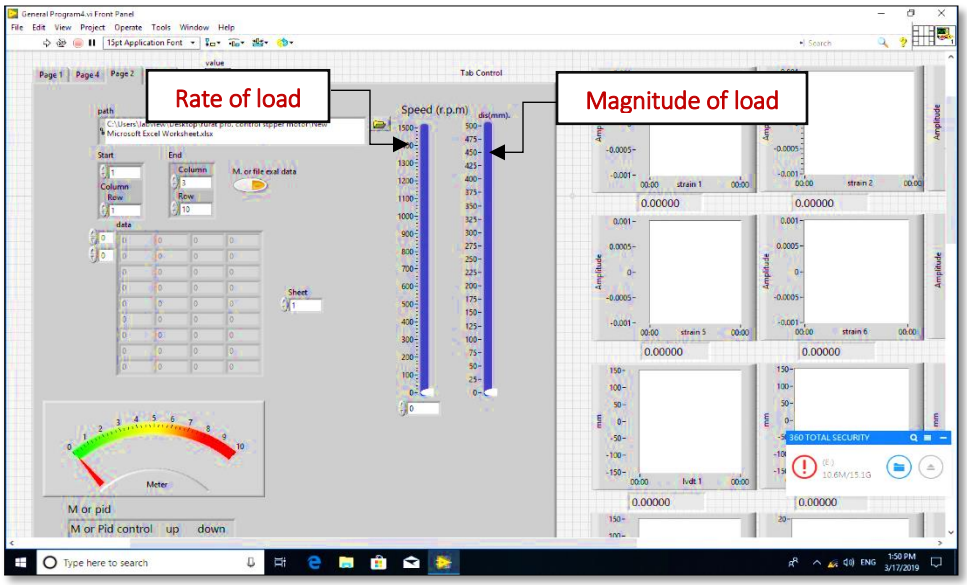

Figure (3.3): LabVIEW Software

3.2.4 Data acquisition system:

Data acquisition was used to record and store load-deflection measurements during the static plate load test, it stores 100 reading per seconds. These huge number of readings performed the total accurate information to the tester in measuring and sensing the occurring displacement due to static load. Plate (3.4) displays the data acquisition which consists of the following parts

- **LVDT:** linear variable displacement transducer with capacity (75 mm) was used to measure the vertical deformations of the soil.
- **Load Cell:** a compression load cell with maximum capacity (20 tons), model (SC 520) was used to measure the applied load, the rated output (R.O) of this load cell is (3 ± 0.0023 mV/V), and has combined error ranged 0.02% to 0.05%, and excitation varied from 10 to15V.
- **LabVIEW Software:** was used for engineering applications that require test, and measurement. This software enabled the user to control the speed and movement of the piston automatically, magnitude of static load, and rate of loading for dynamic load. The data that is read in the program is saved in an Excel file.

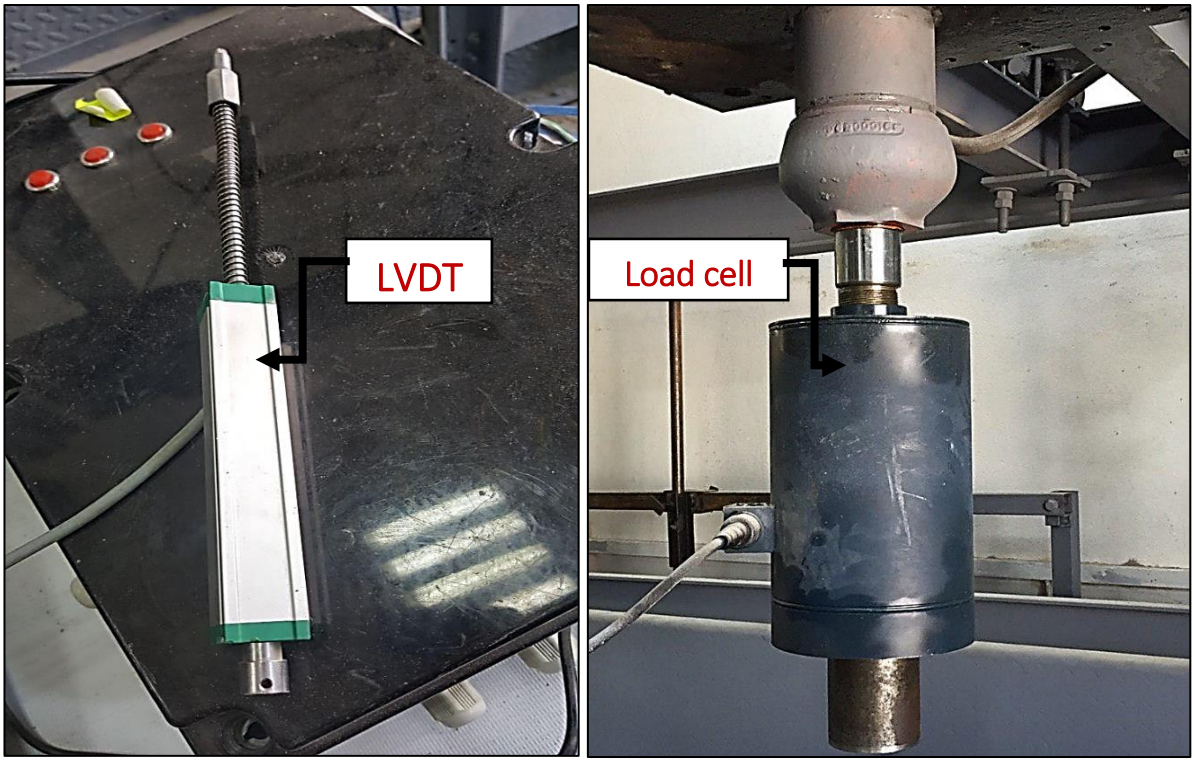

Plate (3.4): Data acquisition

3.3 Subgrade Soils Selection

3.3.1 Site locations:

In this research three types of soil were excavated and collected from different locations in Kerbala city and tested in the laboratory. The first site is located in Al-Meelad in the South-East part of Kerbela city, the classification of this soil was (A-1-b) according to the American Association of State Highway and Transportation Official (AASHTO) soil classification system, and poorly graded sand with silt (SP-SM) according to the Unified Soil Classification System (USCS). The second site is located in Al-Faris in the southern part of Kerbela city, the classification of this soil was (A-3) according to the (AASHTO) soil classification system, and poorly graded sand (SP) according to the (USCS) Soil Classification System. The third site is located in Al-Rofae in the North-West part of Kerbela city, the classification of this soil was (A-7-6) according to the (AASHTO) soil classification system, and lean clay (CL) according to the (USCS). The basic physical and chemical properties of the collected subgrade soils are summarized in Tables (3.2) and (3.3) respectively and Figures (3.5) to (3.12) explains the grain size distribution, Proctor, and CBR tests. Figure (3.4) shows aerial photo of three field sites in Kerbala City.

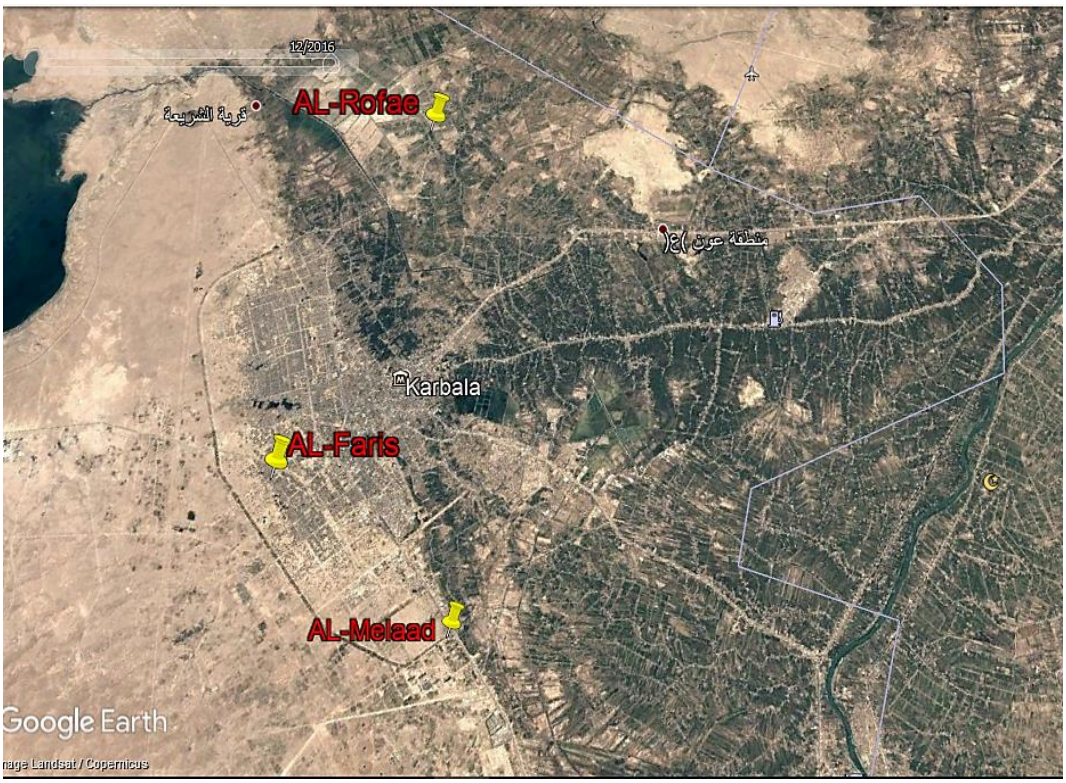

Figure (3.4): Aerial Photo of Three Field Sites in Kerbala City.

Table (3.2): Basic Physical Properties of Subgrade Soils

Property	Test Results			Specification
Soil Classification	A-1-b	A-3	A-7-6	AASHTO M 145
	SP-SM	SP	CL	ASTM D 2487
Coordinates	409911.538 3604114.561	406139.763 3604069.317	40673.683 3617974.787	/
OMC	15.5%	8.75%	18.5 %	ASTM D 1557
Max. Dry Unit Weight	18.85 kN/m^3	21.35 kN/m^3	17.20 kN/m^3	ASTM D 1557
Liquid Limit	/	/	47%	ASTM D 4318
Plasticity Index	NP	NP	24.26 %	ASTM D 4318
Uniformity Coefficient (Cu)	5.25	1.8	/	ASTM D 2487
Curvature Coefficient (Cc)	1.19	0.77	/	ASTM D 2487
Specific Gravity (Gs)	2.72	2.74	2.74	ASTM D 854
CBR Soaked, %	34	78	5.6	ASTM D 1883
CBR Un Soaked, %	53	98	26	ASTM D 1883
Angle of friction (ϕ)	38	36	/	ASTM D 3080

Table (3.3): Basic chemical Properties of Subgrade Soils according to **(B.S Part 3, 1990)**

Property	Test Results %		
	A-1-b soil	A-3 soil	A-7-6 soil
Sulphate, SO_3	9.08	5.68	1.859
Gypsum	19.52	12.21	/
Silicon Dioxide (silica), SiO_2	53.5	71.7	53.4
Calcium Oxides, CaO	26.29	11.17	8.63
Aluminum trioxide, Al_2O_3	4.5	6.24	9.78
Iron oxide, Fe_2O_3	1.6	4.9	8.9
Loss on ignition, L.O.I	11.8	6.2	17.9
PH	1.56	1.1	3.53

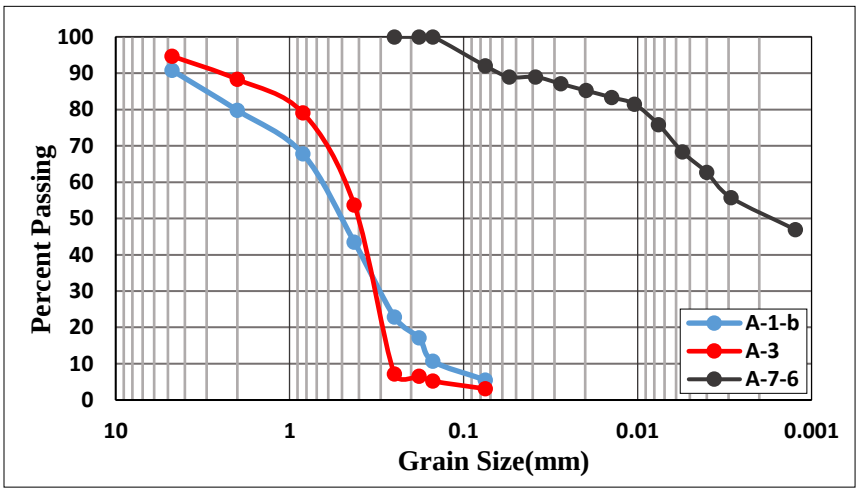

Figure (3.5): Grain Size Distribution of subgrade soils

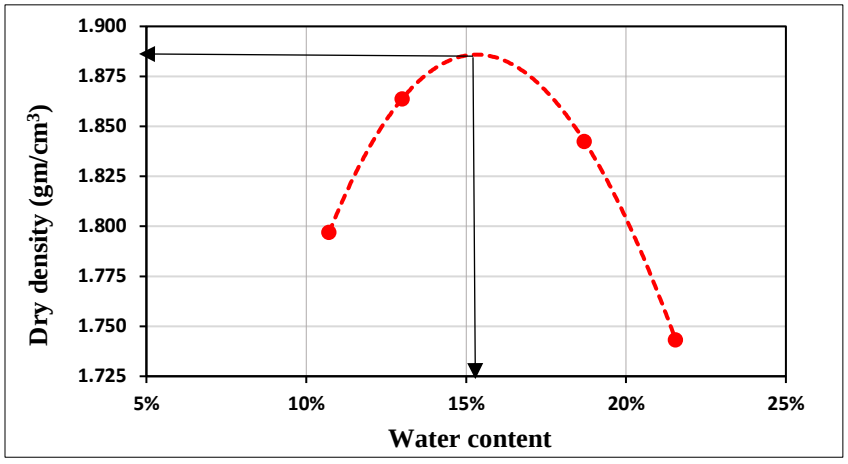

Figure (3.6): Modified Proctor Test Curves for A-1-b soil

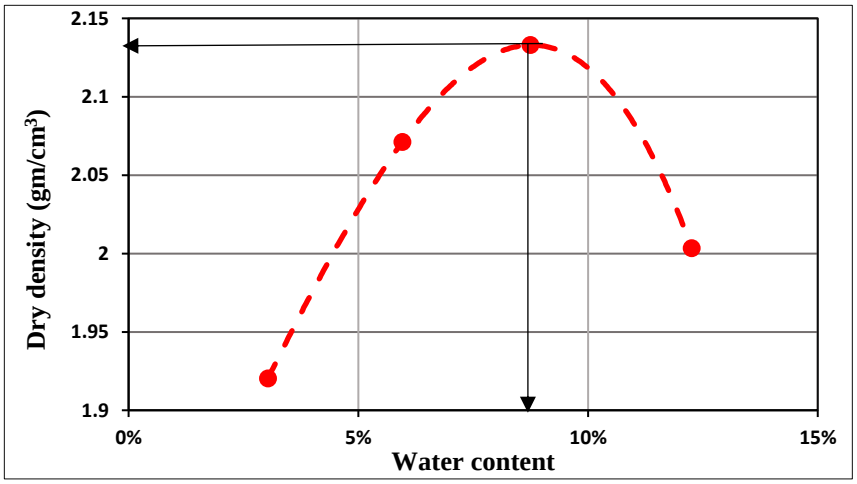

Figure (3.7): Modified Proctor Test Curves for A-3 soil

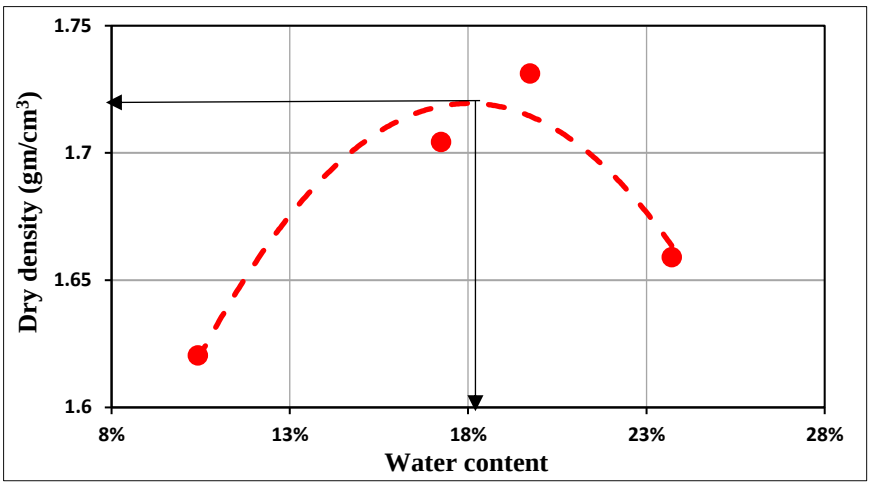

Figure (3.8): Modified Proctor Test Curves for A-7-6 soil

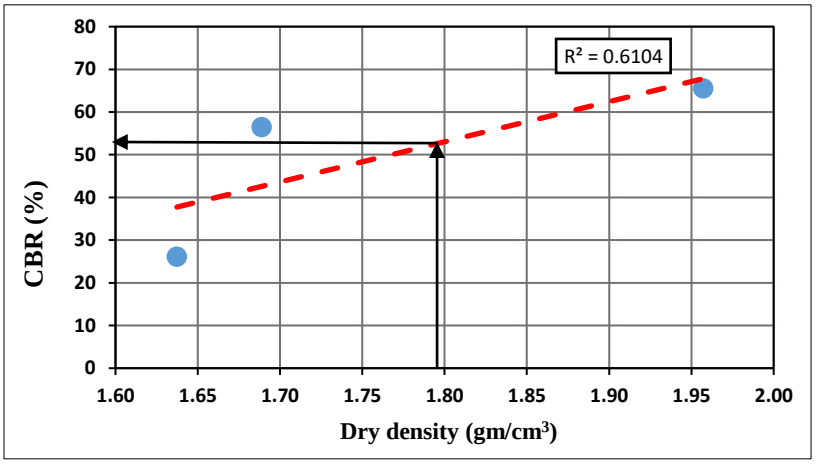

Figure (3.9): Determination of Unsoaked CBR for Desired Dry Unit Weight for A-1-b soil

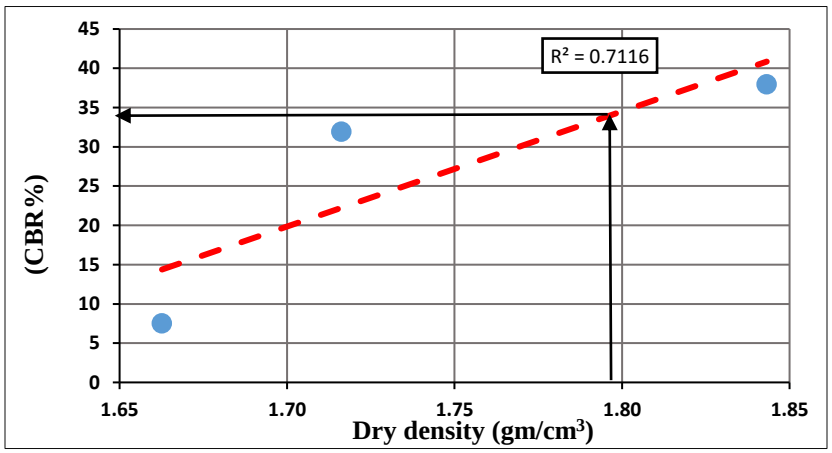

Figure (3.10): Determination of Soaked CBR for Desired Dry Unit Weight for A-1-b soil

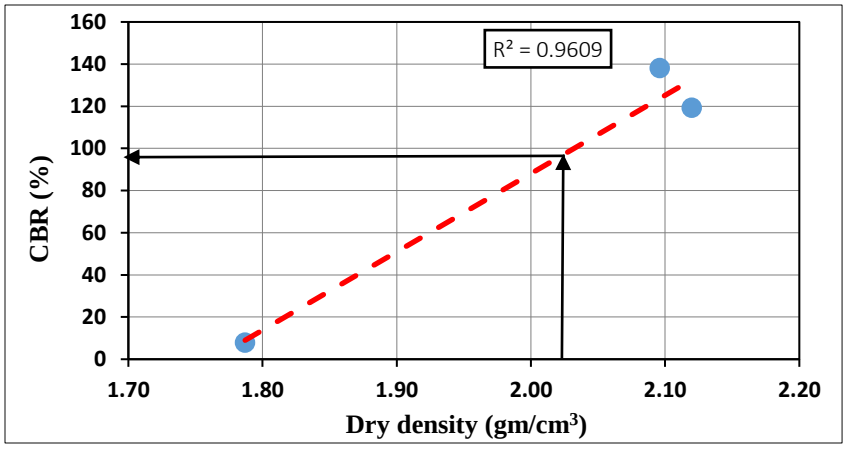

Figure (3.11): Determination of Unsoaked CBR for Desired Dry Unit Weight for A-3 soil.

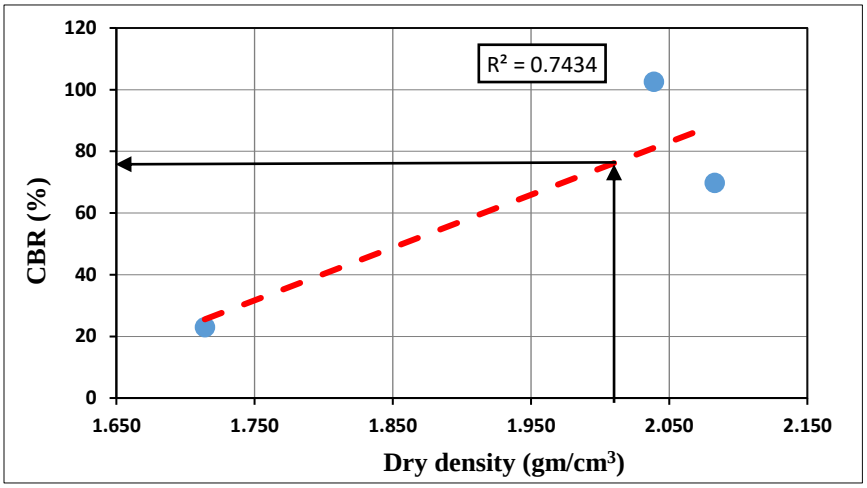

Figure (3.12): Determination of Soaked CBR for Desired Dry Unit Weight for A-3 soil.

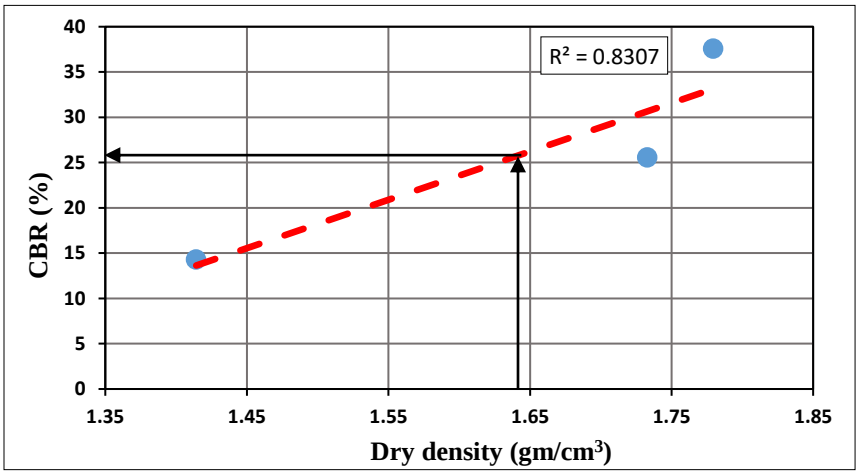

Figure (3.13): Determination of Unsoaked CBR for Desired Dry Unit Weight for A-7-6 soil.

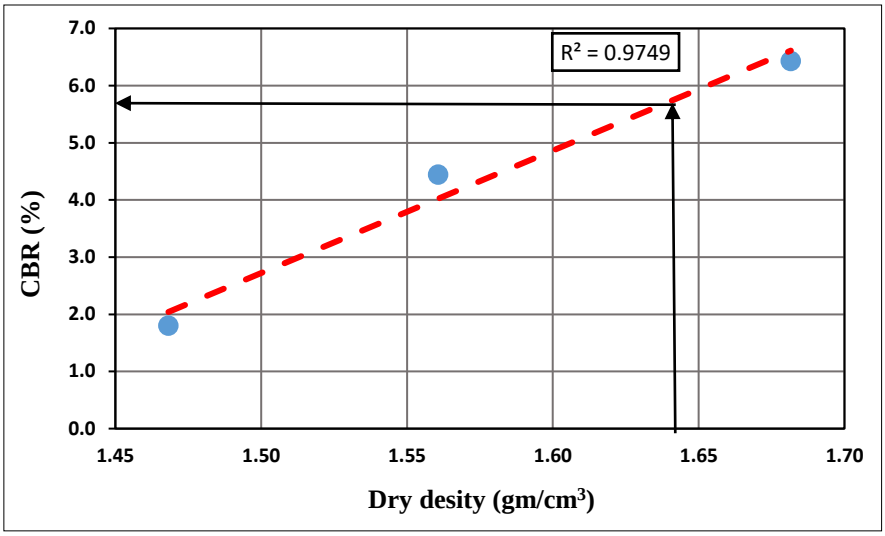

Figure (3.14): Determination of Soaked CBR for Desired Dry Unit Weight for A-7-6 soil.

3.3.2 Preparation of Subgrade Layer:

In this work, three types of subgrade soils were excavated and collected from three locations in Kerbala city. Each subgrade material was prepared and compacted in the laboratory testing-setup, then the structure performance of subgrade layer was evaluated using two in- situ testing devices: [1] light weight deflectometer, and [2] plate load test. In addition, density and water content measurements were taken from conducting sand cone test, core cutter. Approximately (2 m^3) of each soil type was required to construct a (0.6 m) thick of compacted subgrade layer. Subgrade soils were prepared at optimum water content by using electrical mixter with capacity (0.25 m^3) as shown in Plate (3.5). Then, the subgrades were compacted inside the testing steel box as layers (20 cm per layer) until reaching the desired height (0.6 m), as illustrated in Plate (3.6). this desired high of compaction subgrade soils is greater than the depth of influence resulted from both PLT and LWD loads because both PLT and LWD devices create a bulb shape zone of stress under the plates of test. The diameter of significant stress zone extends approximately (0.9 times the diameter of the plate) horizontally from the center line of (300 mm) diameter bearing plate, and (1.5 to 2 times the diameter) vertically. The layers were compacted under a specific compaction effort to achieve a desired degree of compaction. The compaction process was carried out using a plate compactor, and three degree of compaction were selected based on number of passes of the compactor (8, 12, and 16). Once the subgrade

was constructed, its modulus and stiffness properties were measured using PLT and LWD tests. The field moisture content and dry unit weight were obtained using Sand-Cone and Core-Cutter tests method, the sequence of testing was selected as following: three PLT, six LWD, three Sand cone, and three core cutter. Figure (3.15) gives a schematic diagram that describes the layout and locations of the tests.

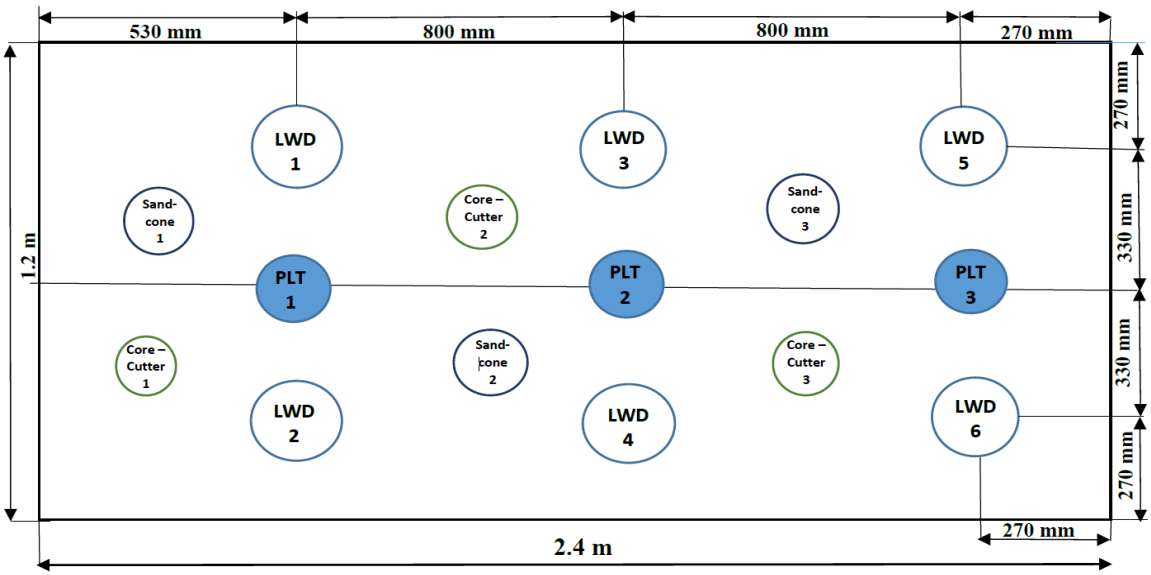

Figure (3.15): The layout of the field tests

Plate (3.5): Electrical Mixter


Plate (3.6): Preparation of Sample

3.4 Testing Methods:

3.4.1 Static plate loading test (PLT)

The plate bearing test was performed according to standard testing procedure presented in **(ASTM D1196, 2004)** and (**AASHTO T222, 2007).** A 300 mm diameter circular steel plate carefully centered under the load cell and jack assembly, another plate with smaller diameter set concentric with, and on top of the bearing plate. The bearing plates must be leveled so; a thin bed of fine sand was required for uniform bearing. As shown in Plate (3.7), two dial gauges with sensitivity 0.01mm/min and one 75 mm LVDT were installed near the edge of the bearing plate (25 mm from the circumference) at an angle of 120º from each other to get the average deflection of the bearing plate. After placing the loading plate, dial gauges and LVDT, a seating load of 0.5 ton was applied to produce a deflection not less than 0.25 mm. When the reading of dials and LVDT came to rest the seating, the seating load was released. The dial gauges were set to zero starting the loading. Then, the load was applied at stages with uniform increments. The number of stages should be enough to permit the recording of a sufficient number of load-deflection points (at least six points should be recorded during the test. After each increment, the load should be maintained until an increase in deflection of not more than 0.03 mm/min for three

consecutive minutes occurs. This procedure was continued until the load capacity has been reached. Plate (3.7) shows the testing.

Plate (3.7): Plate Load Test

From the data obtained through the procedure described above a Load-Deformation curve was obtained by plotting the load for each increment in (kPa) versus the average deflections. The average deflection represents the average of two dials and LVDT readings between the zero and end of each load increment. The curve should be approximately a straight line passing through the origin, otherwise, the curve must be corrected by drawing a straight line between the unit loads of 69 and 207 kPa, as shown in Figure (3.16).

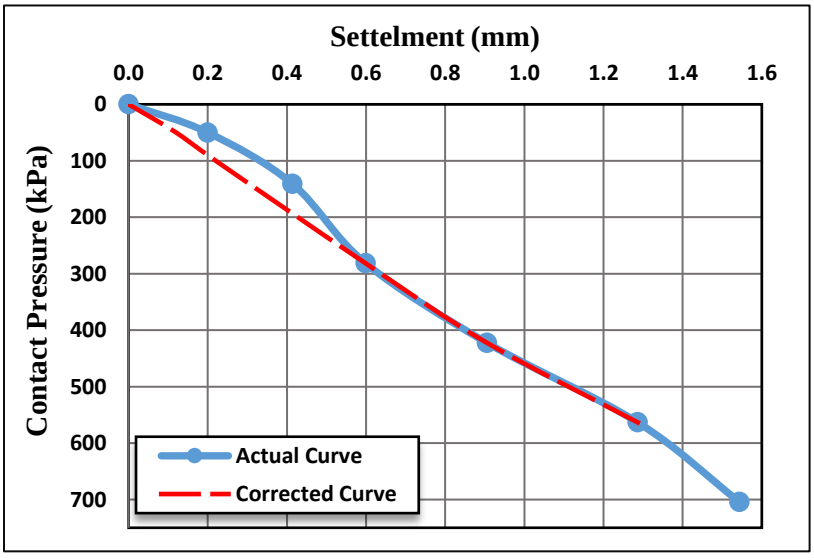

Figure (3.16): Typical load-deformation Curve

3.4.2 Light Weight Deflectometer (LWD)

A manufactured portable LWD was utilized in this study to evaluate dynamic and compaction characteristics of compacted subgrade materials. The principle of working LWD same as of PLT, but it applies a dynamic load not a static. The components and principle of the Zorn ZFG3. LWD device that shown in Figure (3.17), which is used in this study can be summarized as**: (Shaban & Cosentino, 2016)**

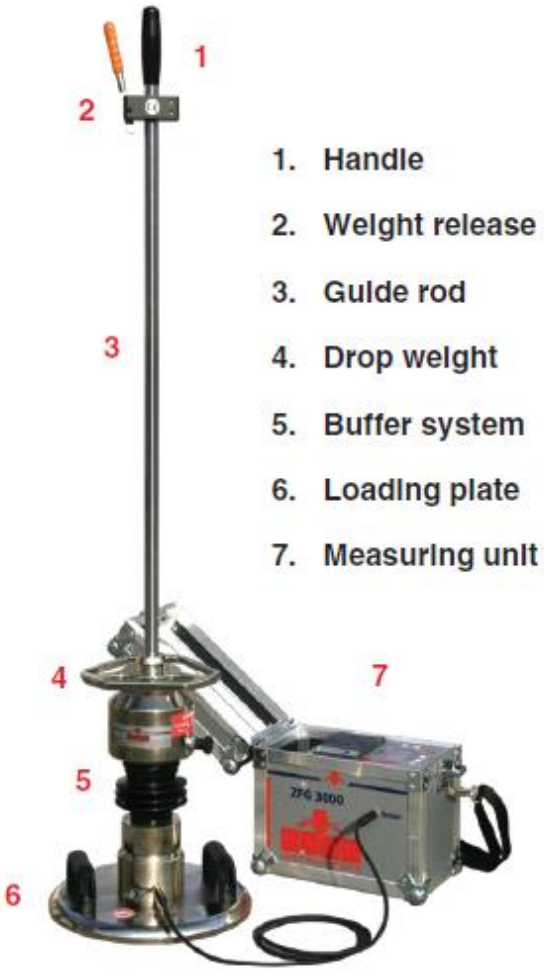

Figure (3.17): Schematic Diagram of the LWD (Zorn ZFG 3.0)

1. A 300-mm diameter loading plate, which place in contact with testing surface to perform a uniform distribution load.
2. 10-kg falling weight drops from 116-cm height, the falling weight designed to be operated by one person and negligible resistance or friction. As explained in **(ASTM E**

2835, 2011) that when the falling weight hits the loading plate resulting a half-sine shaped load on testing surface. As shown in Figure (3.18), three drops were carried out on each testing point to decrease the influence of loose soil particles that might cause unfavorable plastic deformations. The test parameters including dynamic modulus, vertical surface deflection, and degree of compatibility. The surface deflections are measured by integrating impulse velocity readings of an accelerometer fixed inside a circular loading plate, the vertical deflections produced from accelerometer readings are utilized to obtained surface soil modulus based on Boussinesq elastic half-space theory.

3. Buffer system that used to transfer the load to the plate uniformly. **(Akbariyeh, 2015)** explained that increasing the number of buffer leads to increase the system stiffness and reduce pulse duration.
4. Deflection sensors like an accelerometer to measure the dynamic parameter

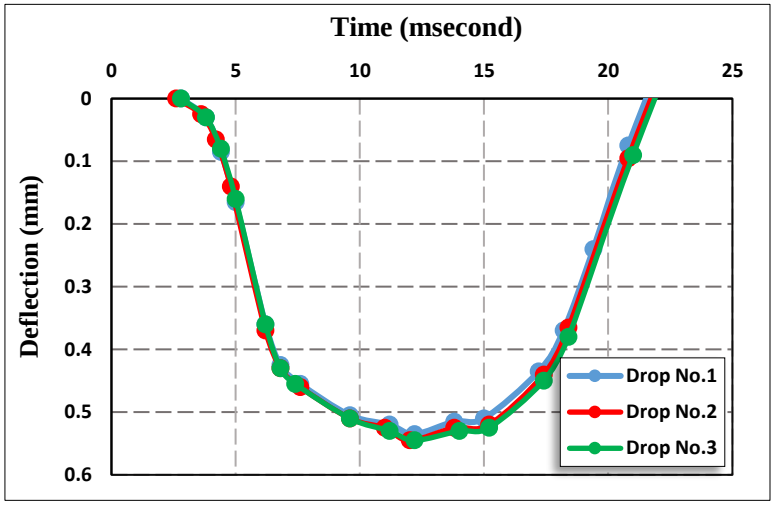

Figure (3.18): Typical results of the light weight deflectometer

3.5 Summary

This chapter explains characterization of the subgrade materials that used in this thesis, the methods used to test materials, the manufacturing of laboratory testing setup, and location of preparation the subgrade soils in this study. The tests are divided in to two phase; laboratory, and laboratory testing setup test. The laboratory tests include the basic physical and chemical tests. While the laboratory testing set up test consist of static and dynamic

tests. The static tests represent by static plate load test (PLT). While the Light Weight deflectometer (LWD) is the dynamic testing devise. Also, the field density's tests performed by the Sand Replacement test and Core – Cutter tests. This chapter explain how the compaction effort of subgrade soils in the laboratory testing setup was performed by using three number of passes of compactor device (8, 12, and 16).

The methodology in this study included preparation the subgrade soils at its optimum water content in the laboratory testing setup, and compacted it in three different degree of compaction depends on number of passes of compaction device. Under each degree of compaction the subgrade soil properties were performed under static and dynamic tests.

Chapter Four

Results of Experimental Tests

4.1: Introduction:

This chapter presents and discusses the results of 126 experimental tests performed on different types of soil, 27 of these tests were carried out under the static load, 54 tests were subjected to the dynamic load, and the remaining 45 testes for other required field tests to determine the field densities and degree of compaction.

4.2: Densities Tests Results:

The degree of compaction and field densities of subgrade soils are summarized in Table (4.1). The field densities were selected based on the number of passes of the compacting device on soil layers. From the results in table below, it can be seen that when increasing the number of passes, the dry density increases, and its increasing is different from one soil to another because it highly influenced by soil type [i.e. grain size distribution, and percentage of fine content], water content, and compaction effort **(Guerrero, 2004)**.

Table (4.1): Field Densities Tests

Type of soil	No. of Passes	Points	Core-Cutter Test			Sand-Cone Test		
			Bulk density (gm/cm3)	Dry density (gm/cm3)	Degree of compaction %	Bulk density (gm/cm3)	Dry density (gm/cm3)	Degree of compaction %
A-1-b	8	1	1.930	1.685	89.37	1.99	1.733	91.95
		2	1.907	1.690	89.65	2.01	1.741	92.36
		3	1.967	1.742	92.43	2.02	1.751	92.89
	12	1	1.902	1.761	93.40	1.96	1.776	94.19
		2	1.850	1.700	90.00	1.91	1.716	91.00
		3	1.934	1.730	92.00	1.96	1.744	92.50
	16	1	1.983	1.843	97.79	2.01	1.857	98.51
		2	1.929	1.801	95.55	2.03	1.830	97.09
		3	2.034	1.855	98.43	1.98	1.860	98.68
A-3	8	1	1.973	1.830	85.73	2.03	1.886	88.33
		2	1.949	1.835	85.93	2.03	1.888	88.41
		3	1.997	1.851	86.69	2.02	1.898	88.89
	12	1	2.026	1.893	88.69	2.09	1.975	92.50
		2	1.977	1.874	87.78	2.01	1.898	88.89
		3	1.962	1.858	87.01	2.00	1.890	88.51
	16	1	2.151	2.023	94.77	2.10	1.974	92.46
		2	2.172	2.030	95.07	2.17	2.035	95.31
		3	2.155	2.039	95.49	2.20	2.047	95.87

Table (4.1): Field Densities Tests-continue

Type of soil	No. of Passes	Points	Core-Cutter Test			Sand-Cone Test		
			Bulk density (gm/cm3)	Dry density (gm/cm3)	Degree of compaction %	Bulk density (gm/cm3)	Dry density (gm/cm3)	Degree of compaction %
A-7-6	8	1	1.870	1.439	83.69	/	/	/
		2	1.817	1.447	84.15	/	/	/
		3	1.863	1.431	83.20	/	/	/
	12	1	1.857	1.520	88.38	/	/	/
		2	1.863	1.491	86.70	/	/	/
		3	1.808	1.479	85.99	/	/	/
	16	1	1.880	1.622	94.03	/	/	/
		2	1.959	1.632	94.90	/	/	/
		3	1.997	1.646	95.70	/	/	/

4.2: Results of Plate Load Test:

Twenty-seven PLT tests were performed on three types of soil under different degree of compaction. The PLT was conducted by applying the load incrementally, the magnitude of maximum applied load used in this study is 50 kN (5 tons). The following characteristics of subgrade materials were extracted from PLT tests:

- **$P_{max.}$:** maximum contact pressure in (kPa) produced from the ratio between applied load and area of the loading plate.
- **$\delta_{max.}$:** maximum settlement of the loading plate under the static load.
- **Ks:** modulus of subgrade reaction in (kPa/mm) obtained from equation (2.1).
- **Es:** Young's modulus determined as a function of maximum surface deflection using the equation below.

$$E_S = \frac{\pi}{4}\frac{pD(1-\boldsymbol{\nu}^2)}{w} \qquad (4.1)$$

The following subsections summarize measurements of PLT tests:

For A-1-b Subgrade soil from Al-Meelad district, the fundamental properties of soil obtained from conducting 9 PLT tests are listed in Table (4.2). It was noted that the values of subgrade reaction modulus obtained from actual load-deformation curve before the correction ranged from 222.6 to 313.6 kPa/mm with an average 255.07 kPa/mm. While the subgrade reaction modulus obtained from corrected load-deflection curve ranged from 313.6 to 431 kPa/mm with an average equal to 361.43 kPa/mm. The values of correction factor varied from 0.61 to 0.79 with average 0.71. The value of elastic modulus ranged

from 21.1 to 55.9 MPa with an average equal to 32.15 MPa. Whereas, the value of maximum contact pressure varied from 432.2 to 732.39 kPa with average value equal to 631.95 kPa. The results also indicated that that maximum settlement varied from 2.7 to 6.47 mm with an average equal to 4.46 mm.

Figure (4.1) shows the average load-deformation curve of PLT tests.

Table (4.2): Summary of plate loading test results for (A-1-b) soil at AL-Meelad

No. of Passes	Points	$P_{max.}$ (kPa)	δ_{max} (mm)	(Ks) from Actual Curve (kPa/mm)	(Ks) from Corrected Curve (kPa/mm)	*Es (MPa)
8	1	563.0	5.200	222.6	313.6	23.20
	2	704.2	6.473	246.4	345.0	23.30
	3	563.0	5.260	287.5	363.0	22.96
12	1	721.4	5.112	222.6	363.2	30.26
	2	432.2	4.390	222.6	345.0	21.17
	3	732.0	6.370	246.4	345.0	24.65
16	1	704.2	3.470	246.4	383.3	43.50
	2	563.0	2.272	287.5	363.5	44.40
	3	704.0	2.700	313.6	431.3	55.90
Average		631.95	4.63	255.07	361.43	32.15
St.dv.		104.83	1.42	33.40	32.52	12.59

Note: *The value of Poisson's ratio used to determine elastic deformation moduli was assumed 0.3

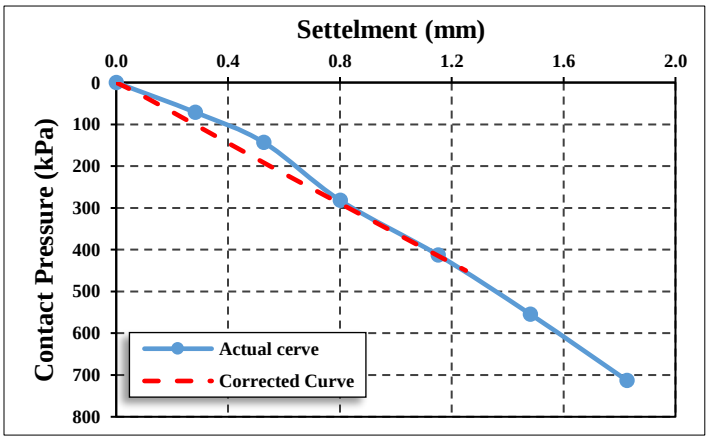

Figure (4.1): Average load – deformation curve for A-1-b soil

For A-3 Subgrade soil from Al-Faris district, the fundamental properties of soil obtained from conducting 9 PLT tests are listed in Table (4.3). The results revealed that the value of subgrade reaction obtained from actual load-deformation curve before correction ranged from 246.43 to 711.3 kPa/mm with an average 401.33 kPa/mm. While after correcting load – deformation curve the value of subgrade reaction modulus range from 246.43 to 766.7 kPa/mm with an average equal to 487.38 kPa/mm. The values of correction factor varied from 0.57 to 1.0 with average 0.86. When the correction factor value reaches

to 1.0 that means the load-deformation curve is a straight line passing through the origin and it doesn't need any correction according to the recommendation of **(AASHTO, 2007),** whereas the elastic modulus varied from 22.35 to 84.67 MPa with an average 58.11 MPa. Maximum settlement of the soil that produced from average readings of dial gauges ranged from 1.75 mm to 4.728 mm with an average equal to 2.6 mm. The value of maximum contact pressure varied from 492.96 to 691.14 kPa with average value equal to 624.52 kPa. Figure (4.2) shows The average load-deformation curve.

Table (4.3): Summary of plate loading test results for (A-3) Soil at (AL-Faris)

No. of Passes	Points	$P_{max.}$ (kPa)	δ_{max} (mm)	(Ks) from Actual Curve (kPa/mm)	(Ks) from Corrected Curve (kPa/mm)	*Es (MPa)
8	1	492.96	4.728	246.4	246.4	22.36
	2	492.96	3.370	255.6	255.6	31.36
	3	492.96	2.013	300.0	300.0	52.51
12	1	690.10	2.583	460.0	460.0	57.30
	2	690.10	2.747	287.5	460.0	53.86
	3	690.10	2.670	345.0	431.3	55.52
16	1	690.10	1.830	711.3	711.3	80.86
	2	690.10	1.750	431.2	755.2	84.56
	3	690.10	1.750	575.0	766.7	84.68
Average		624.52	2.60	401.33	487.38	58.11
St.dv.		98.68	0.97	158.99	209.60	22.29

Note: *The value of Poisson's ratio used to determine elastic deformation moduli was assumed 0.3

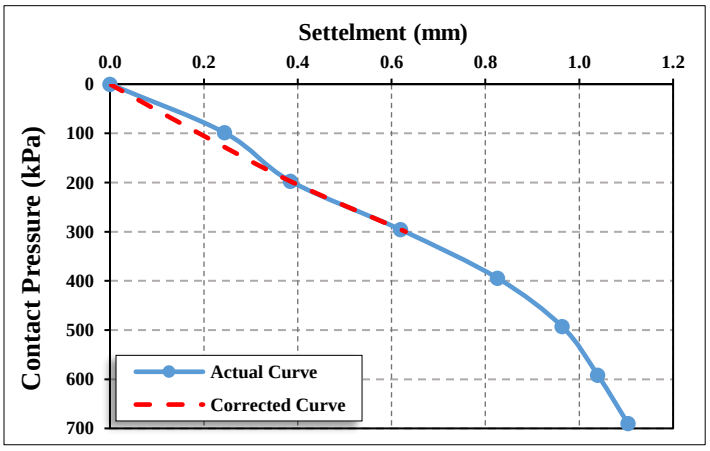

Figure (4.2): Average load – deformation curve for A-3 Soil

For A-7-6 Subgrade soil from Al-Rofae district, the fundamental properties of soil obtained from conducting 9 PLT tests are listed in Table (4.4). It was noted that the values of subgrade reaction modulus obtained from the actual load-deformation curve before

corrected curve ranged 50 to 138 kPa/mm with an average 90.1 kPa/mm. While after correcting load – deformation curve the value of subgrade reaction modulus range from 135.3 to 246.4 kPa/mm with an average equal to 184.3 kPa/mm. The values of correction factor varied from 0.28 to 1.0 with average 0.54. When the correction factor value reaches to 1.0 that means the load-deformation curve is a straight line passing through the origin and it doesn't need any correction according to the recommendation of **(AASHTO, 2007),** The value of elastic modulus ranged from 17 to 43.5 MPa with an average equal to 32.5 MPa. Whereas, the value of maximum contact pressure varied from 492.96 to 690.1 kPa with an average value equal to 624.5 kPa. The results also indicated that maximum settlement varied 3.4 to 6.2 mm with an average equal to 4.49 mm.

Figure (4.4) shows the average load-deformation curve of PLT tests.

Table (4.4): Summary of plate loading test results for (A-7-6) soil at (Al-Rofae)

No. of Passes	Points	$P_{max.}$ (kPa)	δ_{max} (mm)	(Ks) from Actual Curve (kPa/mm)	(Ks) from Corrected Curve (kPa/mm)	*Es (MPa)
8	1	492.96	6.03	138.0	138.0	17.50
	2	492.96	6.20	115.0	138.0	17.00
	3	492.96	5.77	132.7	135.0	18.40
12	1	690.1	4.20	53.1	186.5	35.20
	2	690.1	4.08	57.5	181.6	36.30
	3	690.1	3.90	50.0	172.5	37.90
16	1	690.1	3.44	86.3	230.0	43.01
	2	690.1	3.40	89.6	230.0	43.52
	3	690.1	3.42	88.5	246.4	43.26
Average		624.5	4.49	90.1	184.3	32.5
St.dv.		98.41	1.17	33.14	43.12	11.52

Note: *The value of Poisson's ratio used to determine elastic deformation moduli was assumed 0.3

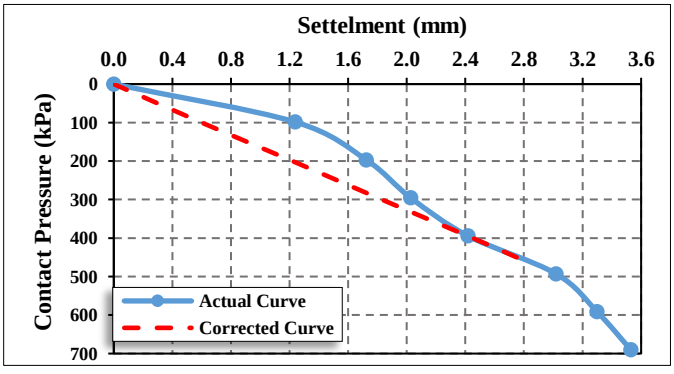

Figure (4.3): Average load – deformation curve for A-7-6 Soil

After all the soils were tested, the values obtained from the experiments were graphed in the following figures in order to explain the relationships between the subgrade reaction

modulus and the obtained dry densities. The modulus of subgrade reaction increased with increasing the dry densities.

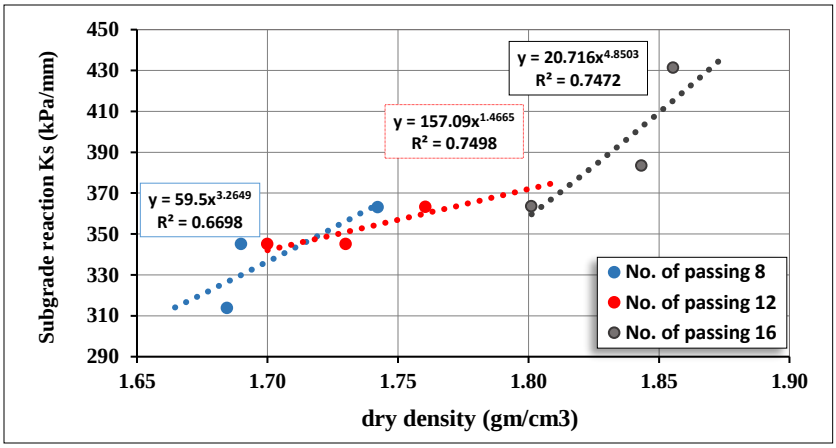

Figure (4.4): Subgrade reaction. vs. dry density for (A-1-b) soil

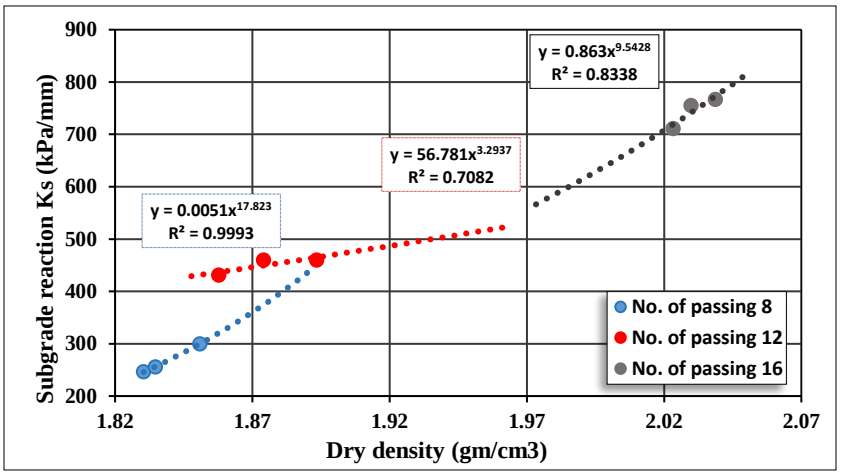

Figure (4.5): Subgrade reaction. vs. dry density for (A-3) soil

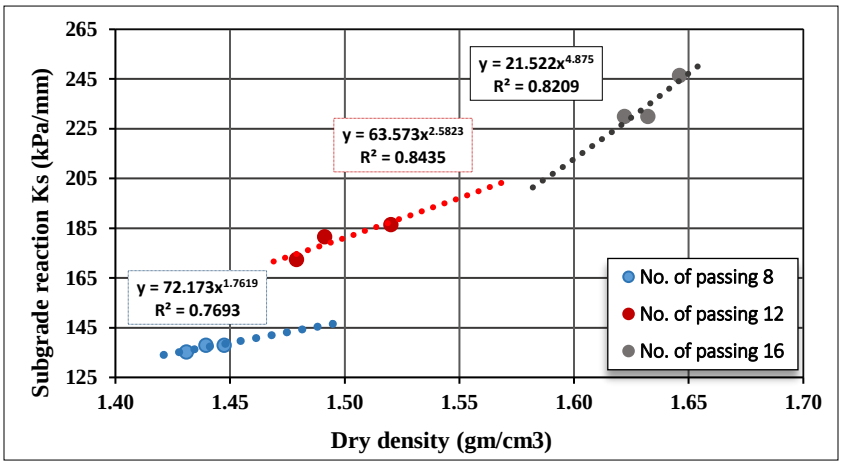

Figure (4.6): Subgrade reaction vs. dry density for (A-7-6) soil

The results also showed that the subgrade reaction modulus increased with increasing the degree of compaction as illustrated in Figures below. Because the compaction process improves the mechanical properties of the soil by reducing the volume of voids containing air and the soil particles get closer due to the new arrangement. That leads to increase the resistance, and reduces the deformation capacity.

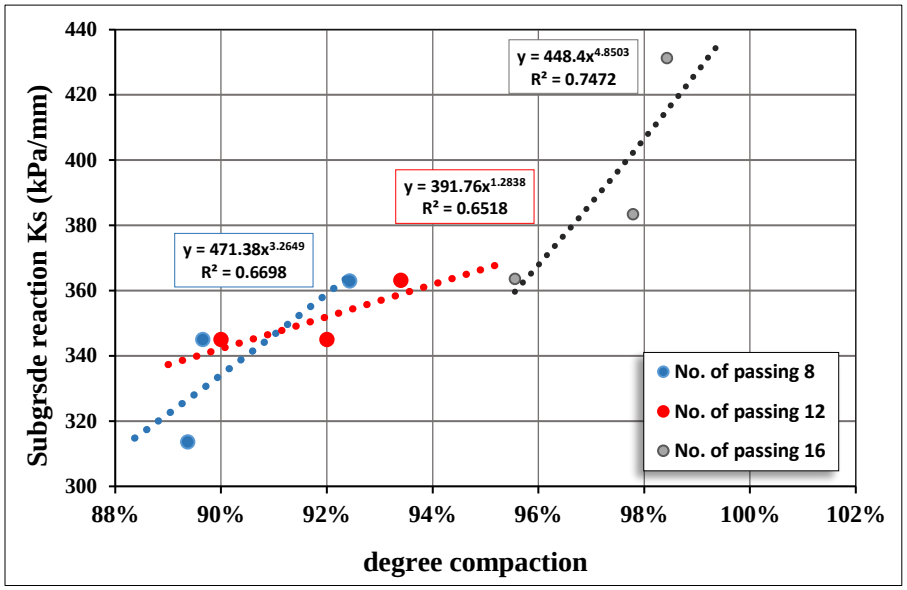

Figure (4.7): Subgrade reaction vs. Degree of compaction for (A-1-b) soil

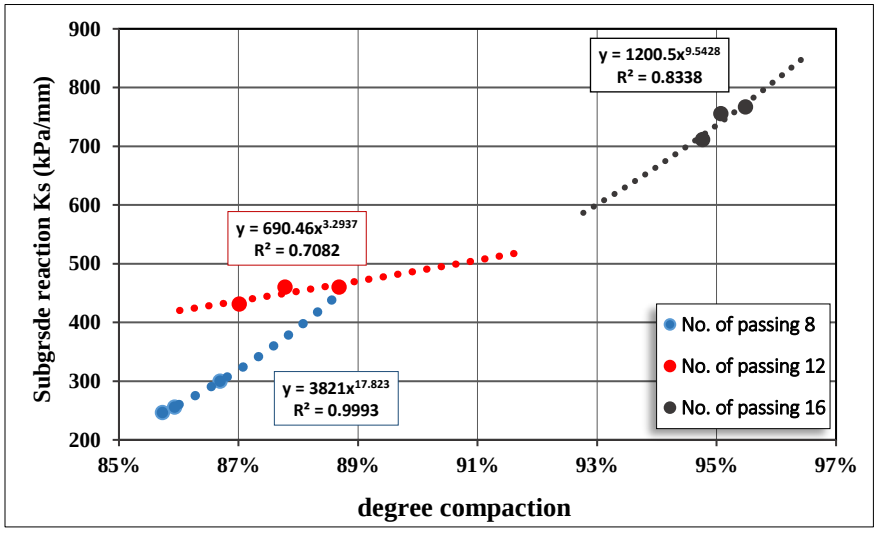

Figure (4.8): Subgrade reaction vs. Degree of compaction for (A-3) soil

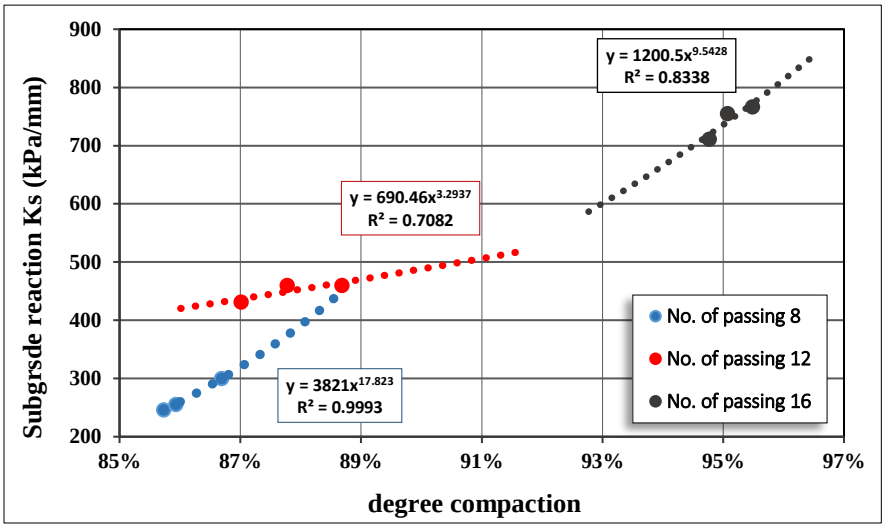

Figure (4.9): Subgrade reaction vs. Degree of compaction for (A-7-6) soil

In general, from the all results above, the higher value of subgrade reaction modulus is 766.7 kPa/mm for the A-3 (AL-Faris) soil, while the lower value is 135 kPa/mm for the A-7-6 (AL-Rofae) soil. Also, the results showed that the subgrade reaction modulus and elastic modulus obtained from A-3 soil are higher than those obtained from A-1-b (AL-Melaad) soil, the reason of this that the A-1-b soil contain the amount of gypsum in it components about 19.52 as illustrated in Table (3.4), this amount of gypsum effect on the strength of soil, as mentioned by **(Razouki et al., 1994), (Razouki and Kuttah, 2004), (Kuttah and Sato,2015),** and **(Razouki and Ibrahim, 2019)** Gypsum is one of the soluble salts that can have a injurious effect on subgrade soils, buildings and earth structures and caused a difficult conditions for roads.

4.3: Results of Light Weight Deflectometer:

The dynamic properties of subgrade materials were obtained by implementing 54 LWD tests on three types of subgrade soils. The LWD parameters measured during this study includes:

- **δ_d:** surface deflection in (mm) obtained from double integration to the acceleration versus time signals of pulse waves recorded by a data acquisition system for the accelerometer located inside the circular loading plate.
- **(E_d):** dynamic modulus in (MPa) measured from back-calculated of the surface deflection using elastic half-space theory developed by Boussinesq.

- **(Dc):** degree of compatibility is determined by dividing the mean value of surface deflection by the mean value of pulse velocity of dynamic impact load generated in a subgrade layer. This parameter gives an indication about compaction characteristics. Generally, if degree of compatibility is less than or equal to 3.5 no further compaction is required. However, if degree of compatibility is greater than 3.5 further compaction is recommended.

The following subsections present the measurements of LWD tests:

For A-1-b Subgrade soil from Al-Meelad district, the results of the 18 LWD tests conducted on different compacted subgrade surfaces are given in Table (4.5). These results were calculated by averaging the values resulted from three consecutive drops. The results exhibited that the vertical displacements ranged from 0.47 to 1.053 mm, with an average deflection of 0.675 mm, Figure (4.10) showed the average data of time-deformation curve. The values of dynamic modulus varied from 21.37 to 47.87 MPa with an average equal to 34.593 MPa. The average value of degree of compatibility was 3.346 ms.
All time-deflection curves of LWD are listed in Appendix (A-1).

Table (4.5): Summary of LWD Results for (A-1-b) Subgrade Soils at (Al-Meelad)

No. of Passes	Points	Surface Deflection (mm)				E_d (MPa)	Dc (ms)
		δ_1	δ_2	δ_3	Mean		
8	1	1.065	1.050	1.044	1.053	21.37	3.649
	2	0.651	0.647	0.624	0.641	35.10	3.163
	3	0.779	0.753	0.723	0.752	29.92	3.679
	4	0.537	0.545	0.549	0.544	41.36	3.101
	5	0.586	0.577	0.557	0.573	39.27	3.209
	6	0.469	0.469	0.471	0.470	47.87	3.422
12	1	0.720	0.721	0.716	0.719	31.29	3.193
	2	0.634	0.627	0.606	0.622	36.17	3.253
	3	0.811	0.802	0.790	0.801	33.28	3.777
	4	0.648	0.639	0.621	0.636	26.85	3.393
	5	0.678	0.667	0.682	0.676	28.09	3.364
	6	0.866	0.830	0.819	0.838	35.38	3.546
16	1	0.663	0.659	0.644	0.655	31.34	3.43
	2	0.716	0.696	0.684	0.699	41.44	3.07
	3	0.731	0.712	0.711	0.718	34.35	3.370
	4	0.570	0.580	0.590	0.580	32.19	3.487
	5	0.545	0.501	0.513	0.520	43.27	3.105
	6	0.675	0.665	0.638	0.659	34.14	3.201
	Average	0.686	0.674	0.666	0.675	34.593	3.365
	St.dv.	0.14	0.13	0.13	0.13	6.41	0.21

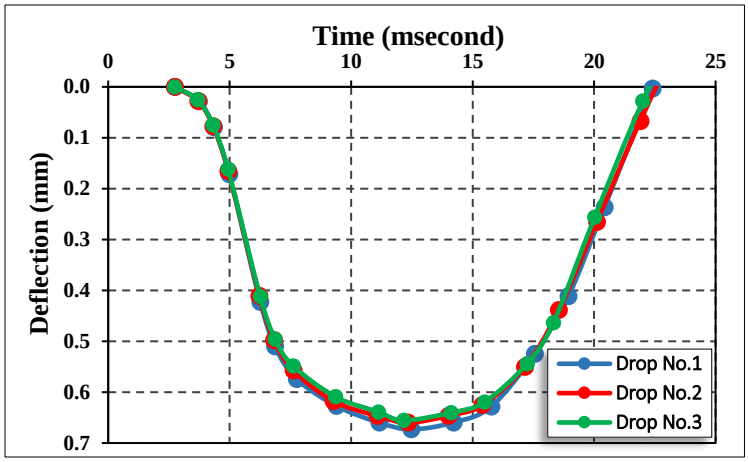

Figure (4.10): Average Time-Deflection Curve for A-1-b soil

For A-3 Subgrade soil from Al-Faris district, the results of the 18 LWD tests conducted in Table (4.6). The results showed that the vertical displacements ranged from 0.391 to 0.675 mm, with an average deflection of 0.553 mm, Figure (4.11) showed the average data of time-deformation curve. The values of dynamic modulus varied from 33.33 to 57.54 MPa with average equal to 47.7 MPa. The average value of degree of compatibility of subgrade soil was 3.075 ms.

All time – deformation curves are listed in Appendix (A-2)

Table (4.6): Summary of LWD Results for (A-3) Subgrade Soils at (Al-Faris)

No of Passes	points	Surface deflection (mm)				Ed (MPa)	Dc (ms)
		δ_1	δ_2	δ_3	Mean		
8	1	0.645	0.646	0.649	0.647	34.78	3.358
	2	0.698	0.670	0.658	0.675	33.33	3.577
	3	0.619	0.624	0.616	0.620	36.76	3.481
	4	0.678	0.667	0.646	0.664	33.89	3.286
	5	0.656	0.634	0.621	0.637	35.32	3.253
	6	0.648	0.632	0.609	0.630	35.71	3.193
12	1	0.457	0.451	0.451	0.453	49.67	2.772
	2	0.405	0.385	0.384	0.391	57.54	2.887
	3	0.423	0.423	0.413	0.420	53.57	2.801
	4	0.511	0.532	0.500	0.514	43.77	2.868
	5	0.624	0.595	0.594	0.604	37.25	2.962
	6	0.486	0.471	0.474	0.477	47.17	2.829
16	1	0.522	0.518	0.499	0.513	42.45	3.094
	2	0.582	0.570	0.56	0.571	41.13	2.995
	3	0.517	0.531	0.543	0.530	44.38	3.107
	4	0.561	0.549	0.530	0.547	39.40	2.919
	5	0.501	0.500	0.504	0.502	44.82	3.069
	6	0.582	0.558	0.561	0.567	39.68	2.894
Average		0.562	0.553	0.545	0.553	41.701	3.075
St.dv.		0.09	0.08	0.08	0.08	6.93	0.24

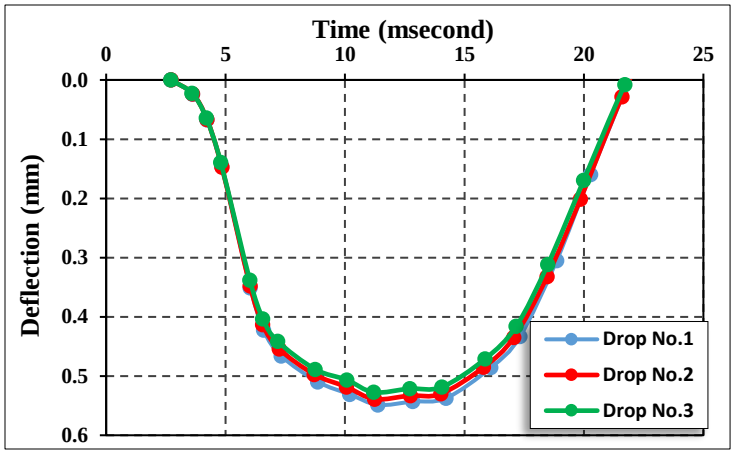

Figure (4.11): Average Time-Deflection Curve for A-3 Soil

For A-7-6 Subgrade soil from Al-Rofae district, the results of the 18 LWD tests conducted on different compacted subgrade surfaces are given in Table (4.7). These results were calculated by averaging the values resulted from three consecutive drops. The results exhibited that the vertical displacements ranged from 1.401 to 2.020 mm, with an average deflection of 1.671 mm, Figure (4.12) showed the average data of time-deformation curve. The values of dynamic modulus varied from 11.14 to 16.11 MPa with an average equal to 13.54 MPa. The average value of degree of compatibility was 4.74 ms.

All time – deformation curves are listed in Appendix (A-3)

Table (4.7): Summary of LWD Results for (A-7-6) Subgrade Soils at (Al-Rofae)

No. of Passes	points	Surface deflection (mm)				Ed (MPa)	Dc (ms)
		δ_1	δ_2	δ_3	Mean		
8	1	1.864	1.844	1.834	1.847	12.18	4.931
	2	1.861	1.871	1.862	1.865	12.06	4.898
	3	1.809	1.752	1.727	1.763	12.76	4.747
	4	2.039	2.001	2.020	2.020	11.14	5.096
	5	1.955	1.932	1.937	1.941	11.59	5.041
	6	1.965	1.958	1.938	1.954	11.51	5.122
12	1	1.502	1.513	1.517	1.511	14.89	4.55
	2	1.711	1.696	1.676	1.694	13.28	4.341
	3	1.59	1.552	1.563	1.568	14.35	4.335
	4	1.705	1.678	1.675	1.686	13.35	4.85
	5	1.681	1.673	1.686	1.680	13.39	5.199
	6	1.665	1.657	1.642	1.655	13.6	5.162
16	1	1.457	1.447	1.454	1.453	13.51	4.318
	2	1.526	1.487	1.478	1.497	13.59	4.794
	3	1.500	1.644	1.555	1.566	15.49	4.410
	4	1.571	1.546	1.550	1.556	15.03	4.645
	5	1.425	1.378	1.399	1.401	16.11	4.484
	6	1.432	1.411	1.427	1.423	15.81	4.385
Average		1.681	1.669	1.663	1.671	13.54	4.74
St.dv		0.20	0.19	0.19	0.19	1.51	0.31

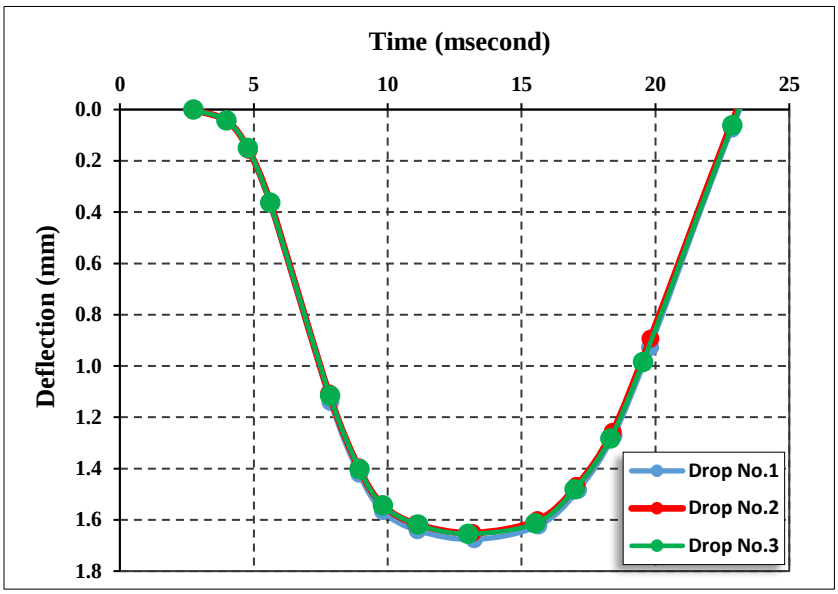

Figure (4.12): Average Time-Deflection Curve for A-7-6 Soil

In general, the following Figures (4.13) to (4.21) below explain that the subgrade reaction modulus increase with increasing the dynamic modulus, and decrease with increasing the degree of compatibility and surface deflection.

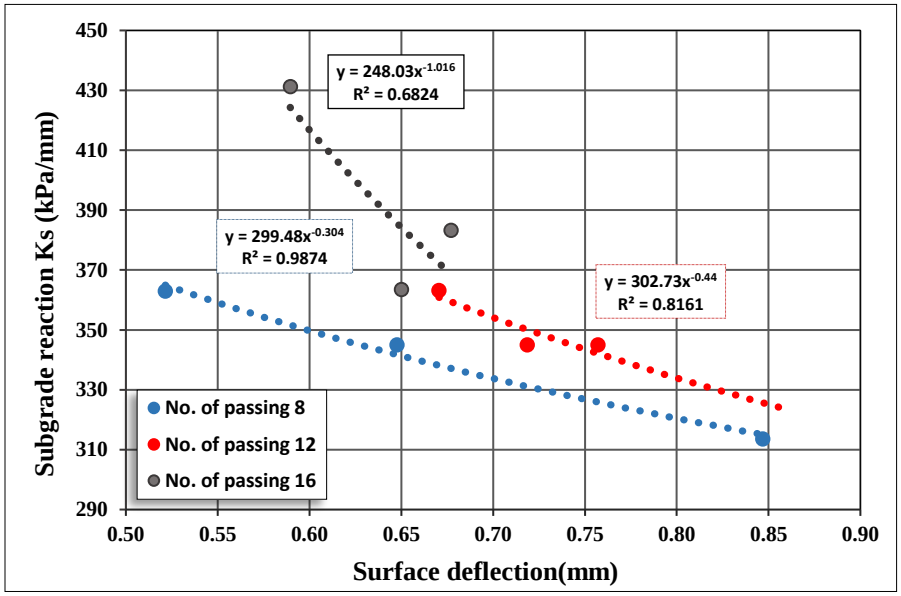

Figure (4.13): Subgrade reaction. Vs. LWD Surface deflection for A-1-b soil

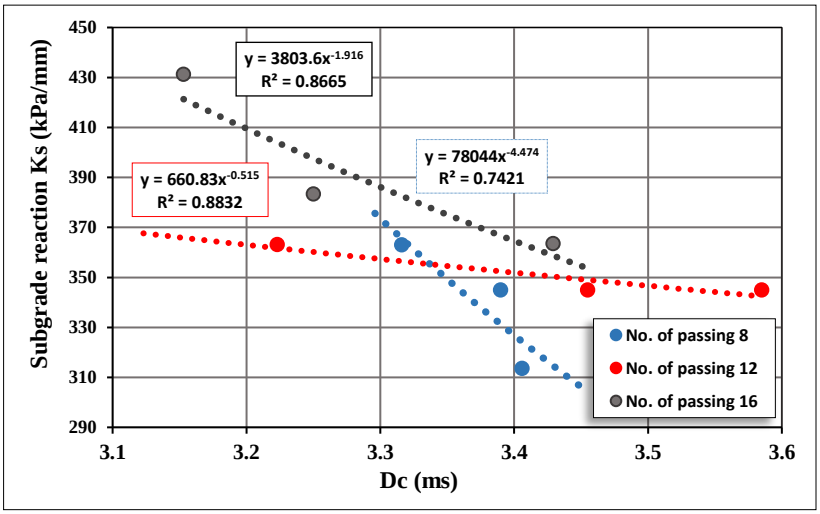

Figure (4.14): Subgrade reaction. vs. LWD degree of compatibility for A-1-b soil

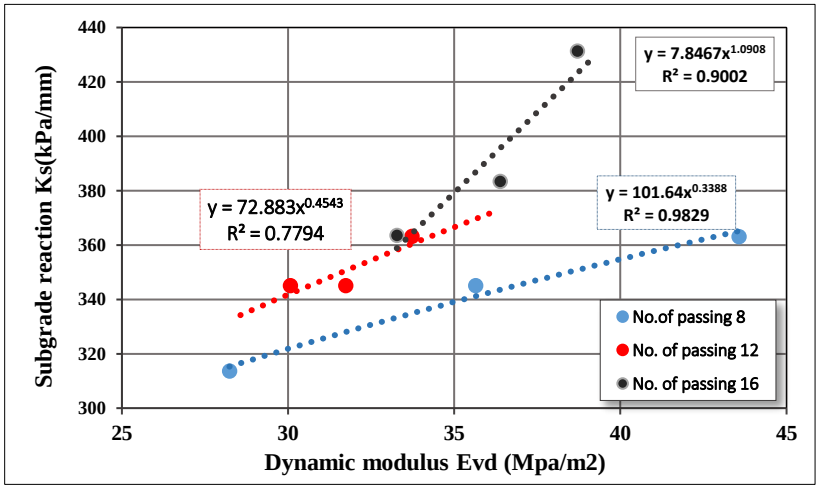

Figure (4.15): Subgrade reaction. vs. LWD dynamic modulus for A-1-b soil

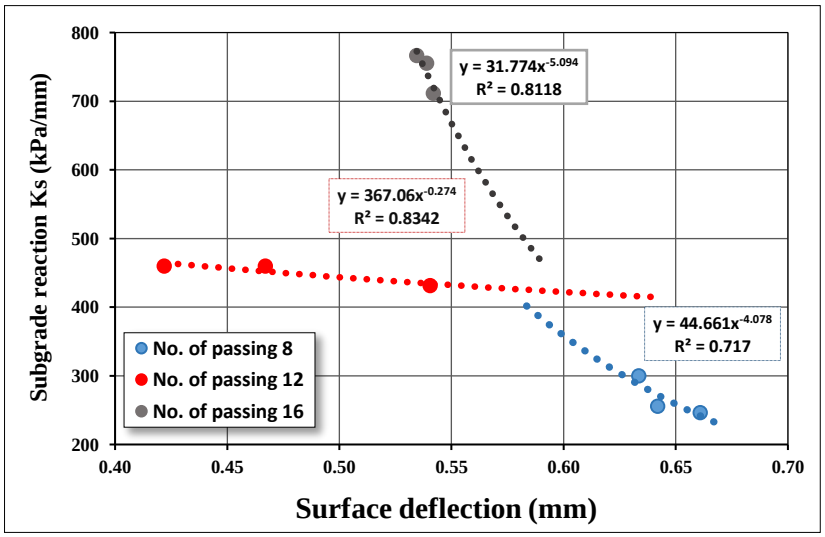

Figure (4.16): Subgrade reaction. vs. LWD Surface deflection for A-3 soil

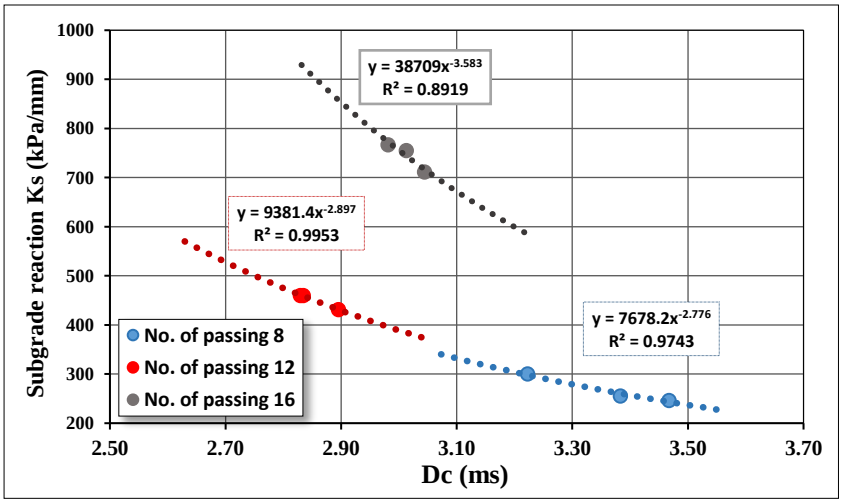

Figure (4.17): Subgrade reaction. vs. LWD degree of compatibility for A-3 soil

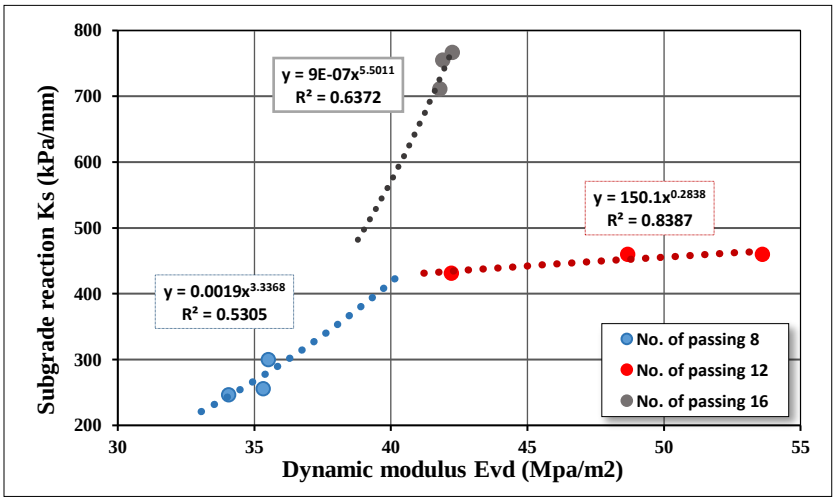

Figure (4.18): Subgrade reaction. vs. LWD dynamic modulus for A-3 soil

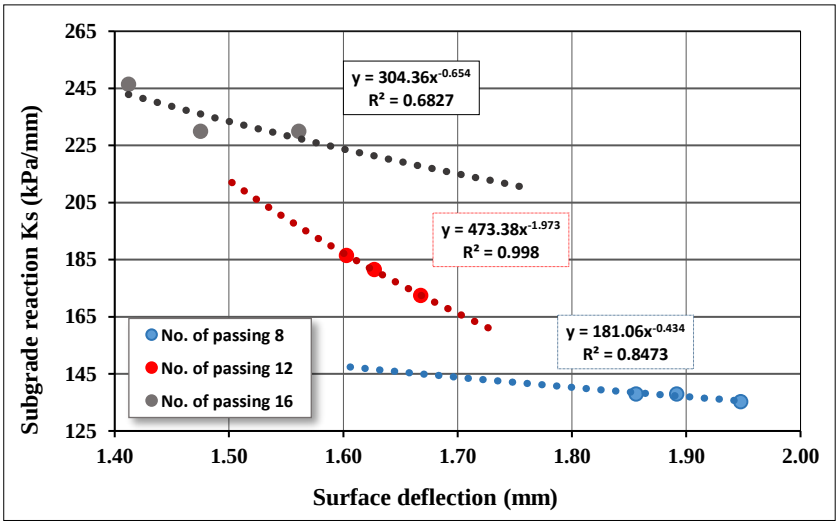

Figure (4.19): Subgrade reaction. vs. LWD Surface deflection for A-7-6 soil

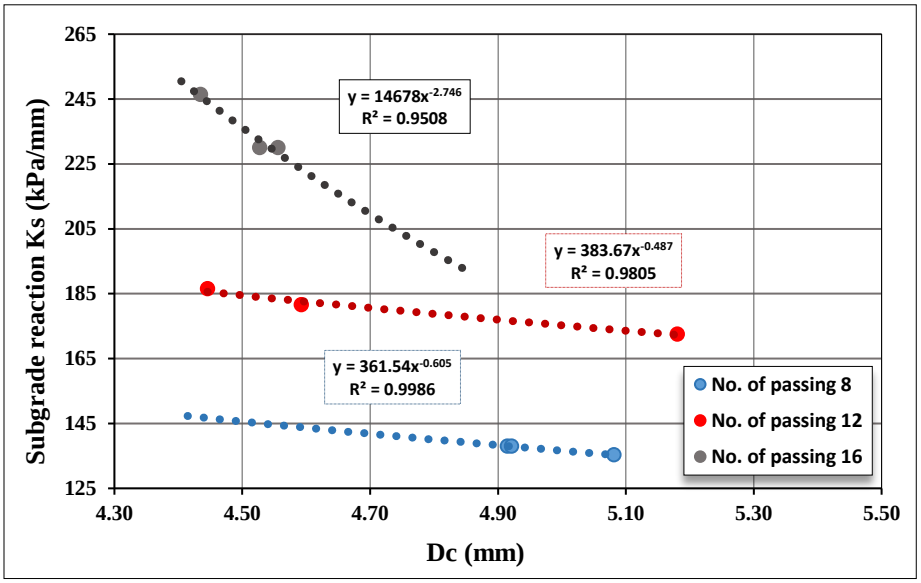

Figure (4.20): Subgrade reaction. vs. LWD degree of compatibility for A-7-6 soil

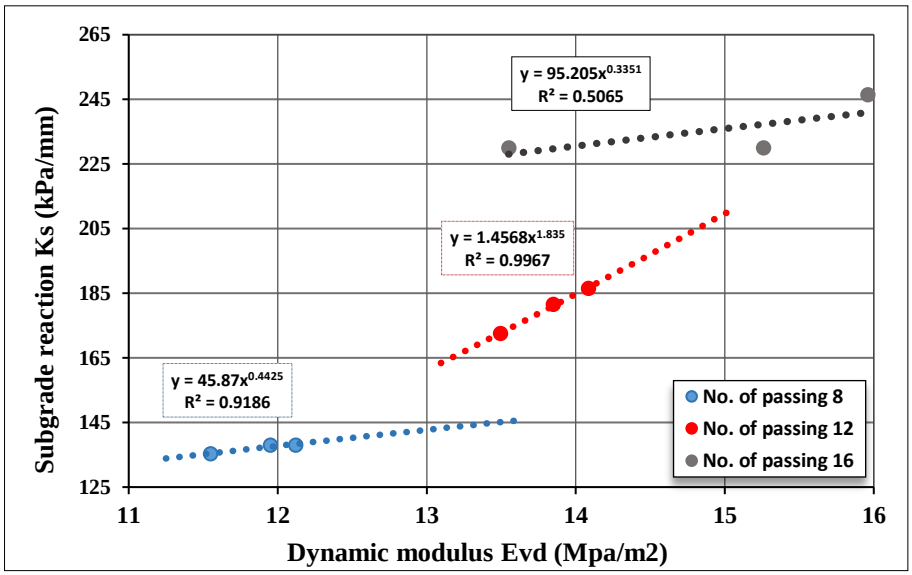

Figure (4.21): Subgrade reaction. vs. LWD dynamic modulus for A-7-6 soil

4.4 : Summary

This chapter included the testing results for characterizing the subgrade soils using three different soils. The results divided into three phases;

1. Results obtained from static plate load test, these results include the surface deflection, elastic modulus, and the modulus of subgrade reaction before and after correction the load – deformation curve,

2. Results obtained from light weight deflectometer (LWD) test. Three dynamic measurements were obtained from (LWD) test includes; dynamic modulus, surface deflection, and degree of compatibility.
3. Results obtained from field densities tests, Sand-Cone test and Core- cutter test. From these test identified the degree of compaction of soil preparation and both dry and wet unit weight.

From the results, the degree of compaction of subgrade soil increase with increasing the number of passes of compaction devises, and this lead to increase the characteristics of subgrade soils under each static and dynamic tests.

Chapter Five

Statistical Analysis and Modeling

5.1: Introduction:

The experimental research program was conducted with two testing devices, the plate load test (PLT) and the light weight deflectometer (LWD), to evaluate the characteristics of subgrade soils. The testing measurements obtained from these two devices were compared and analyzed statistically using regression analysis to examine feasible relationships between PLT and LWD data. The analysis results have been divided into two sections:

- Granular subgrades collected from Al-Melaad and Al-Faris district.
- Clay subgrades collected from Al-Rofae soil.

5.2: Statistical Analysis:

Statistical analysis is used to develop a mathematical model between dependent and independent variables, and to describe how these variables related with each other. In this study regression analysis was carried out to find out the most valid statistical models that determines the subgrade reaction (Ks). A statistical software called SPSS [Statistical Package for Social Sciences] was utilized to perform an extensive regression analysis in the least square errors, and analyze the relationships among the results obtained from PLT tests with those determined from the LWD tests.

5.3: Regression analysis:

Regression analysis is an important and powerful method That provides the following things:

- Description the relationships among the dependent and independent variables statistically.
- Testing the hypotheses about the relationships between variables.

The best-known types of regression analysis are the following:

1. Linear Regression Analysis

Linear regression is the first and most common type of regression analysis that extensively utilized in practical application, it is classified as:

- Simple linear regression: presents the linear relationships between a dependent variable and one independent variable and it is given as in the form below:

$$Y = a + b.X + e \qquad (5.1)$$

Where:

Y : dependent variable.
X : independent variable.
a : Constant. Represent y-intercept
b : the slope of the regression line
e : is the error term; the error in predicting the value of Y

- Multiple linear regression: is a technique that allows additional factors to enter the analysis separately, it is used to predict the value of a dependent variable based on the value of two or more other variables.

$$Y = a_0 + a_1.X_1 + a_2.X_2 + \cdots + a_nX_n \qquad (5.2)$$

Where:

Y : dependent variable.
X_1, and X_2 : independent variables.
a_0 : Constant. Represent y-intercept
a_1, a_2... a_n : slope of the regression lines

2. Nonlinear regression analysis

Nonlinear regression is a form of regression analysis in which dependent or criterion variables are modeled as a non-linear function of the model parameters and depends on one or more independent variables. The relationships between the dependent and independent variables in this regression are modeled as non-linear (typically curve) as if every value of Y was a random variable. The goal of the model is to make the sum of the squares as small as possible. There are several models of this regression; logarithmic,

trigonometric functions, exponential functions, and other fitting methods. **(Archontoulis and Miguez,2013).**

5.4 : Correlation between variables.

Correlation is a statistical method that shows the relation between two variables or the degree of the strong relation, when variables move in the same direction it's called positive correlation, otherwise the negative correlation occurs. The coefficient of correlation ranges between -1 to 1. The degree of correlation is classified into five points based on the value of the coefficient: **(Montgomery et al, 2011).**

- High degree of correlation, when the value of coefficient is above 0.75.
- Moderate degree of correlation, when the coefficient ranges between 0.50 to 0.75.
- Low degree of correlation occurs when the value of coefficient ranges from 0.25 to 0.5
- Absence of correlation when the value is less than 0.25.

5.5 : Some Definitions about Accuracy of Regression Models:

The accuracy of statistical models was evaluated based on some statistical parameters;

- **Coefficient of Determination (R^2):** which is defined as the number representing the variance ratio in the dependent variable that can be predicted from the independent variable and has a value from 0 to 1. When the value is equal to one, this means a perfect correlation because all points lie on the suggested least square line. It can be expressed mathematically as below:

$$R^2 = 1 - \frac{\sum_{i=1}^{n}\left(Y_i - \hat{Y}_i\right)^2}{\sum_{i=1}^{n}\left(Y_i - \hat{Y}_i\right)^2 + \sum_{i=1}^{n}(Y_i - \bar{Y}_i)^2} \qquad (5.3)$$

- **Root Mean Square Error (RMSE):** it is a measure of the difference between the predicted values from the regression model and the values actually measured that is being modelled:

$$\text{RMSE} = \sqrt{\frac{\sum_{i=1}^{n}\left(Y_i - \hat{Y}_I\right)^2}{n}} \qquad (5.4)$$

- **Mean Absolute Error (MAE):** Measures the average size of errors in a range of predictions, without considering their direction. It is the mean on the test sample of absolute differences between the prediction and the actual observation.

Where:

$$MAE = \frac{\sum_{i=1}^{n}|Y_i - \hat{Y}_i|}{n} \quad (5.5)$$

$\boldsymbol{Y_i}$**:** Observation value.
$\hat{Y}_i$**:** Predicted value.
$\overline{\boldsymbol{Y}}_{\boldsymbol{i}}$**:** Mean of observed values
$\boldsymbol{n}$**:** Number of samples.

- **Residual** (e): is the measure of vertical distance between the data points and the line of equality to describe the adequacy of the model.

  Residual = Observed value - Predicted value

- **Analysis of Variance (ANOVA)** is a statistical technique used to test difference between two or more means, for significance of regression ANOVA test the following **(Montgomery, 2011).**

  1. Regression sum of squares (SS_R).
  2. Error or residual sum of squares (SS_E).
  3. Total of Sum squares (SS_T).
  4. Mean Square of regression (MS_R).
  5. Mean square of residual or error (MS_E).

5.6 : Results and Discussion of statistical Analysis

The statistical analysis results have been spilt into two sections; [1] Results of granular soils, [2] Results of clay soil.

1. For granular subgrade soils

The testing results data obtained from the experimental work were divided randomly into 12 results to generate the model and the other 6 is used to validate the model. The first step to model preparations is the correlation between the variables by using SPSS Pearson's analyzed statistically. A correlation analysis was carried out and summarized in Table (5.1).

Table (5-1): Correlation between variables for granular subgrade soils

		Ks	Ed	δd	ɣdry	Dc	Wc
Ks	Pearson Correlation	1	0.604*	-0.529*	0.815**	-0.602**	-0.561*
	Sig. (2-tailed)	---	0.033	0.024	0.000	0.008	0.054
Ed	Pearson Correlation	0.604*	1	-0.950**	0.459*	-0.783**	-0.561
	Sig. (2-tailed)	0.033	---	0.000	0.016	0.000	0.054
δd	Pearson Correlation	-0.529*	-0.950**	1	-0.527**	0.678**	0.644**
	Sig. (2-tailed)	0.024	0.000	---	0.054	0.002	0.004
ɣdry	Pearson Correlation	0.815**	0.459*	-0.527**	1	-0.675**	-0.765**
	Sig. (2-tailed)	0.000	0.016	0.054	---	0.002	0.000
Dc	Pearson Correlation	-0.602**	-0.783**	0.678**	-0.675**	1	0.679**
	Sig. (2-tailed)	0.008	0.000	0.002	0.002	---	0.002
Wc	Pearson Correlation	-0.561	-0.461*	0.644**	-0.765**	0.679**	1
	Sig. (2-tailed)	0.054	0.054	0.004	0.000	0.002	---

Note: *. Correlation is significant at the 0.05 level (2-tailed).

**. Correlation is significant at the 0.01 level (2-tailed).

This table shows:

1. The correlation between the dependent variable (Ks) and some independent variables like LWD surface deflection (δd), degree of compatibility (Dc), and water content is negative moderate correlation, which indicates that any decrease in these values leads to increase Ks, and vice versa. Also, this degree of correlation can develop an acceptable theoretical model between Ks and any one of these variables.
2. The LWD measurements (i.e., Ed, δd, and Dc) have high to moderate correlation with each other. It was noted that there is a negative high correlation between Ed and (δd, and Dc). Whereas the correlation between (δd) and (Dc) is positive moderate correlation, which means the surface deflection increases with increasing degree of compatibility.
3. The dry unit weight has the most significant correlation to Ks, it has a high positive correlation with Ks. While with water content the dry density has negative high correlation.
4. The correlations between the dry density and LWD measurements ranged from moderate to low. Moderate positive correlation with E_d, negative correlation with D_c, and low negative correlation with surface deflection (δ_d).

Based on the results of correlations and the independent variables developing three set of regression models were developed as clarified below

1.1 : Regression models based on LWD testing data:

In this phase, the non-linear regression analyses were conducted to develop three theoretical models that can be used to predict the modulus of subgrade reaction (Ks) as a function of LWD measurements including: Ed, δd, and Dc. Table (5.2) summarizes the statistical predictors of these non-linear correlation models and associated R^2, and MSE values.

For first model, a non-linear regression model was developed to predict the subgrade reaction modulus as a function of LWD dynamic modulus. The results of ANOVA test are listed in Table (5.3), it explains that the mean square error (MSE) is low and equal 3453 kPa/mm (3.45 MPa/mm) and sum of residual is lower than the sum of regression, which sustained the significance of the model. While, from the same table, the high value of the R^2 (0.92) indicates a perfect prediction. Thus from these values a conclusion can be drawn that the developed model for K-Ed is good. Figure (5-1) shows the adequacy of the model and this figure indicates that an acceptable scatter can recognized between predicted and measured Ks. From the same figure it can recognized that all values are within the significant level boundaries. Figure (5.2) shows the scatter of residual points around the mean zero. In this Figure the residuals are plotted against the independent variable (Ed) to determine if the regression model provides an adequate fit to the data or if any underlying assumptions are violated. From the same figure, the two largest residuals do not fall extremely close to a straight line. By calculating the two largest standardized residuals [$d = e/\sqrt{\sigma^2}$ were (-2.01, 1.6)]and these are not far outside the nominal standardized residuals that range between (-2, 2).

For the second model, a non-linear regression model was developed to predict the subgrade reaction modulus as a function of LWD surface deflection. The results of ANOVA test are listed in Table (5.4), which explains that the mean square error (MSE) is low and equal 9013.439 kPa/mm (9.013MPa/mm) and the sum of residuals is lower than the sum of regression, which sustained the significance of the model. While, from the same table, the high value of the R^2 (0.83) indicates a good prediction. Thus, from these values

a conclusion can be drawn that the developed model for K- δd is good. Figure (5-3) shows the adequacy of the model and this figure indicates that an acceptable scatter can be recognized between predicted and measured Ks. From the figure it can be recognized that all values with in the significant level boundaries. Figure (5.4) shows the scatter of residual points around the mean zero. In this Figure the residuals are plotted against the independent variable (δd). From the same figure, the two largest residuals do not fall extremely close to a straight line. By calculating the two largest standardized residuals [$d = e/\sqrt{\sigma^2}$ were (-2.1, 0.9)]and these are not far outside the nominal standardized residuals that range between (-2, 2).

Table (5.2): Summary of statistical models based on LWD data for granular subgrade soils

Predictor	**Model**	**R^2**	**MSE MPa/mm**
E_d (MPa)	$Ks = 9.32E_d + \frac{-46.89}{(E_d - 42.39)} + \frac{-23.38}{(E_d - 41.81)}$	0.92	3.45
δd (mm)	$Ks = 365.714 + \frac{-0.032}{1.06\delta d - 0.57} + \frac{-0.427}{0.55 - 1.03\delta d}$	0.832	9.013
Dc (ms)	$Ks = 1494.4 + \frac{-824.75}{3772.4 + 414.5\,(Dc)^2 - 2501.9\,Dc} - 337.62Dc$	0.93	4.875

- **Note:** Ks in (kPa/mm)

Table (5.3): ANOVA[a] test of Ks –Ed model for granular subgrade soils

Source	**Sum of Squares**	**df**	**Mean Squares**
Regression	2280973.785	5	456194.757
Residual	24172.764	7	3453.252
Uncorrected Total	2305146.550	12	/
Corrected Total	337624.073	11	/

Note: Dependent variable: Ks

a. R squared = 1 - (Residual Sum of Squares) / (Corrected Sum of Squares) = 0.92

Table (5.4): ANOVA[a] test of Ks – δd model for granular subgrade soils

Source	Sum of Squares	df	Mean Squares
Regression	2495706.187	7	356529.455
Residual	45067.194	5	9013.439
Uncorrected Total	2540773.381	12	/
Corrected Total	268663.762	11	/

Note: Dependent variable: Ks

a. R squared = 1 - (Residual Sum of Squares) / (Corrected Sum of Squares) = 0.832

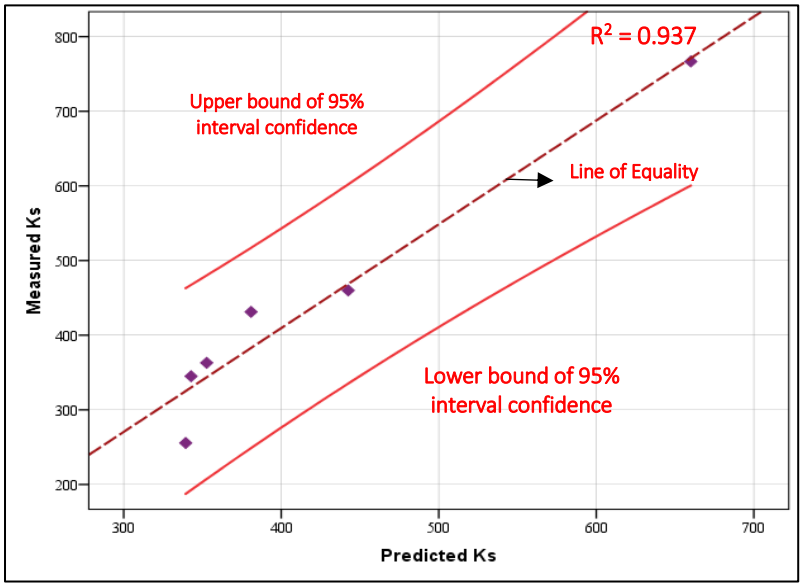

Figure (5.1): Predicted vs. measured modulus – LWD dynamic modulus model for granular subgrade soils.

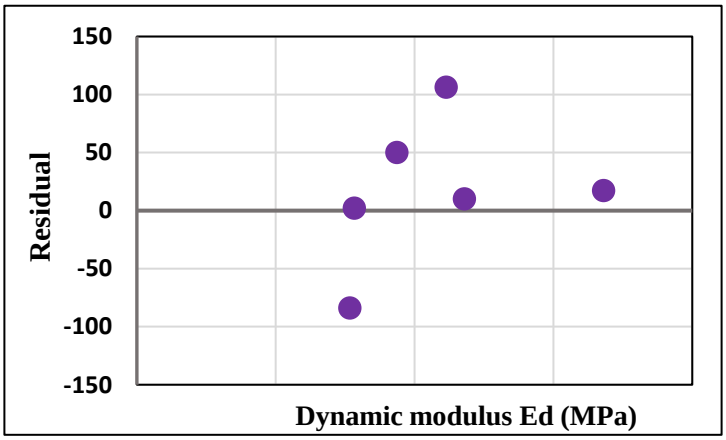

Figure (5.2): residuals vs. dynamic modulus – LWD dynamic modulus model for granular subgrade.

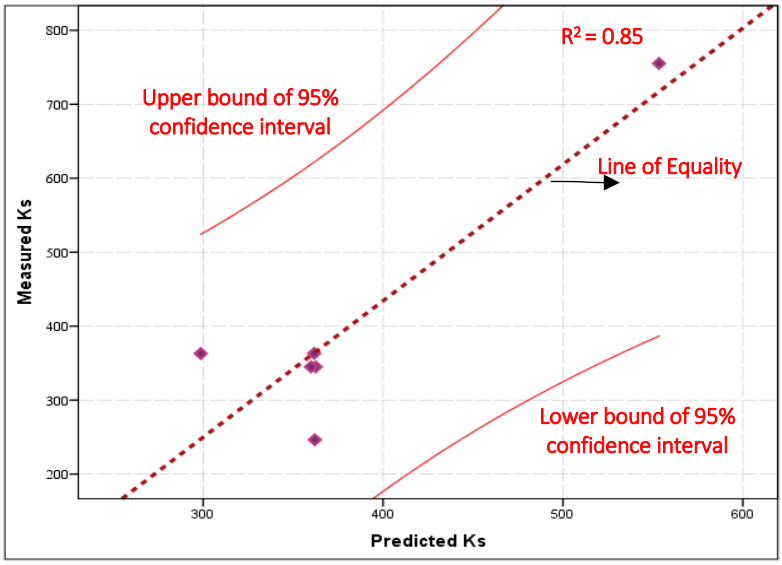

Figure (5.3): Predicted vs. measured modulus – Surface deflection model for granular subgrade.

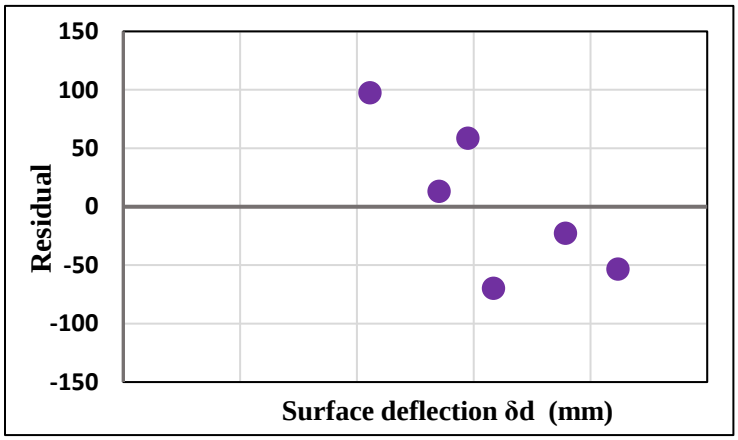

Figure (5.4): residuals vs. surface deflection – LWD surface deflection model for granular subgrade soils.

For the third model, a non-linear regression model with high value of R^2 equal to 0.93 was developed to predict the subgrade reaction modulus as a function of LWD degree of compatibility. The results of ANOVA test are summarized in Table (5.5), it explains that the mean square error (MSE) is low and equal 4857.733kPa/mm (4.857 MPa/mm) and the sum of residual is lower than the sum of regression, which is good for the significance of the model. Figure (5.5) explains the adequacy of the model and the acceptability of scattered between the predicted and measured Ks. From the figure, it can be recognized that all values within the significant level boundaries. Figure (5.6) shows the scatter of residual points around the mean zero. In this Figure the residuals are plotted against the

independent variable (Dc) to check the normality assumption. By calculating the two largest standardized residuals [$d = e/\sqrt{\sigma^2}$ were (-0.46, 0.75)]and these are not far outside the nominal standardized residuals that range between (-2, 2).

Table (5.5): ANOVA[a] test of Ks – Dc model for granular subgrade soils

Source	Sum of Squares	df	Mean Squares
Regression	2631624.887	6	438604.148
Residual	24288.665	5	4857.733
Uncorrected Total	2655913.552	11	/
Corrected Total	389463.757	10	/

Note: Dependent variable: Ks

a. R squared = 1 - (Residual Sum of Squares) / (Corrected Sum of Squares) = 0.93

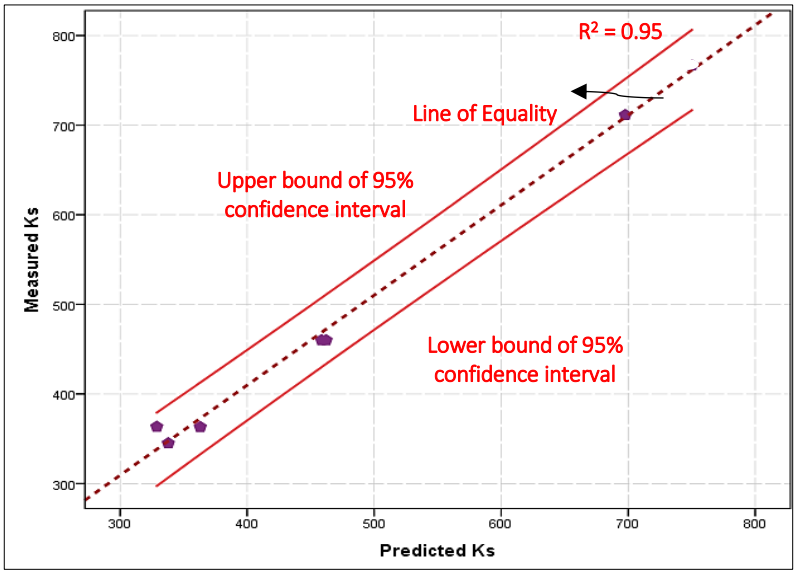

Figure (5.5): Predicted vs. measured modulus – degree of compatibility model for granular subgrade soils.

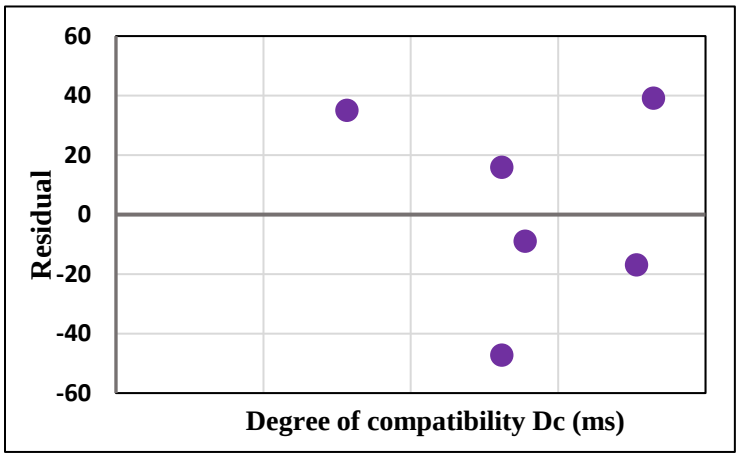

Figure (5.6): residuals vs. degree of compatibility – LWD degree of compatibility model for granular subgrade soils.

1.2 : Regression models based on basic soil properties.

In the second phase, basic soil properties were used to develop a cubic regression model with R^2 equals to 0.9 to predict the modulus of subgrade reaction Ks as a function of dry density. This model is summarized in Table (5.6), and the results of ANOVA test are illustrated in Table (5.7). It explains that the mean square error 3262kPa/mm (3.262 MPa/mm) and the sum of residue are low in compare with the sum of regression which is good for the significance of the model. Figure (5.7) explains the adequacy of the model and the acceptability of scattered between the predicted and measured Ks. From the figure it can be recognized that all values are within the significant level boundaries. Figure (5.8) shows the scatter of residual points around the mean zero. In this Figure the residuals are plotted against the independent variable (γ_{dry}) to check the normality assumption. By calculating the two largest standardized residual [$d = e/\sqrt{\sigma^2}$ were (-0.66, 0.42)]and these are not far outside the nominal standardized residual that range between (-2, 2).

Table (5.6): Summary of statistical model based sol properties for granular subgrade soils.

Predictor	Model	R^2	MSE MPa/mm
γ_{dry} (gm/cm^3)	Ks =5533.9 - 5086.8 $*$ $\gamma_{dry}{}^2$ + 1934.8 $*$ $\gamma_{dry}{}^3$	0.90	3.262

▪ **Note:** Ks in (kPa/mm)

Table (5.7): ANOVA[a] test of Ks-dry densities model for granular subgrade soils

Source	Sum of Squares	df	Mean Squares
Regression	2516617.884	3	838872.628
Residual	29358.797	9	3262.089
Uncorrected Total	2545976.681	12	/
Corrected Total	292747.347	11	/

Note: Dependent variable: Ks

a. R squared = 1 - (Residual Sum of Squares) / (Corrected Sum of Squares) = 0.90

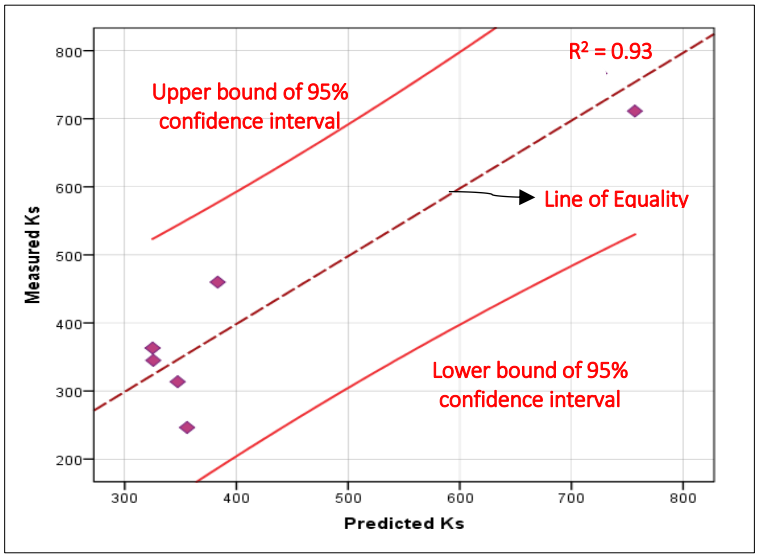

Figure (5.7): Predicted vs. measured modulus – dry density for granular subgrade.

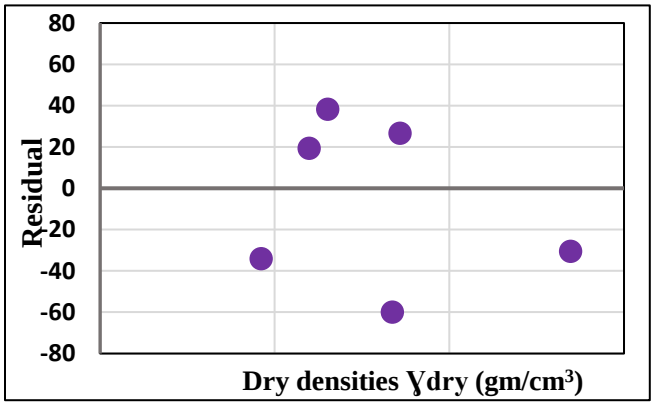

Figure (5.8): residuals vs. dry density – basic soil properties model for granular subgrade.

1.3 : Regression models based on a combination of LWD data and basic soil properties.

In the third phase, both basic soil properties and LWD measurements were used to develop a regression model to predict the modulus of subgrade reaction Ks.

A non-linear model with R^2 equals to 0.87 was developed to predict the modulus of subgrade reaction Ks as a function of the dynamic modulus (Ed) and dry density (γ_{dry}) as explained in Table (5.8). The results of ANOVA test are summarized in Table (5.9), it explains that the mean square error (MSE) is low and equal 2595.177 kPa/mm (2.595 MPa/mm) and sum of residual is lower than the sum of regression, which indicates a good prediction. Thus from these values, a conclusion can be drawn that the developed model for K- γ_{dry} and Ed is good. Figure (5.9) shows the adequacy of the model and this figure indicates that an acceptable scatter can be recognized between predicted and measured Ks.

From the same figure it can be recognized that all values are within the significant level boundaries. Figures (5.10), and (5.11) show the scatter of residual points around the mean zero. In these Figures the residuals are plotted against the independent variables (Ed) and (γ_{dry}) respectively to check the normality assumption. From these figures the two largest residual do not fall extremely close to a straight line. By calculating the two largest standardized residual [$d = e/\sqrt{\sigma^2}$ were (-0.58, 0.48)]and these are not far outside the nominal standardized residual that range between (-2, 2).

Table (5.8): Summary of statistical model based (soil properties + LWD measurements) for granular subgrade soils.

Predictor	Model	R^2	MSE MPa/mm
γ_{dry} (gm/cm^3) Ed (MPa)	Ks =$18616 + 7.53E_d + 5841.4(\gamma_{dry})^2 - 20833\gamma_{dry}$	0.87	2.595

▪ **Note:** Ks in (kPa/mm)

Table (5.9): ANOVA[a] test of Ks- Ed + γ_{dry} model for granular subgrade soils

Source	Sum of Squares	df	Mean Squares
Regression	2042212.732	4	510553.183
Residual	20761.420	8	2595.177
Uncorrected Total	2062974.151	12	/
Corrected Total	161186.755	11	/

Note: Dependent variable: Ks

a. R squared = 1 - (Residual Sum of Squares) / (Corrected Sum of Squares) = 0.87

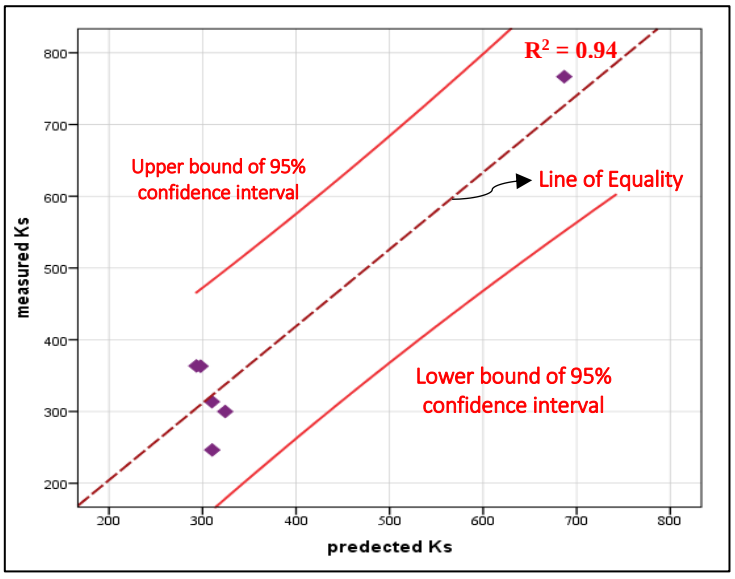

Figure (5.9): Predicted vs. measured modulus – (γ_{dry} and Ed) for granular subgrade.

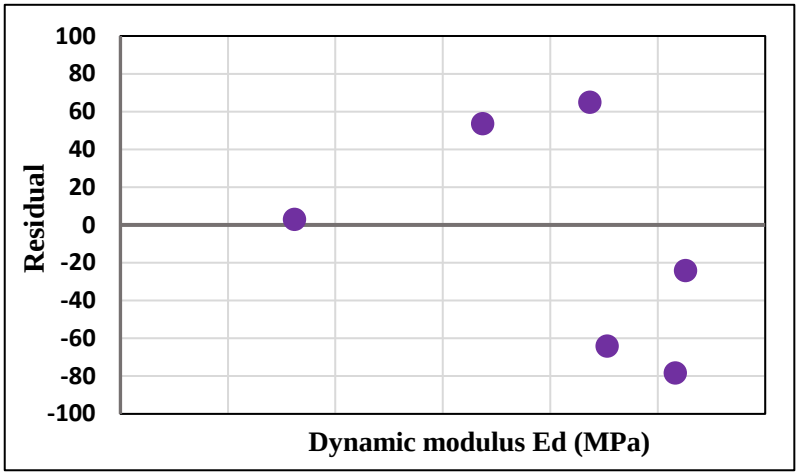

Figure (5.10): residuals vs. dynamic modulus – (γ_{dry} and Ed) for granular subgrade.

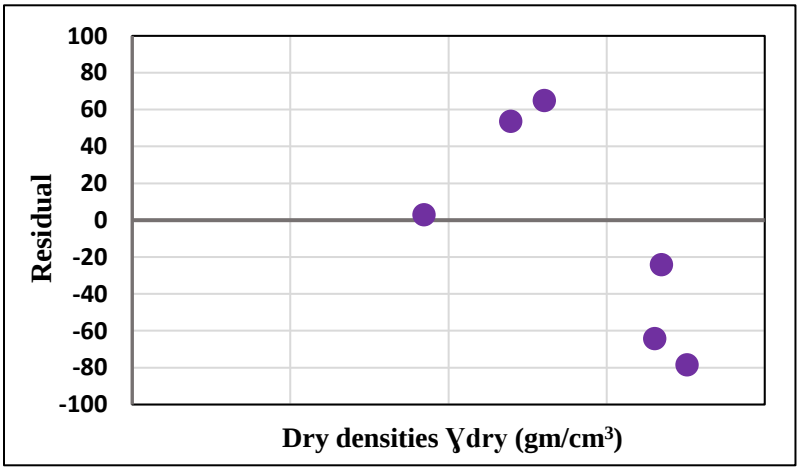

Figure (5.11): residuals vs. dry density - (γ_{dry} and Ed) for granular subgrade.

2. For clayey subgrade soils data

The results data obtained from the experimental work was analyzed statistically into two phases based on the personal correlations analysis and independent variables that used in developing simple regression models that will be improved in the future studies. A personal correlation analysis between dependent and independent variables were carried out and summarized in table (5.10).

This table shows:

1. The correlation between dependent variable (Ks) and some independent variables like LWD surface deflection (δd), degree of compatibility (Dc), and water content is negative high correlation, which means that any decrease in these value lead to increase Ks, and vice versa. Also this degree of correlations is good for acceptable model.

2. The LWD measurements (Ed, δd, and Dc) have high to moderate correlation between each other. The correlation between Ed and δd is high negative correlation. And the correlation between (δd) and (Dc) is positive high correlation, which means that the surface deflection increases with the increase of degree of compatibility. Whereas the correlation between Ed and Dc is negative moderate correlation. This degree of correlation between the independent variables is not suitable to collect these independent variables in one model with Ks.
3. The dry density has the most significant correlation to Ks, it has a high positive correlation with Ks. While with water content the dry density has negative high correlation.
4. The correlation between the dry density and LWD measurements is high, positive with Ed, and negative with Dc and surface deflection (δd).

Table (5.10): Correlation between variables for clayey subgrade soils

		Ks	Ed	δd	ɣdry	Dc	Wc
Ks	Pearson Correlation	1	0.910**	-0.961**	0.984**	-0.768*	-0.861**
	Sig. (2-tailed)	---	0.001	0.000	0.000	0.016	0.003
Ed	Pearson Correlation	0.910**	1	-0.907**	0.865**	-0.748*	-0.746*
	Sig. (2-tailed)	0.001	---	0.001	0.003	0.020	0.021
δd	Pearson Correlation	-0.961**	-0.907**	1	-0.906**	0.767*	0.835**
	Sig. (2-tailed)	0.000	0.001	---	0.001	0.016	0.005
ɣdry	Pearson Correlation	0.984**	0.865**	-0.906**	1	-0.763*	-0.820**
	Sig. (2-tailed)	0.000	0.003	0.001	---	0.017	0.007
Dc	Pearson Correlation	-0.768*	-0.748*	0.767*	-0.763*	1	0.529
	Sig. (2-tailed)	0.016	0.020	0.016	0.017	---	0.143
Wc	Pearson Correlation	-0.861**	-0.746*	0.835**	-0.820**	0.529	1
	Sig. (2-tailed)	0.003	0.021	0.005	0.007	0.143	---

Note: *. Correlation is significant at the 0.05 level (2-tailed).

**. Correlation is significant at the 0.01 level (2-tailed).

Based on the results of personal correlations and the independent variables, two sets of regression models were developed as clarified below.

2.1 : Regression models based on LWD testing data:

In this phase, regression analysis was conducted to develop three theoretical models that can be used to predict the modulus of subgrade reaction (Ks) as a function of LWD measured data Ed, δd, and Dc. Table (5.11) summarizes the statistical predictors of these models and associated R^2, and MSE values.

For the first model, a simple linear model was developed to predict the subgrade reaction modulus as a function of LWD dynamic modulus with good value of $R^2 = 0.83$. The results of ANOVA test are summarized in Table (5.12), which explains that the mean square error (MSE) is low and equal 366 kPa/mm (0.366 MPa/mm) and the sum of residual is lower than the sum of regression, which sustained the significance of the model. Table (5.13) explains the testing of residual for developing model, as shown in the table the mean of residual and standard residuals equal to zero, and that is an important condition for acceptable model.

For the second model, a simple linear model with value of R^2 equal to 0.92 was developed to predict the subgrade reaction modulus as a function of LWD surface deflection. Table (5.14) summarizes the ANOVA test, it explains that the mean square error (MSE) is low and equal 163 kPa/mm (0.163 MPa/mm) and the sum of residual is lower than the sum of regression, which sustained the significance of the model. Table (5.15) explains the testing of residual for developing model, as shown in table the mean of residuals and standard residuals equal to zero, and that is an important condition for acceptable model.

Table (5.11): Summary of statistical models based on LWD data for clayey subgrade soils

Predictor	Model	R^2	MSE MPa/mm
E_d (MPa)	$Ks = 26.36E_{vd} - 172.55$	0.83	0.366
δd (mm)	$Ks = 551.73 - 219.87\delta d$	0.92	0.163
Dc (ms)	$Ks = -116112.3 + (74405.1 * Dc) - (15815.6 * Dc^2) + (1116.9 * Dc^3)$	0.8	0.593

▪ **Note:** Ks in (kPa/mm)

For the third model, the subgrade reaction modulus was predicted as a function of LWD degree of compatibility with value of R^2 equal to 0.801. Table (5.16) summarizes the ANOVA test, it explains that the mean square error (MSE) is low and equal 593.28 kPa/mm (0.0.593 MPa/mm) and sum of residual is lower than the sum of regression, which sustained the significant of the model.

Table (5.12): ANOVA[a] test of Ks- LWD dynamic modulus for clayey soil

Model	Sum of Squares	df	Mean Square
Regression	12310.929	1	12310.929
Residual	2562.194	7	366.028
Total	14873.122	8	/

a. Dependent Variable: Ks
b. Predictors: (Constant), Ed

Table (5.13): Residuals statistics[a] of Ks- LWD dynamic modulus for clayey soil

	Minimum	Maximum	Mean	Std. Deviation	N
Predicted Value	131.890	248.130	184.255	39.228	9
Residual	-12.340	45.393	0.000	17.896	9
Std. Predicted Value	-1.335	1.628	0.000	1.000	9
Std. Residual	-0.645	2.373	0.000	0.935	9

a. Dependent Variable: Ks

Table (5.14): ANOVA[a] test of Ks- LWD surface deflection for clayey subgrade soil

Model	Sum of Squares	df	Mean Square
Regression	13727.374	1	13727.374
Residual	1145.748	7	163.678
Total	14873.122	8	/

a. Dependent Variable: Ks
b. Predictors: (Constant), δd

Table (5.15): Residuals Statistics[a] of Ks- LWD surface deflection for clayey soil

	Minimum	Maximum	Mean	Std. Deviation	N
Predicted Value	123.425	241.27	184.255	41.423	9
Residual	-12.779	21.485	0.000	11.967	9
Std. Predicted Value	-1.468	1.376	0.000	1.000	9
Std. Residual	-0.999	1.679	0.000	0.935	9

a. Dependent Variable: Ks

Table (5.16): ANOVA[a] test of Ks- LWD degree of compatibility for clayey subgrade soil

Model	Sum of Squares	df	Mean Square
Regression	317457.689	4	79364.422
Residual	2966.421	5	593.284
Uncorrected Total	320424.110	9	/
Corrected Total	14873.122	8	/

Dependent variable: Ks

a. R squared = 1 - (Residual Sum of Squares) / (Corrected Sum of Squares) = .801.

2.2 : Regression models based on basic soil properties.

In the second phase, basic soil properties were used to develop regression models to predict the modulus of subgrade reaction Ks as a function of dry density and water content. Table (5.17) summarizes the statistical predictors of these models and associated R^2, and MSE values.

For the first model, the subgrade reaction modulus was developed as function of dry density. A simple linear regression model with high value of R^2 equal to 0.96 was developed. Table (5.18) summarizes the ANOVA test, which explains the sum of residue is lower than the sum of regression which sustained the significance of the model. Also, in the same table the mean square error is 67.224kPa/mm (0.067 MPa/mm) which is acceptable value for the significance of the model. Table (5.19) explains the testing of residuals for developing model, as shown in the table, the mean of residual and standard residual is equal to zero, and that is an important condition for acceptable model.

Table (5.17): Summary of statistical model based soil properties for clayey subgrade

Predictor	Model	R^2	MSE MPa/mm
γ_{dry} (gm/cm^3)	Ks = 485.61γ_{dry} - 555.32	0.96	0.067
Wc	Ks = 409.014Wc - 9.387	0.742	0.548

▪ **Note:** Ks in (kPa/mm)

Table (5.18): ANOVA[a] test of Ks- dry density for clayey subgrade soil

Model	Sum of Squares	df	Mean Square
Regression	14402.553	1	14402.553
Residual	470.569	7	67.224
Total	14873.122	8	/

a. Dependent Variable: Ks

b. Predictors: (Constant), γ_{dry}

Table (5.19): Residuals Statistics[a] of Ks- dry density model for clayey subgrade soil

	Minimum	Maximum	Mean	Std. Deviation	N
Predicted Value	139.5798	243.9852	184.2556	42.43017	9
Residual	-9.34946	12.88385	0.000	7.66949	9
Std. Predicted Value	-1.053	1.408	0.000	1.000	9
Std. Residual	-1.140	1.571	0.000	.935	9

[a.] Dependent Variable: Ks

For the second model, the subgrade reaction modulus was predicted as function of water content. A simple linear regression model with acceptable value of R^2 equal to 0.742 was developed. Table (5.20) summarizes the ANOVA test, which explains that the sum of residue is lower than sum of regression which sustained the significance of the model. Also, in same table the mean square error is 548.800kPa/mm (0.548 MPa/mm) which is acceptable value for the significance of the model. Table (5.21) explains the testing of residual for developing model, as shown in the table the mean of residual and standard residual is equal to zero, and that is an important condition for acceptable model.

Table (5.20): ANOVA[a] test of Ks- water content for clayey subgrade soil

Model	Sum of Squares	df	Mean Square
Regression	11031.520	1	11031.520
Residual	3841.603	7	548.800
Total	14873.122	8	/

a. Dependent Variable: Ks

b. Predictors: (Constant), Wc

Table (5.21) : Residuals Statistics[a] of Ks- water content model for clayey subgrade soil

	Minimum	Maximum	Mean	Std. Deviation	N
Predicted Value	125.5367	226.9128	184.2556	37.13408	9
Residual	-33.41540	37.32191	.00000	21.91347	9
Std. Predicted Value	-1.581	1.149	.000	1.000	9
Std. Residual	-1.426	1.593	.000	.935	9

[a.] Dependent Variable: Ks

5.7 : Summary

To understand the significant of the different parameters in characterizing of dynamic properties, and basic soil properties. Or both of them of the subgrade reaction modulus its necessary to Conduct a statistical modeling. However, this chapter proved the ability to introduce an acceptable model to predict the subgrade reaction modulus from dynamic measurements obtained from (LWD) test, basic soil properties, and both of them.

Chapter Six

Finite Element Analysis

6.1: Introduction

The finite element method is one of the most powerful ways to solve differential equations, especially when these equations are applied to complex structures with complex boundary conditions. These complex structures can be either two or three-dimensional shapes which are sub-divided into a number of triangular or quadrilateral elements, as shown in Figure (6.1). Then, solve differential equations, over these elements.

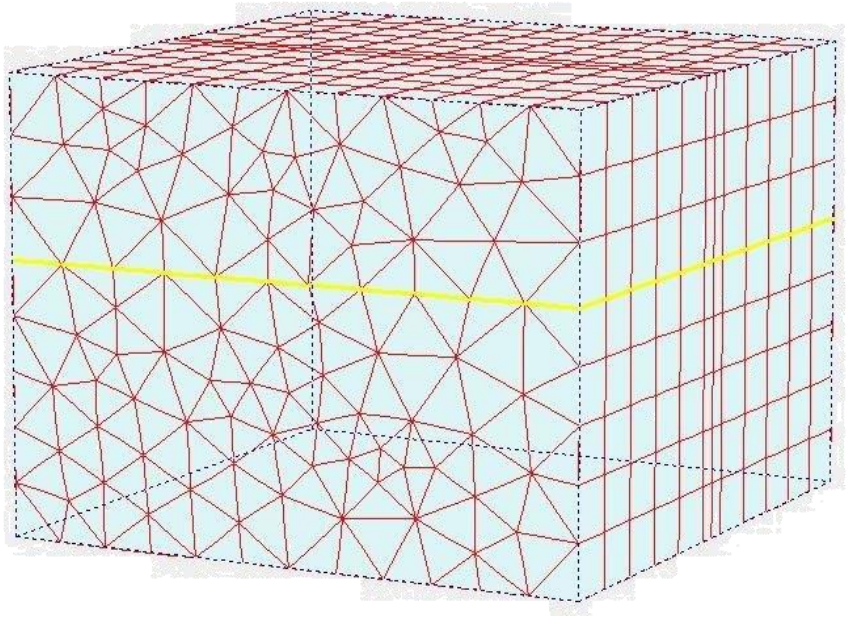

Figure (6.1): Three-dimensional shape subdivided into elements.

The basic idea in the method of specific elements is to find a solution to a complex problem by replacing it with a simpler one. Because replacing the actual problem with a simpler solution, an approximate solution will be found instead of the exact one. The finite element analysis has been widely used in the field of structural mechanics to solve different types of engineering problems, such as heat conduction, fluid dynamics, seepage flow, and electric and magnetic fields. **(Rao, 2011).**

In this chapter, 3D finite element program commercially known as (Plaxis– Plasticity Axi-Symmetry), was used to model subgrade layer. PLAXIS 3D is a special finite element software used to implement deformation, stability, and flow analysis for various types of geotechnical applications. Nowadays, this program is mostly used by geotechnical engineers to analyze the foundation of different structure, because it provides better understanding on the behavior of soil under various loading condition, static and dynamic. The main focus of using Plaxis 3D in this study was to create a 3D subgrade model to:

- Simulate LWD impulse load to find time-deflection.
- Simulate PLT static load to find load-deflection curve of subgrades.

A comprehensive description of the material's constitutive models, geometry and boundary conditions, mesh and element configurations, dynamic loading techniques, and static loading techniques are presented in detail in the following subsections:

6.2: Material Characteristics:

To simulate the behavior of a soil, Plaxis provides four models; linear elastic model, Mohr-coulomb model, hardening soil model, and Soft soil creep model to allow the user to select suitable mechanical behavior of the soil. In this study, the finite element calculation is divided in to two phases;

In the first phase, finite element modeling has been analyzed to examine vertical surface deflection under static load to develop load-deflection curve to obtain subgrade reaction modulus. Based on previous studies carried by **(Teodoru and Toma, 2009), (Palix et al, 2011), (Demir et al, 2013),** and **(Ahirwar, and Mandal, 2017),** the behavior of soil was simulated by Mohr-coulomb model, this linearly elastic- perfectly plastic model considered as a first approximation of soil behavior, this model involves five parameters as an input data namely;

- Young's modulus (E) is the basic elastic modulus. In this study, the modulus of elasticity varied from 21.17 to 84.67 MPa was used in this work
- Poison's ratio (ν), as recommended in **(PLAXIS 3D Reference Manual, 2013)** this parameter ranges between 0.3 and 0.4 which gives a realistic ratio K_0 less than 1, In this study, ν was assumed 0.3.

- Cohesion (c) in (kN/m^2) is determined from unconfined compression test for undisturbed clay specimen. In this study, the cohesion coefficient was obtained from the equation derived by **(Ersoy et al.,2013):**

$$C = 265\left(\frac{PI}{LL}\right)^{2.78} \quad (6.1)$$

Where:

PI: is the plasticity index.

LL: is the liquid limit.

- Friction angle (φ), is entered in degree, it is used to model the effective friction of soil by means of Mohr's stress circle, in this study this value obtained from direct shear test and it ranged from 5.58º for A-7-6 soil to 38º for A-1-b soil.
- Dilatancy angle (ψ) this value is much smaller than friction angle, for clayey soil this value is equal to zero, but for sands it depends on both the friction angle and density of the sand, the order of magnitude is; **(PLAXIS 3D Reference Manual, 2013)**

$$\psi = \varphi - 30 \quad (6.2)$$

In the second phase, the surface deflection under impulse LWD loading condition was calculated using linear elastic model to simulate the soil behavior. Based on the results obtained from **(Ameri et al, 2012), (Kalliainen et al,2016),** and **(Shaban,2016)** they found that using linear elastic properties for subgrade layer produces acceptable degree of accuracy, this model based on Hooke's law of isotropic linear elasticity, and involves two parameters, young's modulus E, and poisons ratio ν.

The 150 mm radius loading plate in both phases was modeled as explained by **(Demir et al, 2013).** It was assumed to be isotropic, and the basic geometry parameters of the loading plate include the thickness, d = 0.015 m, elastic modulus, E = 7.33 ×10^5 kPa, Poisson's ratio, ν= 0.10, and the unit weight of the plate material, γ= 0.02 kN/m^3.

6.3: Geometry and Boundary Conditions

A 3D finite element tool which typically requires much more computational time, but provides ideal results was utilized to model subgrade. A geometry model consists of

boreholes and horizontal work planes (x-y) planes. The work planes define geometry lines and structures, while the local soil layers, ground surface level, and pore water pressure were defined in the boreholes.

In this work, model was created with dimensions similar to those in the experimental work as shown in Figure (6.2), this large geometric model (1.5 m width × 2.4 m length × 0.65 m deep) would help to avoid undesirable reflection of the scattered wave source of the dynamic load, and the stress bulb due to the static load

To minimize the influence of the stress distribution, the boundary conditions were chosen. A fixed support was used in the edges and in the bottom base of the model to prevent any movement in the horizontal direction, while the surface of the model is free in all directions, these general fixities of the boundaries are automatically imposed by Plaxis 3D.

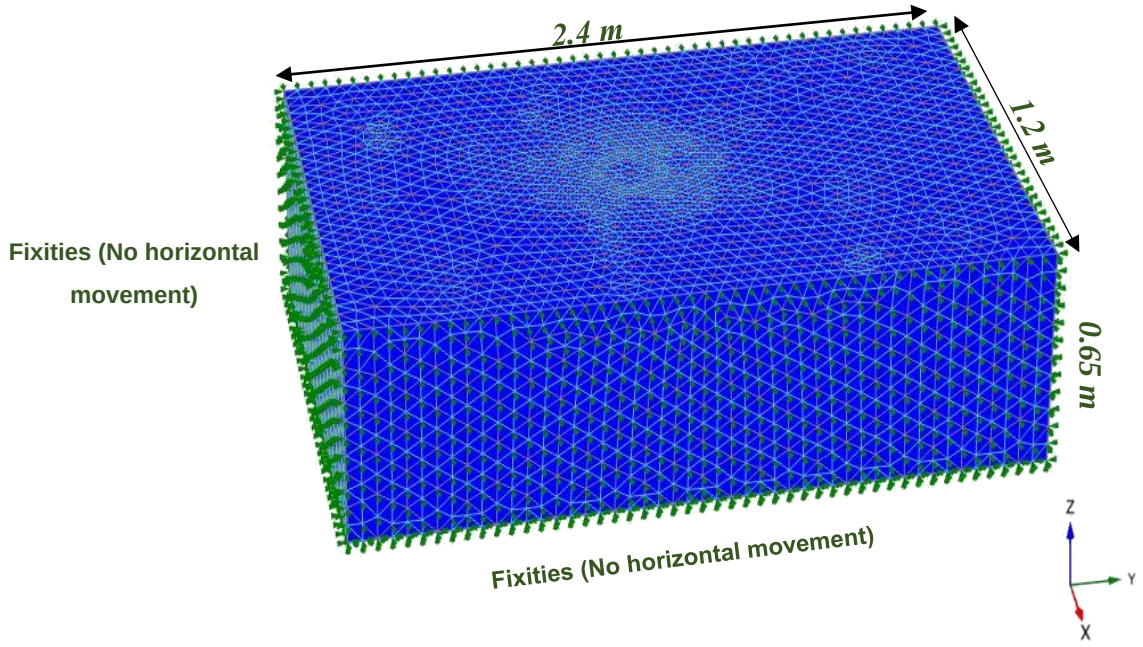

Figure (6.2): Geometry and boundary conditions of 3D Finite Element Model.

6.4: Mesh and Element Configurations:

After the geometry model is created and material properties are fully defined to subgrade soil layer, the geometry has to be divided into fine elements called finite element mesh, these elements are interconnected at specified joints lie on the element boundaries called nodal points, as illustrated in Figure (6.3).

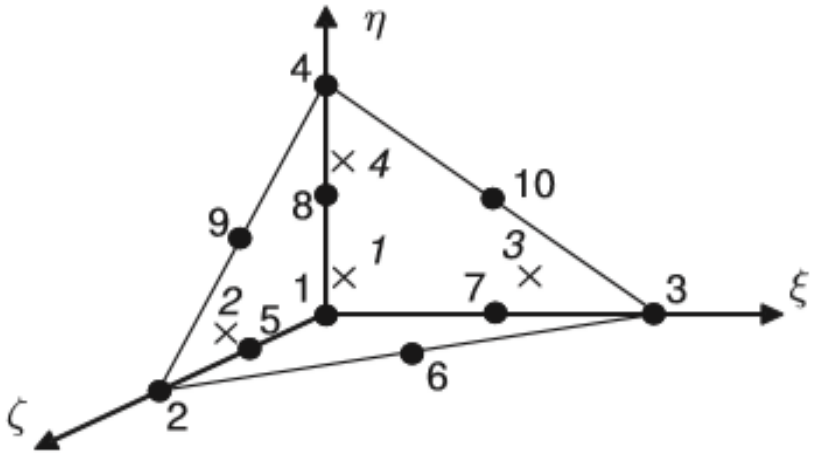

Figure (6.3): 3D soil elements (10-node tetrahedrons).

in this project the subgrade soil modeled as tetrahedral element with 10-nodes fine element, used the automatic meshing procedure, i.e. target element size was 0.7, polyline tolerance angle was 30° and surface angle tolerance 15°. These dimensions for finite element were selected after several analyses on different mesh size, so the surface deflection is not affected by the boundary conditions. The developed mesh has 60,106 nodes and 41,281 elements, as shown in Figures (6.4) and (6.5).

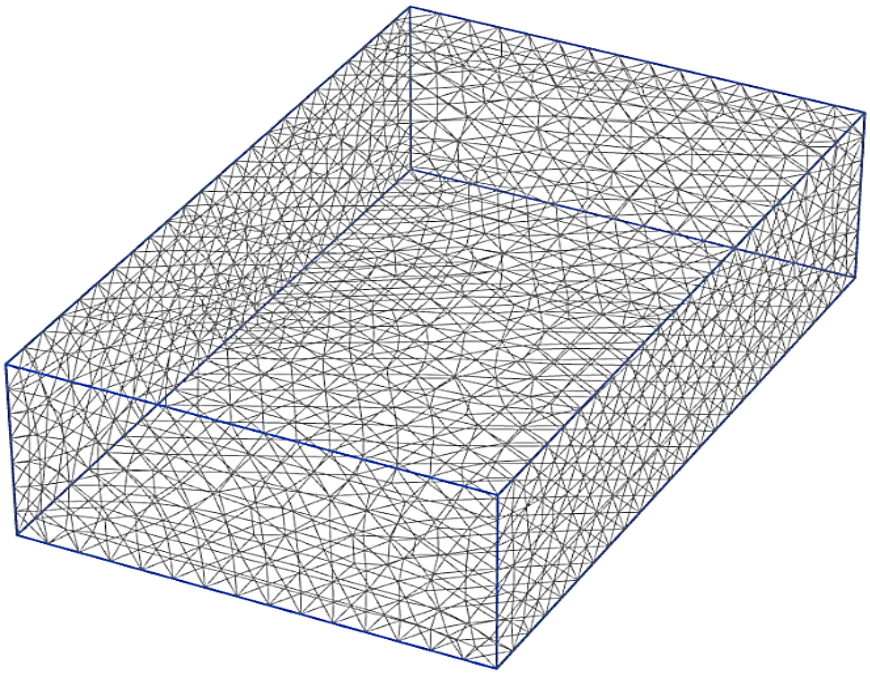

Figure (6.4): Ten – nodes finite element mesh.

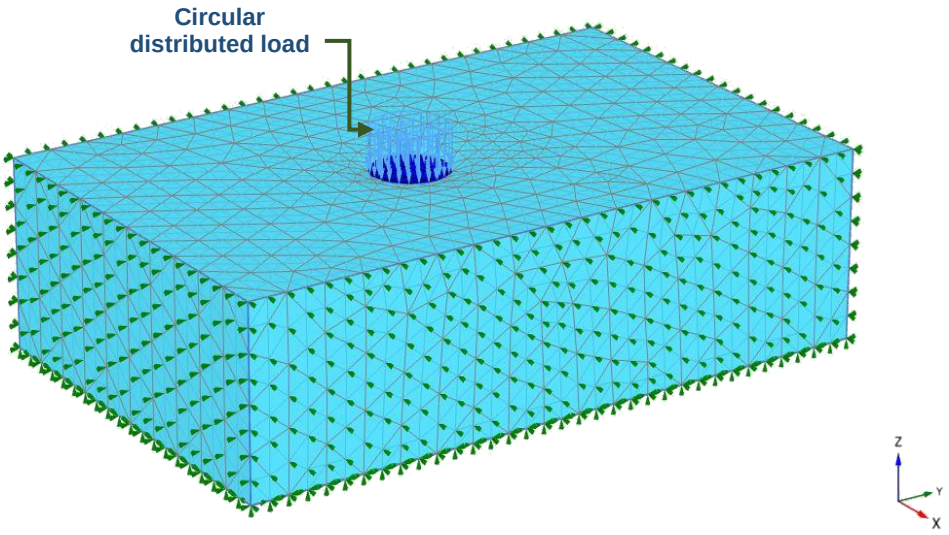

Figure (6.5): Developed geometry with loading plate

6.5: Loading Condition:

6.5.1: Static loading condition:

Twenty-seven PLT tests for three types of subgrade soils that used in the experimental work were simulated numerically using Plaxis 3D software. The vertical static loads were increased in steps, and the plate displacements were calculated under each load step to develop load-deformation curves, then the modulus of subgrade reaction was calculated from the simulated load-deformation curve.

6.5.2: Dynamic loading condition:

Soil layers are often subjected to various dynamic loading conditions, as in earthquake and traffic load…etc. In this study, 54 impulse LWD were developed to simulate the traffic load.

LWD impulse load generates compressive pulse stress with 100 kPa amplitude and a pulse time of 0.018 seconds. This stress simulates a tire pressure generated from a truck with axle 100 kN weight moving at speed 80 kN/hr. As shown in Figures (6.6) and (6.7), this stress is defined as follows:

$$F = \acute{M}.\dot{F}.sin(2\pi ft + \theta_{\circ}) \qquad (6.3)$$

Where:

F : Applied pressure at Time (t).
Ḿ : Amplitude multiplier = 100
Ḟ : Input value of load = 7.07 KN
f **:** Loading frequency = 27.4 Hz
$\emptyset_o$**:** Initial phase angle = 5 degree.

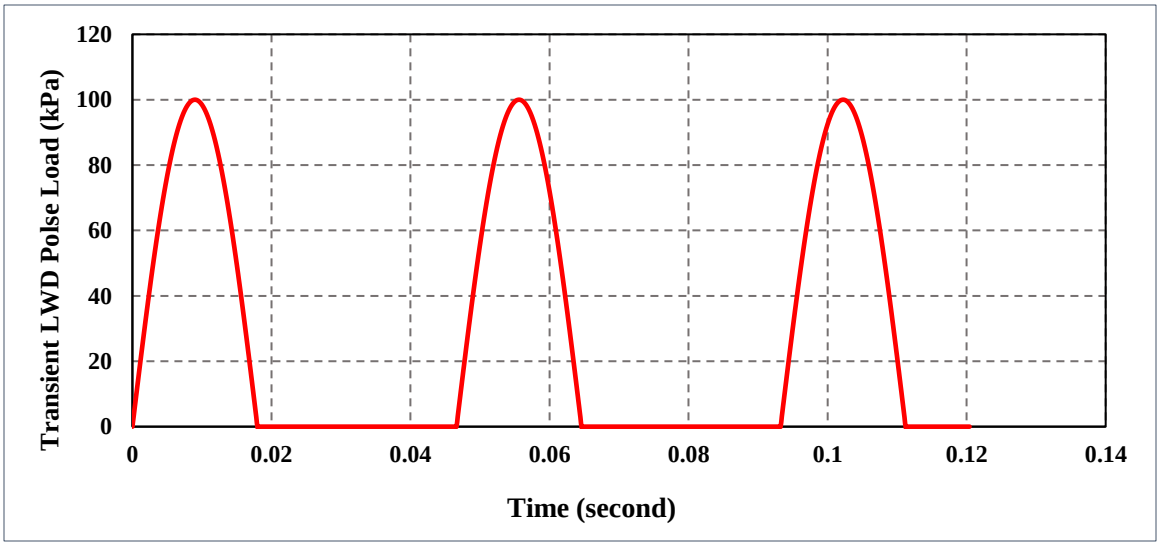

Figure (6.6): Normalized transient pulse load of LWD (Shaban,2016)

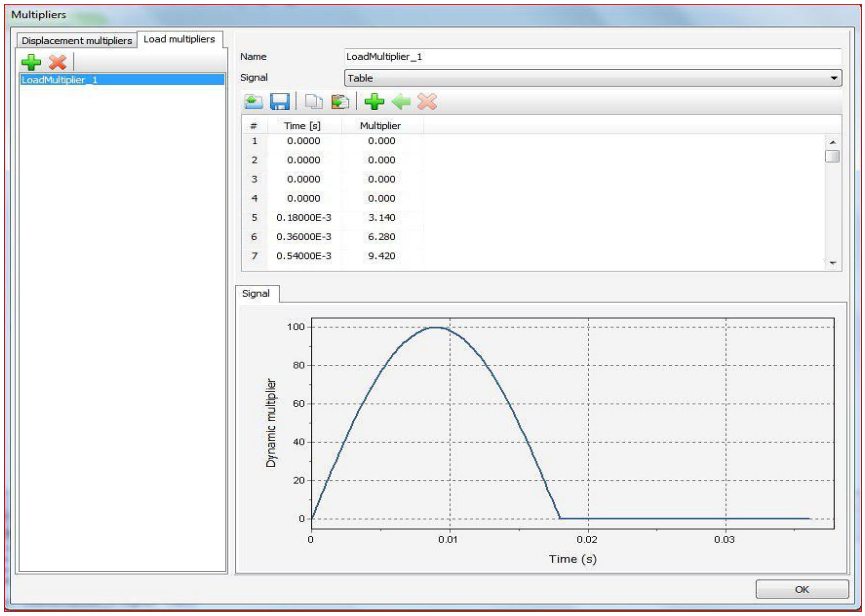

Figure (6.7): Dynamic loading signal, imported from an Excel sheet.

6.6 : FE Calculations:

Finite element calculations were divided into three phases:

1. Initial phases: this phase represents the starting point for further calculation, which defines the initial stress for the soil model taking into account weight of material and loading history of it by using K_0 procedure, where K_0 is the coefficient of lateral earth pressure at rest. The required parameters in the development procedures of initial stresses are two K_0 values, one value is specified for the y-direction, and the other value is specified for the x-direction:

$$K_{0,y} = \frac{\sigma`_{yy}}{\sigma`_{zz}} \qquad (6.4)$$

$$K_{0,x} = \frac{\sigma`_{xx}}{\sigma`_{zz}} \qquad (6.5)$$

In engineering practice, the K_0 value for a normally consolidated soil is frequently assumed to be connected to the angle of internal friction according to Jaky's empirical expression **(Jaky, 1948):**

$$K_0 = 1 - \sin\phi \qquad (6.6)$$

2. Plastic calculation phase: loading at this stage can be defined as changing the load composition, stress, weight, strength, or stiffness of the elements.
3. Dynamic calculation phase: the applied dynamic loading is the result of multiplying the dynamic load multiplier by the input value of the dynamic load. The critical time step is defined by the newmark time integration scheme in which the time step is constant during the analysis. This phase is activated in the calculation of LWD impulse load.

6.7 : Results and Discussion of Finite Element Calculation:

The results of numerical models with PLAXIS 3D software that used to simulate the experimental work were divided into two subsections: [1] results of surface deflection

obtained from LWD dynamic load, and [2] results of maximum surface deflection, and subgrade reaction modulus obtained from PLT static load.

6.7.1: LWD Finite Element Results

The surface deflections resulted from finite element modeling δ_{FEM} were compared with the experimental surface deflection $\delta_{EXP.}$ For three types of subgrade soils of A-1-b, A-3, and A-7-6, the results are summarized in Tables (6.1) that presents FE and experimental surface deflections. The following subsections summarize the LWD finite element results:

For A-1-b soil, the output of finite element surface deflection varied from 0.525 to 1.02 mm with an average value 0.672 mm and standard deviation equal to 0.134. While for A-3 soil the surface deflection obtained from finite element modeling range from 0.44 to 0.661 mm with an average equal 0.57 mm and standard deviation 0.065. And for clayey soil A-7-6 the results show that the value of surface deflection varies from 1.168 to 1.766 mm with an average value 1.429 mm and standard deviation equal to 0.178.

Table (6.1): Summary of experimental and FE for LWD surface deflection of subgrade soils

Test No.	A-1-b		A-3		A-3	
	$\delta_{EXP.}$ (mm)	$\delta_{FEM.}$ (mm)	$\delta_{EXP.}$ (mm)	$\delta_{FEM.}$ (mm)	$\delta_{EXP.}$ (mm)	$\delta_{FEM.}$ (mm)
1	1.053	1.012	0.647	0.640	1.847	1.568
2	0.641	0.651	0.675	0.661	1.865	1.584
3	0.752	0.727	0.620	0.613	1.763	1.460
4	0.544	0.584	0.664	0.644	2.020	1.766
5	0.573	0.597	0.637	0.643	1.941	1.698
6	0.470	0.525	0.630	0.640	1.954	1.708
7	0.719	0.769	0.453	0.494	1.511	1.280
8	0.622	0.639	0.391	0.444	1.694	1.466
9	0.801	0.721	0.420	0.470	1.568	1.314
10	0.636	0.647	0.514	0.545	1.686	1.407
11	0.676	0.671	0.604	0.605	1.680	1.409
12	0.838	0.753	0.477	0.504	1.655	1.387
13	0.655	0.664	0.513	0.553	1.453	1.419
14	0.699	0.694	0.571	0.565	1.497	1.406
15	0.718	0.691	0.530	0.535	1.566	1.234
16	0.580	0.559	0.547	0.576	1.556	1.256
17	0.52	0.542	0.502	0.535	1.401	1.168
18	0.659	0.648	0.567	0.598	1.423	1.196
average	0.675	0.672	0.553	0.570	1.671	1.429
St. dv	0.134	0.110	0.085	0.065	0.192	0.178

6.7.1.1: T-Test Analysis for LWD finite element results.

Since the data are fewer than 30, the variations between experimental and FE results were conducted using a paired T-Test method. The results for the three soils are presented in Table (6.2):

For A-1-b subgrade soil, the results of the T-Test analysis were [t (17) = -0.37, probability = 0.75 > 0.05] which means there is no significant variance between predicted and measured surface deflection and decrease value is 0.003 with confidence interval 95%, see Figure (6.8).

For A-3 subgrade soil, the T-Test results showed that there is a significant variance between simulated and measured surface deflection, this small variation can be attributed to many reasons, such as the test conditions, the FE model cannot predict the soil behavior accurately, and mesh size. T-Test analysis were [t (17) = 3.09, probability = 0.008 < 0.05], the mean increase value 0.017 with 95% of confidence interval, as illustrated in Figure (6.9).

For A-7-6 subgrade soil, the paired T-Test result was [t (17) = -14.27, probability > 0.05] that means there is a significant variance between predicted and measured surface deflection, this variation can be attributed to many reasons, such as the test conditions, the FE model cannot predict the soil behavior accurately, some soil properties, which are assumed due to the lack of testing devices and mesh size. And the mean decrease value is 0.242 with confidence interval 95%, as illustrated in Figure (6.10).

Table (6.2): Summary of T-Test Analysis for LWD finite element results of subgrade

Soil Type	Surface deflection data	No. of Samples	Mean (mm)	Standard Deviation	Paired Sample T-test Method	
A-1-b	$\delta_{FEM.}$ Measurements	18	0.672	0.110	$t_{n-1} = \frac{\bar{x}d}{[std/\sqrt{n}]}$	− 0.37
					Probability	0.75 > 0.05
	$\delta_{EXP.}$ Measurements	18	0.675	0.134	Variance	Non-significant
A-3	$\delta_{FEM.}$ Measurements	18	0.570	0.065	$t_{n-1} = \frac{\bar{x}d}{[std/\sqrt{n}]}$	3.09
					Probability	0.008 < 0.05
	$\delta_{EXP.}$ Measurements	18	0.553	0.085	Variance	significant

. **Note:** If the value of probability is greater than 0.05 there is no significant variance between variables.

Table (6.2): Summary of T-Test Analysis for LWD finite element results of subgrade - continue

Soil Type	Surface deflection data	No. of Samples	Mean (mm)	Standard Deviation	Paired Sample T-test Method	
A-7-6	$\delta_{FEM.}$ Measurements	18	1.429	0.178	$t_{n-1} = \frac{\bar{x}d}{[std/\sqrt{n}]}$	-14.2
					Probability	< 0.05
	$\delta_{EXP.}$ Measurements	18	1.671	0.192	Variance	significant

. **Note:** If the value of probability is greater than 0.05 there is no significant variance between variables.

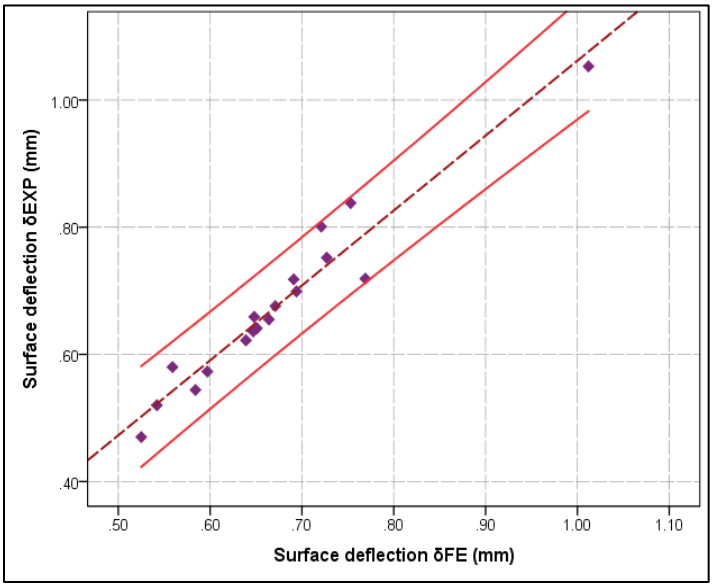

Figure (6.8): Predicted vs. measured LWD surface deflection for A-1-b soil

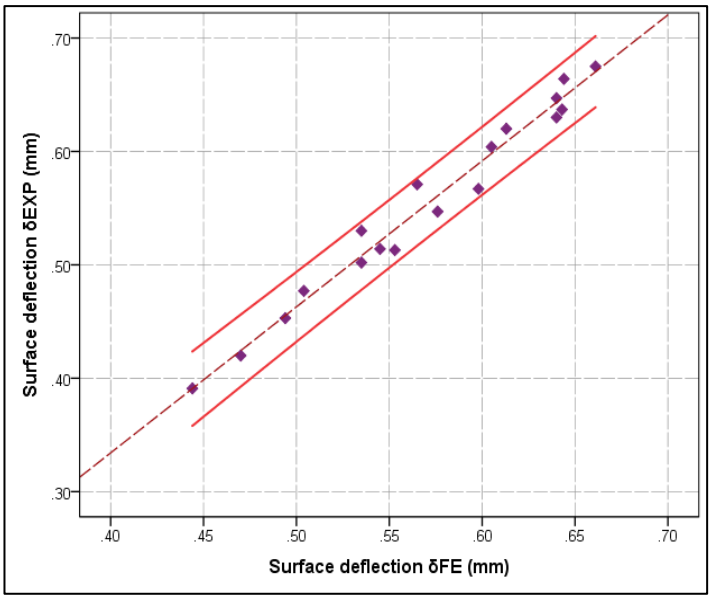

Figure (6.9): Predicted vs. measured LWD surface deflection for A-3 soil

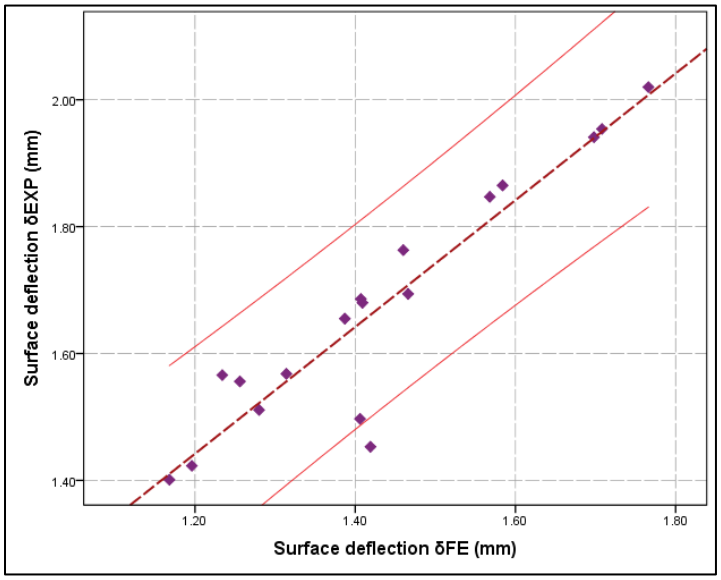

Figure (6.10): Predicted vs. measured LWD surface deflection for A-7-6 soil

The typical output of finite element for LWD tests are presents in the following Figures (6.11) through (6.13). The geometry model of 3D finite element with circular dynamic load of LWD were illustrated in the Figure (6.11), this figure explains the zone that affected by the applied load. As mentioned in the experimental work that the impact load obtained from LWD causes the stresses zone within the soil like a bulb with a diameter of twice the diameter of loading plate, see Figure (6.12).

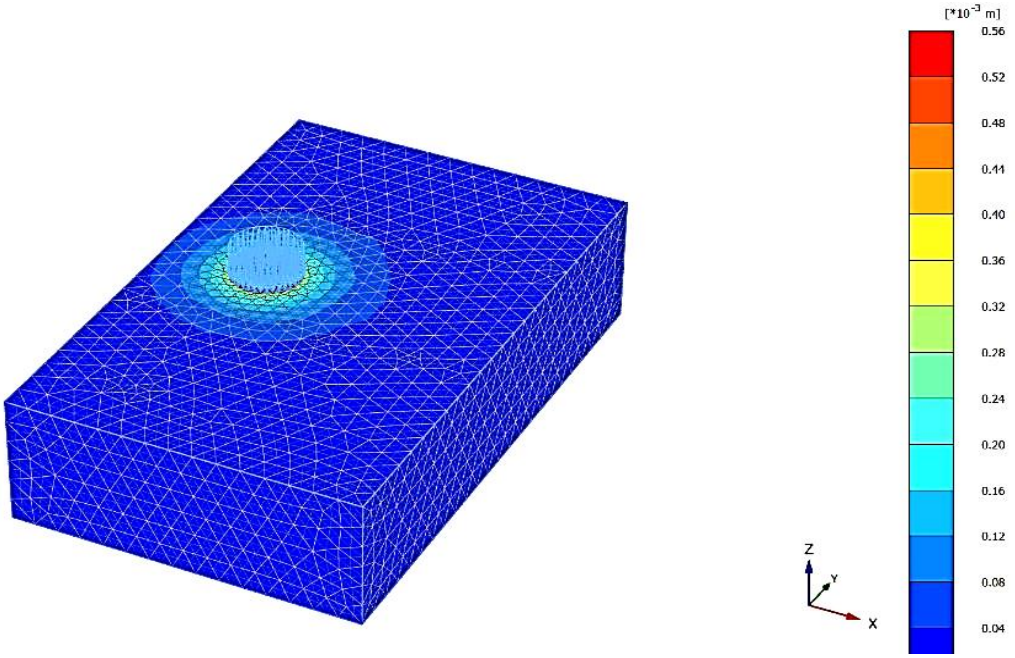

Figure (6.11): 3D Finite element model of LWD test

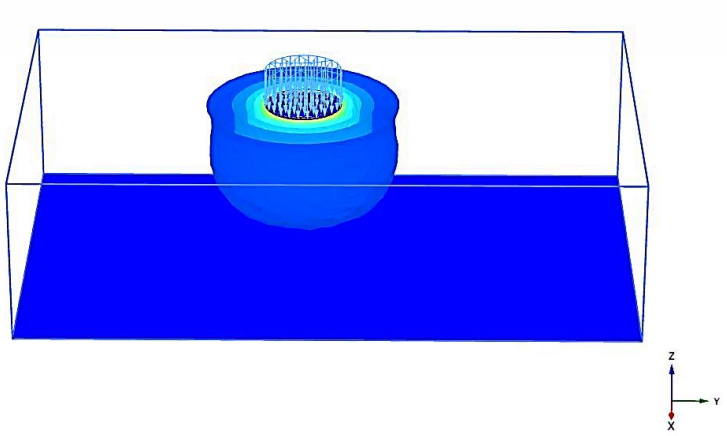

Figure (6.12): Bulbe of influence zone of LWD load

To explain the displacement through the subgrade layer, take the cross-section of FE model as shown in Figure (6.13), the red color represents the highest effect of the load on the soil surface, which gives the highest displacement of the soil, then the effect of the load decreases downwards which is represented in a blue color. Also, this figure explains the deformation in the mesh under the load.

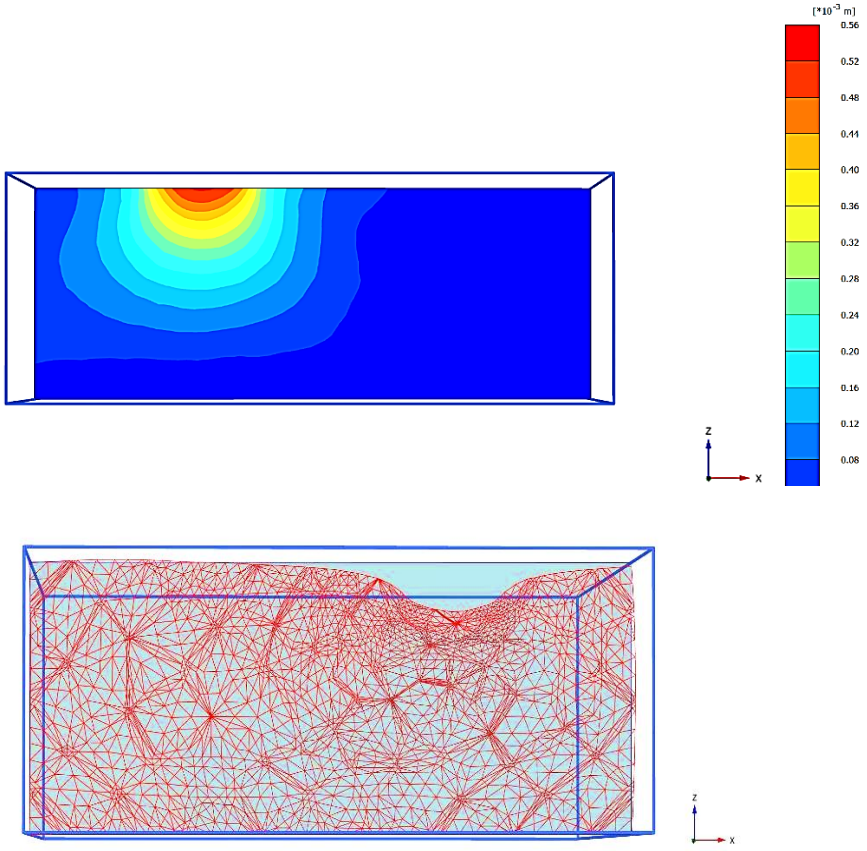

Figure (6.13): Distribution of displacements in simulated subgrade soil.

6.7.2: PLT Finite Element Results

Under the same loading condition that used in the experimental work, the PLT tests were simulated numerically to find the maximum surface deflection, and to develop load-deformation curve, from which the subgrade reaction modulus was predicted. The FE results for three soils are summarized in Table (6.3):

For A-1-b subgrade soil, it was noticed that the maximum settlement ranged from 2.3 to 6.7 mm with an average value of 4.78 mm. Whereas the modulus of subgrade reaction Ks ranged from 287.5 to 492 kPa/mm with an average value of 343.82 kPa/mm. Figure (6.14) displays a typical compression load-deformation curve.

For A-3 subgrade soil, it was noticed that the maximum settlement ranged from 2.1 to 5.010 mm with an average value 3.11 mm. Whereas the modulus of subgrade reaction Ks ranged from 197.14 to 766 kPa/mm with an average value 490.47 kPa/mm. Figure (6.15) displays a typical compression load-deformation curve.

For A-7-6 subgrade soil, the results showed that the maximum settlement ranged 3.52 to 6.2 mm with an average value 4.494 mm. Whereas the modulus of subgrade reaction Ks ranged from 135.2 to 293.6 kPa/mm with an average value 209.379 kPa/mm. Figure (6.16) displays a typical compression load-deformation curve.

All compression load-deformation curves are summarized in Appendix B

Table (6.3): Summary of Experimental and FE results for PLT test

Type of soil	Test No.	$\delta_{EXP.}$ (mm)	$\delta_{FEM.}$ (mm)	$K_{S\ (EXP).}$ kPa/mm	$K_{S\ (FEM).}$ kPa/mm
A-1-b	1	5.20	4.80	313.6	300.0
	2	6.47	6.20	345.0	328.6
	3	5.26	5.06	363.0	345.0
	4	5.11	5.70	363.2	321.0
	5	4.39	4.85	345.0	287.5
	6	6.37	6.70	345.0	328.5
	7	3.47	4.40	383.3	328.6
	8	2.72	3.04	363.5	363.2
	9	2.70	2.30	431.3	492.0
A-3	1	4.73	5.01	246.43	197.1
	2	3.37	4.40	255.56	255.6
	3	2.01	2.68	300.00	363.2
	4	2.58	3.20	460.00	492.8
	5	2.75	3.10	460.00	431.3
	6	2.67	2.89	431.25	460.0

Table (6.3): Summary of Experimental and FE results for PLT test-continue

Type of soil	Test No.	$\delta_{EXP.}$ (mm)	$\delta_{FEM.}$ (mm)	Ks (EXP). kPa/mm	Ks (FEM). kPa/mm
A-3	7	1.83	2.25	711.30	690.0
	8	1.75	2.10	755.20	766.0
	9	1.75	2.40	766.70	758.2
A-7-6	1	6.03	6.00	138.00	143.7
	2	6.20	6.85	138.00	135.2
	3	5.77	5.53	135.29	146.8
	4	4.20	3.98	186.49	222.6
	5	4.08	4.30	181.58	197.4
	6	3.90	4.18	172.50	181.6
	7	3.44	3.25	230.00	276.0
	8	3.40	3.80	230.00	287.5
	9	3.42	3.50	246.43	293.6

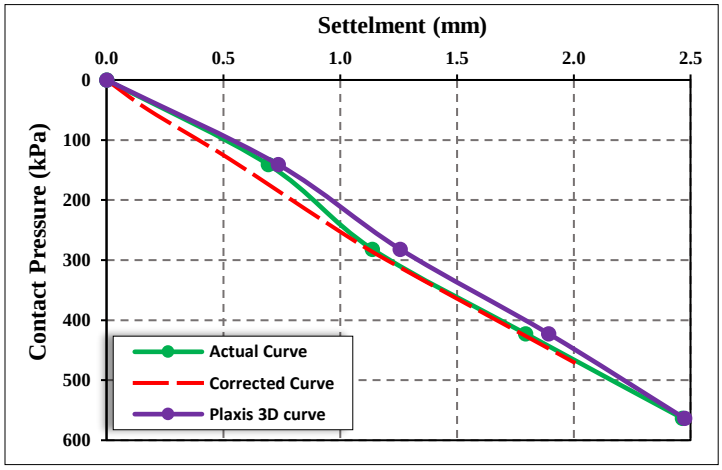

Figure (6.14): Typical curve- compression between the experimental and the numerical simulation for surface settlement for A-1-b

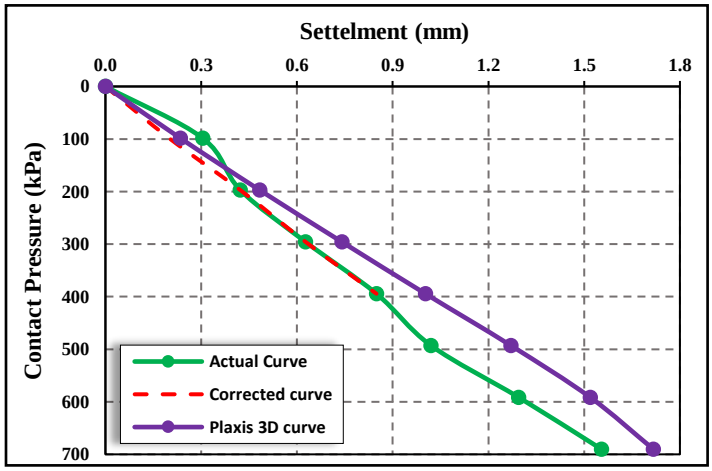

Figure (6.15): Typical curve- compression between the experimental and the numerical simulation for surface settlement for A-3

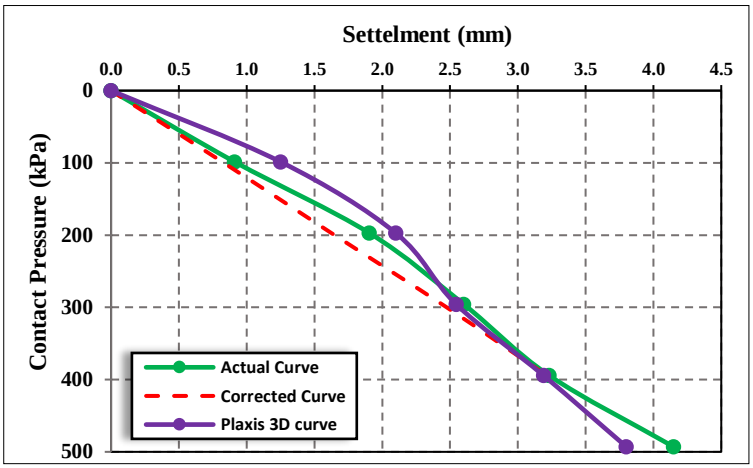

Figure (6.16): Typical curve- compression between the experimental and the numerical simulation for surface settlement for A-7-6

6.7.2.1: T-Test Analysis for PLT finite element results.

Since the data are fewer than 30, the variations between experimental and FE results were conducted using a paired T-Test method. The results for the three soils are presented in Table (6.4):

For A-1-b subgrade soil, the results of the analysis were [t (8) = 0.93, probability = 0.17 > 0.05] which means there is no significant variance between predicted and measured surface deflection and the mean increase value is 0.15mm with confidence interval 95%, see Figure (6.17). Whereas in the modulus of subgrade reaction Ks, the T-Test results showed that there is no significant variance between simulated and measured subgrade reaction modulus, [t (8) = -1.49, probability = 0.35 > 0.05], the mean decreased 17.614 kPa/mm with 95% interval as illustrated in Figure (6.18).

For A-3 subgrade soil, the T-Test results showed that the [t (8) = -6.0, probability 0.0 < 0.05] which means there is a significant variance between predicted and measured surface deflection, this small variation can be attributed to many reasons, such as the test conditions, the FE model cannot predict the soil behavior accurately, mesh size. and the mean decrease value is 0.15mm with confidence interval 95% as explained in Figure (6.19). Whereas in the modulus of subgrade reaction Ks, the T-Test result showed that there is no significant variance between simulated and measured subgrade reaction modulus, [t (8) = -0.27, probability = 0.75 > 0.05], the mean decreased 3.088 kPa/mm with 95% interval, see Figure (6.20).

For A-7-6 subgrade soil, the T-Test results were [t (8) = - 1.03 probability = 0.35 > 0.05] which means there is no significant variance between predicted and measured surface deflection and the mean decrease value is 0.105mm with confidence interval 95%, see Figure (6.21). Whereas in the modulus of subgrade reaction Ks, the T-Test results showed that there is a significant variance between simulated and measured subgrade reaction modulus, [t (8) = -3.47, probability = 0.008 < 0.05]. This variation can be attributed to many reasons, such as the test conditions, the FE model cannot predict the soil behavior accurately, some soil properties, which are assumed due to the lack of testing devices. and mesh size, the mean decreased -25.125 kPa/mm with 95% interval, as illustrated in Figure (6.22).

Table (6.4): Summary of T-Test analysis of PLT test for subgrade soil

Type of soil	Measurements data	No. of Samples	Mean (mm)	Standard Deviation	Paired Sample T-test Method
A-1-b	$\delta_{FEM.}$	9	4.783	1.412	$t_{n-1} = \frac{\bar{x}d}{[std/\sqrt{n}]}$ 0.93
	$\delta_{EXP.}$	9	4.633	1.421	Probability 0.17 > 0.05
	Ks $_{(FEM).}$	9	343.82	59.84	$t_{n-1} = \frac{\bar{x}d}{[std/\sqrt{n}]}$ − 1.49
	Ks $_{(EXP).}$	9	361.43	32.52	Probability 0.35 > 0.05
A-3	$\delta_{FEM.}$	9	3.11	0.98	$t_{n-1} = \frac{\bar{x}d}{[std/\sqrt{n}]}$ − 6.0
	$\delta_{EXP.}$	9	2.604	0.97	Probability 0.0 < 0.05
	Ks $_{(FEM).}$	9	490.47	208.953	$t_{n-1} = \frac{\bar{x}d}{[std/\sqrt{n}]}$ − 0.27
	Ks $_{(EXP).}$	9	487.38	209.59	Probability 0.75 > 0.05
A-7-6	$\delta_{FEM.}$	9	4.599	1.235	$t_{n-1} = \frac{\bar{x}d}{[std/\sqrt{n}]}$ − 1.03
	$\delta_{EXP.}$	9	4.494	1.171	Probability 0.35 > 0.05
	Ks $_{(FEM).}$	9	209.37	63.649	$t_{n-1} = \frac{\bar{x}d}{[std/\sqrt{n}]}$ − 3.74
	Ks $_{(EXP).}$	9	184.254	43.124	Probability 0.008 < 0.05

Note If the value of probability is greater than 0.05 there is no significant variance between variables

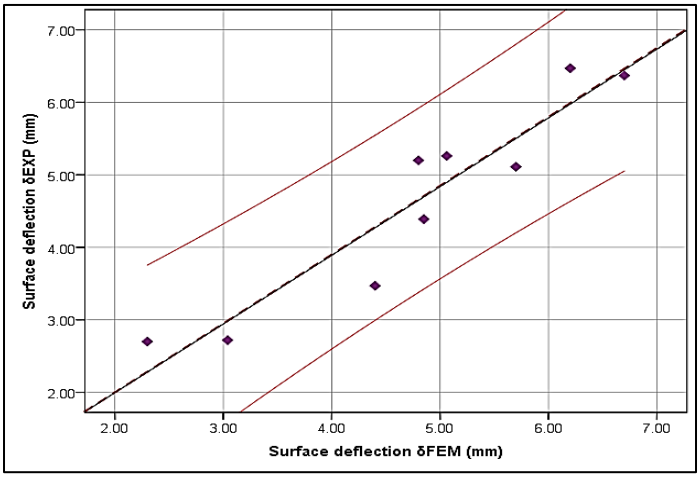

Figure (6.17): Predicted vs. measured maximum surface deflection for A-1-b soil

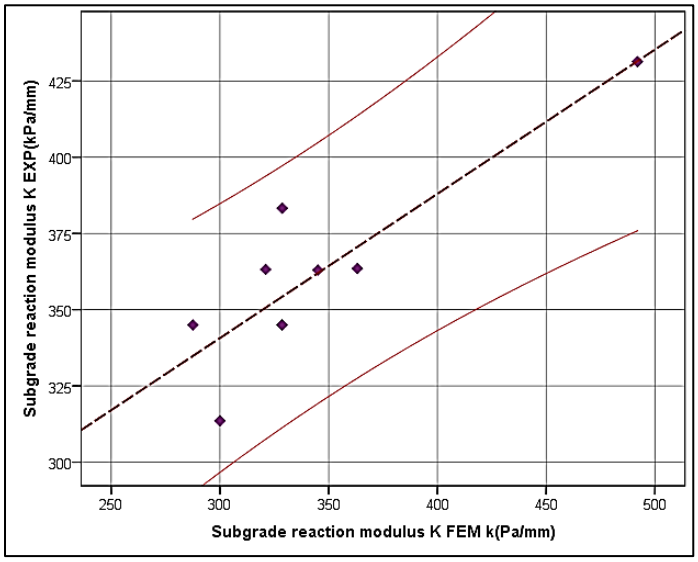

Figure (6.18): Predicted vs. measured modulus of subgrade reaction for A-1-b soil

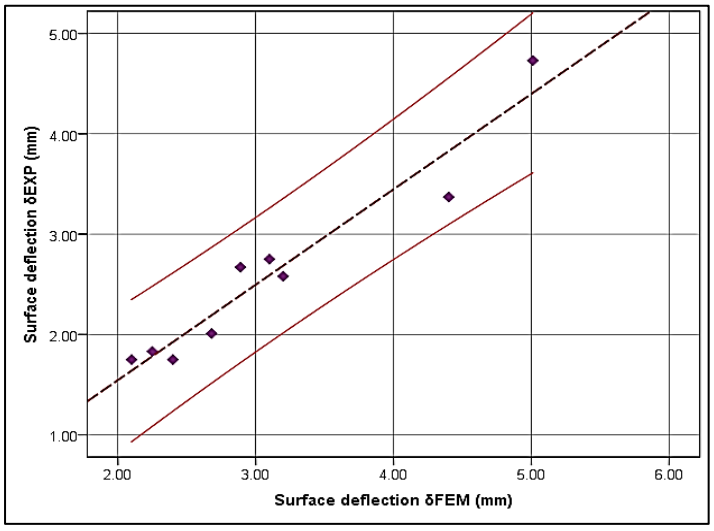

Figure (6.19): Predicted vs. measured maximum surface deflection for A-3 soil

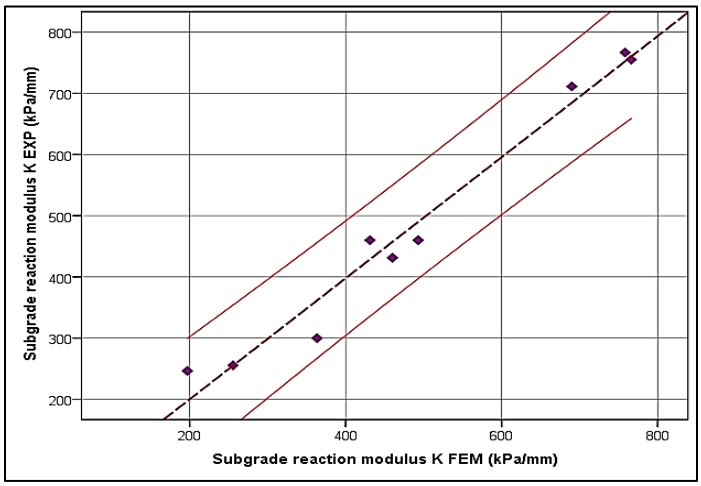

Figure (6.20): Predicted vs. measured modulus of subgrade reaction for A-3 soil

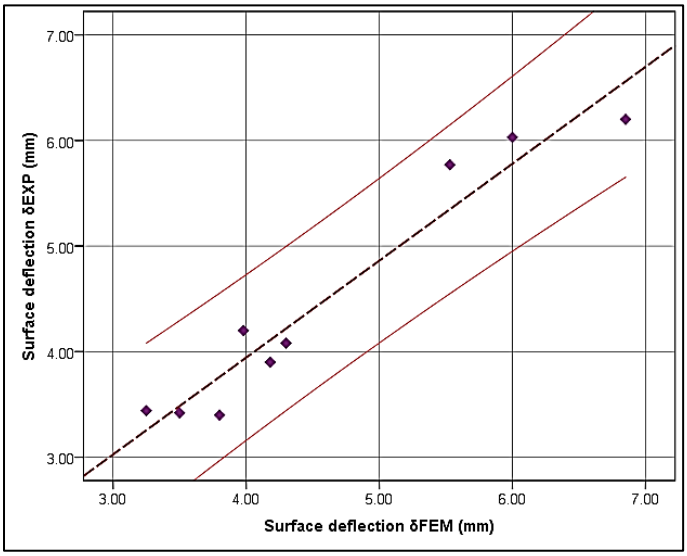

Figure (6.21): Predicted vs. measured maximum surface deflection for A-7-6 soil

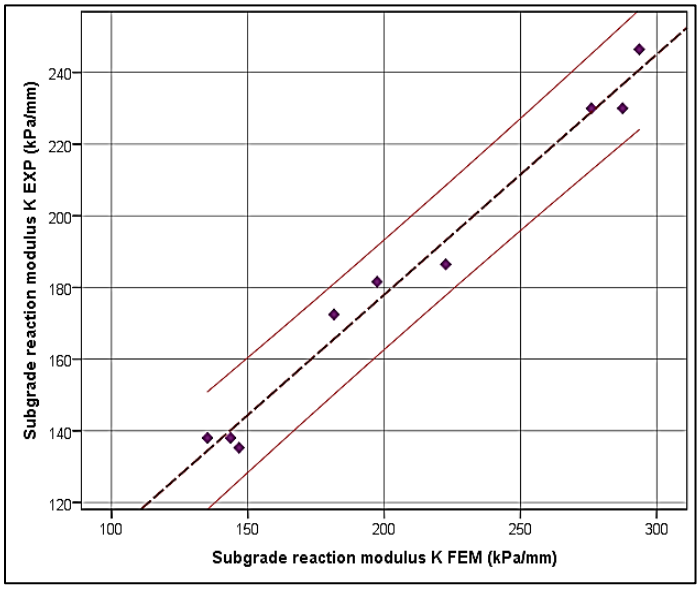

Figure (6.22): Predicted vs. measured modulus of subgrade reaction for A-7-6 soil

The typical output of finite element for PLT tests are presents in the following Figures (6.23) through (6.26). The geometry model of 3D finite element with circular static load of PLT were illustrated in the Figure (6.23), this figure explains the zone that affected by the applied load. The distribution of load through the subgrade layers explained in Figure (6.24). As mentioned in the experimental work that the static load obtained from PLT causes the stresses zone within the soil like a bulb with a diameter of twice the diameter of loading plate, see Figure (6.25).

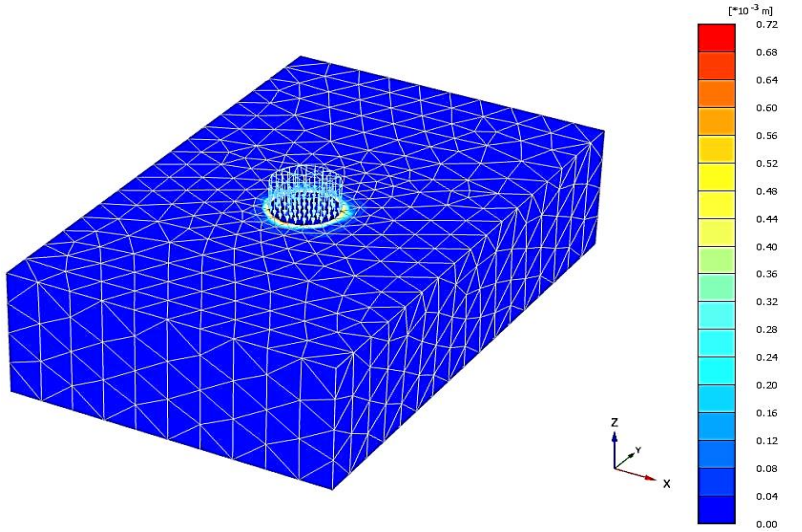

Figure (6.23): 3D Finite element model of PLT test

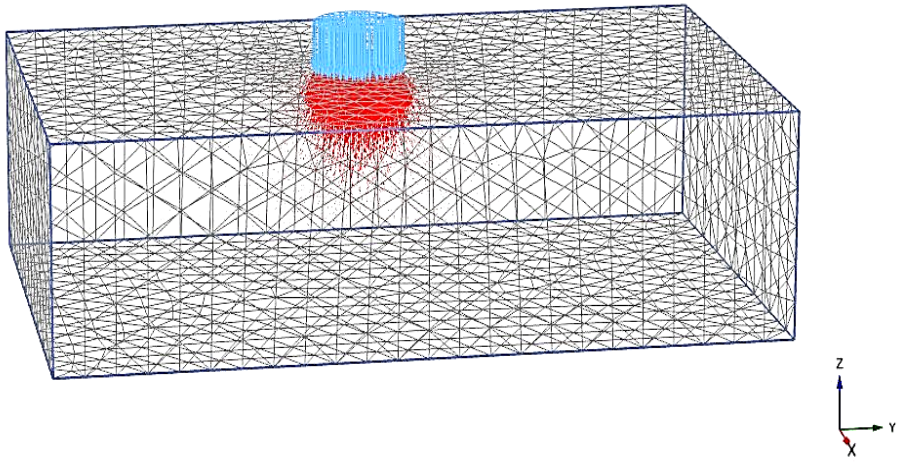

Figure (6.24): Distribute the load through the soil layer

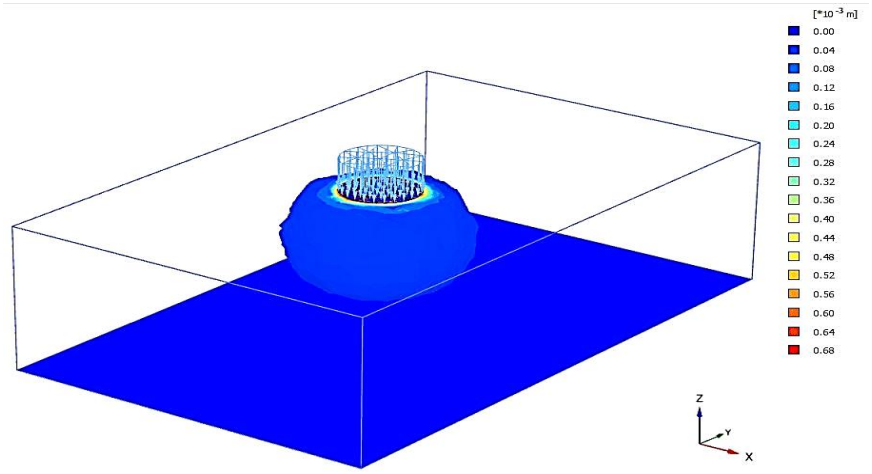

Figure (6.25): Bulbe of influence zone of PLT load

To explain the displacement through the subgrade layer, take the cross-section of FE model as shown in Figure (6.26), the red color represents the highest effect of the load on the soil surface, which gives the highest displacement of the soil, then the effect of the load decreases downwards which is represented in a blue color. Also, this figure explains the deformation in the mesh under the load.

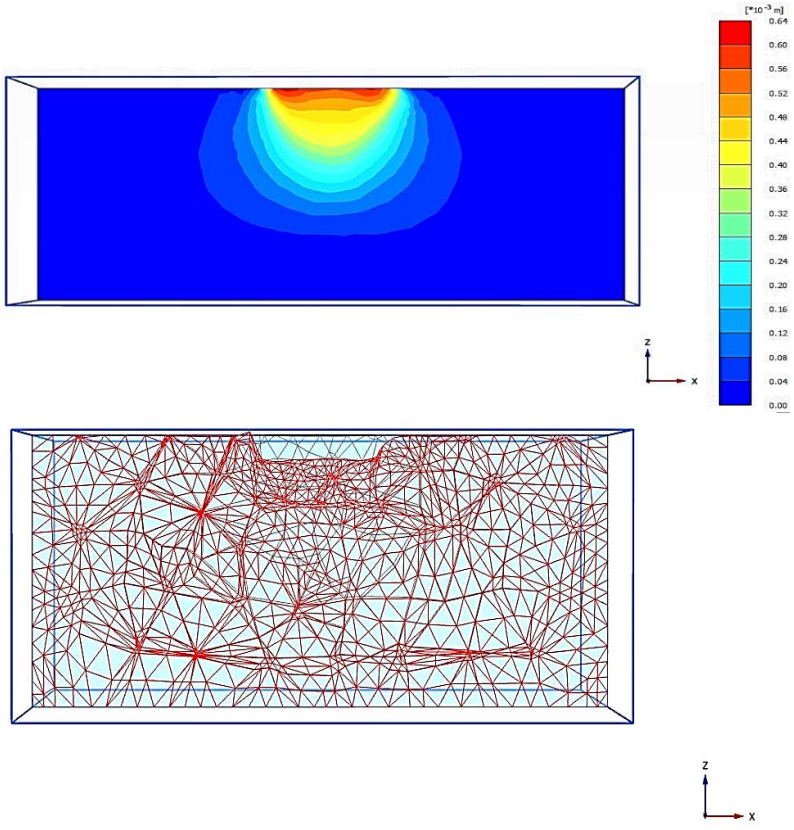

Figure (6.26): Distribution of displacements in simulated subgrade soil

2.8 : Summary

In this chapter explained the finite element model that developed in dimensions (1.2 m width, 2.4m length, and 0.65m depth). These dimensions are similar to those used in experimental work. the boundary conditions were chose as fixed in all directions and in base as used in the experimental work. using two types of loading conditions; static to simulate the static plate load test and developed load – deformation curve obtained subgrade reaction modulus from it. And dynamic loading condition to simulate the light weight deflectometer test to identify the maximum surface deflection. Also this chapter include the T-Test that used to analysis the experimental and finite element results to explained the variance between the results.

Chapter Seven

Conclusions and Recommendations

7.1 Conclusions

Based on the results of the experimental and theoretical work, the following conclusions are drawn:

1- From the laboratory tests the results of physical soil properties showed that the higher value of California bearing ratio and maximum dry unit weight were obtained for A-3 subgrade soil. While the higher optimum moisture content reach to (18.5%) was for A-7-6 subgrade soil.

2- The results of laboratory setup investigation indicated that the degree of compaction of subgrade soils increase with increasing the number of passes of compaction device. Increasing the degree of compaction of subgrade soils was caused to increase the dry unit weight, LWD dynamic modulus, and elastic modulus while a decrease in moisture content, surface deflection, and degree of compatibility.

3- In general, the results of laboratory setup illustrate that the modulus of subgrade reaction increases with increasing the LWD dynamic modulus, and dry unit weight of soils. However, the results illustrated that the modulus of subgrade reaction modulus decreases with the increase of the LWD surface deflection, degree of compatibility, and moisture content of soils.

4- From statistical analysis the results showed that good correlation between PLT and LWD measurements for both granular and fine subgrade soils. The relations obtained from statistical analysis, were linear for some models and non-linear for others.

5- For granular soils, a high correlation was obtained between the subgrade reaction modulus and LWD degree of compatibility with the coefficient of determination (R^2 = 0.93), and mean square error (MSE= 4.875). Additionally, a good agreement was identified between the LWD surface deflection and the subgrade reaction modulus with a coefficient of determination (R^2 = 0.83), and mean square error (MSE= 9.13). While for fine soil (clayey soil) the higher correlation was between the subgrade reaction

modulus and LWD surface deflection with a coefficient of determination (R^2 = 0.0.92), and mean square error (MSE= 0.163).

6- The statistical results also showed that the basic soil properties that represented by field densities and water content are well related with the subgrade reaction modulus. It was found that the field densities have the most significant correlation than water content to predict subgrade reaction modulus with a coefficient of determination equal to (R^2 = 0.90, and 0.96) for granular and fine subgrade soils respectively.

7- The results of the multiple non-linear regression analysis for granular subgrade soils showed that the inclusion of the dry density along with LWD dynamic modulus gives a regression model with good reliability in prediction the subgrade reaction modulus. The R^2 and MSE values were 0.87 and 2.595, respectively.

8- The results of numerical models with Plaxis 3D software revealed a good agreement with the results obtained from the experimental work. It was found that the mean difference between numerical and experimental results of LWD surface deflection ranged from 0.003 to 0.242. and the T-Test results indicated that there is no significant variance between measured and predicted data in most data.

9- Also, numerical analysis showed a well acceptance between measured subgrade reaction and predicted from simulated model with low mean difference range from 3.088 kPa/mm to 25.15 kPa.

10- The results of numerical simulation showed that the mean difference between experimental work and numerical simulation in terms of PLT surface deflections varied from 0.105 to 0.15 mm. and there is no significant variance between the most data.

11- The results of this work showed the possibility of employing the LWD devices as an effective non-destructive tool to rapidly and reliably predict the subgrade reaction modulus of pavement materials and soil embankments

7.2 Recommendations for Future Work

1. Developing a simple procedure to determine the subgrade reaction modulus for stabilized subgrade soils.
2. It is recommended to conduct further field tests (i.e., PLT and LWD) to revalidate the theoretical models developed in this study.
3. Future research should be considered to investigate the strength characteristics of base and subbase layers using LWD.
4. Evaluate soil properties using repetitive plate load test and compare the results with those obtained from dynamic LWD.

References

AASHTO M145, (2012),"Standard Specification for Classification of Soils and Soil-Aggregate Mixtures for Highway Construction Purposes," American Association of State and Highway Transportation Officials, Washington, DC.

AASHTO T222, (2007), "Nonrepetitive static plate load test of soil and flexible pavement components for use in evaluation and design of airport and highway pavements. "American Association of State Highway and Transportation Officials, Washington, DC.

Abu-Farsakh M. Y., Nazzal, M. D., Alshibli, K. and Seyman, E. (2004), " Assessment of In-situ Test Technology for Construction Control of Base Course and Embankments", Louisiana Department of Transportation and Development Louisiana Transportation Research Center, No. 736-02-0995.

Abu-Farsakh M. Y., Nazzal, M. D., Alshibli, K. and Seyman, E. (2005), " Application of Dynamic Cone Penetrometer in Pavement Construction Control", Transportation Research Record: Journal of the Transportation Research Board, No. 1913, Transportation Research Board of the National Academies, Washington, D.C., 2005, pp. 53–61.

Adam C., Adam D., Kopf F., and Paulmichl I., (2009), "Computational validation of static and dynamic plate load testing", Acta Geotechnical, Springer, vol. 4, pp. 35–55

Ahirwar S. K., and J. N. Mandal., (2017). "Finite Element Analysis of Flexible Pavement with Geogrids." Transportation Geotechnics and Geoecology (TGG), vol. 2017, 17-19 May 2017, PP. 411-416 Saint Petersburg, Russia.

Akbariyeh, N. (2015). "A new technique for the estimation of the elastic moduli of pavement layers from light weight Deflectometer data." The university of Texas at arlinton, August 2015, master thesis.

Alavi, S., and Lecates, F., (2002), " Falling Weight Deflectometer Usage.", NCHRP Synthesis 381, Transportation Research Board of the National Academic, Washington, DC.

Ameri, M., Salehabadi, E. G., Nejad, F. M., and Rostami, T. (2012). "Assessment of Analytical Techniques of Flexible Pavements by Finite Element Method and Theory of Multi-Layer System." Journal Basic Applied Science Research, 12(11), 11743-11748.

Archontoulis S. V. and Fernando E. Miguez., (2013).,"Nonlinear Regression Models and Applications in Agricultural Research." Agronomy Journal: Agron. J. 105:1–13 (2013).

ASTM D1195, (2004), "Standard Test Method for repetitive Static Plate Load Tests of Soils and Flexible Pavement Components, for Use in Evaluation and Design of Airport and Highway Pavements." ASTM International, West Conshohocken, PA.

ASTM D1196, (2004), "Standard Test Method for Nonrepetitive Static Plate Load Tests of Soils and Flexible Pavement Components, for Use in Evaluation and Design of Airport and Highway Pavements." ASTM International, West Conshohocken, PA.

ASTM D1557–12, (2012), "Standard Test Methods for Laboratory Compaction Characteristics of Soil Using Modified Effort," American Society for Testing and Materials (ASTM), West Conshohocken, PA.

ASTM D1883–07, (2007), "Standard Test Method for CBR (California Bearing Ratio) of Laboratory-Compacted Soils," American Society for Testing and Materials (ASTM), West Conshohocken, PA.

ASTM D2011, (2011), " Standard Test Method for Density and Unit Weight of Soil in Place by Sand-Cone," American Society for Testing and Materials (ASTM), West Conshohocken, PA.

ASTM D2487 – 11, (2005), "Standard Practice for Classification of Soils for Engineering Purposes (Unified Soil Classification System)," American Society for Testing and Materials (ASTM), West Conshohocken, PA.

ASTM D2937, (2004), " Standard Test Method for Density of Soil in Place by the Drive-Cylinder Method." ASTM International, West Conshohocken, PA.

ASTM D3080 – 3080M, (2007), "Standard Test Method for Direct Shear Test of Soils Under Consolidated Drained Conditions," American Society for Testing and Materials (ASTM), West Conshohocken, PA.

ASTM D4318 – 10, (2005), "Standard Test Methods for Liquid Limit, Plastic Limit, and Plasticity Index of Soils", American Society for Testing and Materials (ASTM), West Conshohocken, PA.

ASTM D854 – 14, (2014), " Standard Test Methods for Specific Gravity of Soil Solids by Water Pycnometer", American Society for Testing and Materials (ASTM), West Conshohocken, PA.

ASTM E2583-07, (2011), "Standard Test Method for Measuring Deflections with a Light Weight Deflectometer (LWD)." ASTM International, West Conshohocken, PA.

B.S Part 3. (1990), "Chemical and electro-chemical tests" , British Standard, Methods of test for Soils for civil engineering purposes, vol. 1377-3, pp.40

Barker, W. R. and Alexander, D. R., (2012)."Determining the Effective Modulus of Subgrade Reaction for Design of Rigid Airfield Pavements Having Base Layers.", Report No. 12-2 (ERDC/GSL TR), US Army Corps of Engineers, Engineer Research and Development Center, Geotechnical and Structures Laboratory.

Bhatia H. S, (2016). ‘‘Sustainable models for better design of foundation systems’’. International journal of education research studies, MAR-APRIL, 2016, VOL-I, ISSUE-VI. P.P 475-488

Biot, M. A. (1937). "Bending of Infinite Beams on an Elastic Foundation," Journal of Applied Mechanics Trans. Am. Soc. Mech. Eng., Vol. 59, 1937, pp. A1-A7.

Bowles, J. E. (1998). "Foundation Analysis and Design, ", 6 the Edition, McGrow-Hill International Press, 1998

British standards code, (1999). ‘‘Code of practice for site investigations’’ British standard BS 5930:1999.

Burhani A., (2016), "Correlation Study on the Falling Weight Deflectometer and Light Weight Deflectometer for the Local Pavement Systems. " Thesis for master degree, Russ College of Engineering and Technology of Ohio University

CRD-C 655-95. (1995). "Standard test method for determining the modulus of soil reaction." Handbook for Concrete and Cement. U.S. Army Corps of Engineers.

Dalili S. M, Huat B., and Jaafar, M. (2013). "Review of static soil-framed structure interaction. ", interaction and multiscale mechanics (2013), Vol. 1, PP. 51-81,

David H. and Mooney, Michael A., "Influence of Lightweight Deflectometer Characteristics on Deflection Measurement. ", Geotechnical Testing Journal, Vol. 36, No. 2, 2013, pp. 216–226, doi:10.1520/GTJ20120034. ISSN 0149-6115.

Demir, A. Abdulazim Yildiz, Mustafa Laman, and Murat Ornek., (2013). "Experimental and numerical analyses of circular footing on geogrid-reinforced granular fill underlain by soft clay." Springer, Acta Geotechnics (2014), Vo. 9: pp. 711–723,

Dutta. S. C., and Roy. R., (2002) "A critical review on idealization and modeling for interaction among soil–foundation–structure system.", Computers and structures, Elsevier Science, Vol. 80 (2002), PP.1579-1594.

Egyptian Code, "Soil Mechanics and Foundation," Organization, Cairo, 2001.

Ersoy, H. M., Seda C¸ ellek1, Bilgehan K., ˙Idris Baykan, and Robert L Parsons. (2013), "Estimation of the soil strength parameters in Tertiary volcanic regolith (NE Turkey) using analytical hierarchy process." J. Earth Syst. Sci. 122, No. 6, December 2013, pp. 1545–1555.

Federal Aviation Administration (2009). "Airport Pavement Design and Evaluation." Advisory Circular 150/5320-6E, Office of Airport Safety and Standards, Washington, DC.

Ferretti. E, (2013). ‘‘The second order solution of Boussinesq’s problem’’. Research and Applications in Structural Engineering, Mechanics and Computation – Zingoni (Ed.) © 2013 Taylor & Francis Group, London, ISBN 978-1-138-00061-2

Fleming, P. R., Frost, M. W., and Lambert, J. P., (2007), " A Review of the Light Weight Deflectometer (LWD) For Routine Insitu Assessment of Pavement Material Stiffness. ", Transportation Research Record: Journal of the Transportation Research Board, Vol. 7359, No.07-1586 Submitted 14/11/06.

Jaky, J., 1948. "Pressure in silos". In Proc. 2nd International. Conference. Soil Mechanics and Foundation Engineering, Vol. 1, pp. 103-107.

Kalliainen, A. Pauli Kolisoja, and Antti Nurmikolu. (2016)., "3D Finite Element Model as a Tool for Analyzing the Structural Behavior of a Railway Track" International Conference on Transportation Geotechnics (ICTG 2016), Procedia Engineering, Vo. 143, 2016, PP. 820–827.

Khazanovich, L., Tayabji, S. D., and Darter, M. I. (2001). "Back calculation of layer parameters for LTPP test sections, Volume I: Slab on elastic solid and slab on dense-liquid foundation analysis of rigid pavements. " Technical Rep. No. FHWA-RD-00-086, Federal Highway Administration, McLean, Va.

Kim D.S., Park S. Y. (2011), "Relationship Between the Subgrade Reaction Modulus and the Strain Modulus Obtained Using a Plate Loading Test. " World Congress, Railway Research, may 22-26-2011.

Kuttah DK, and Sato KS., (2015), "Review on the effect of gypsum content on soil behavior. " Transportation Geotechnics 2015, Elsevier, pp. 2214-3912.

Lin, D., Liau, C., and Lin, J., 2006, "Factors Affecting Portable Falling Weight Deflectometer Measurements, " J. Geotech. Geoenviron. Eng., Vol. 132, No. 6, 804–808.

Louay, N. M., Munir, D. N., Murad, Y. A., and Alshibli, K. (2009). "Estimation of Subgrade Soils Resilient Modulus from In-Situ Devices Test Results." Journal of Testing and Evaluation (ASTM), 37(3), 1-9.

Madhira, M., Abhishek, S.V., and Rajyalakshmi K. (2015). "Modelling Ground – Foundation Interaction.", Innovations in Structural Engineering. PP.91-106

Marradi A., Pinori U., and Betti G., (2014). ‘‘Subgrade and Foundation Dynamic Performance Evaluation by Means of Lightweight Deflectometer Tests.’’ Transportation Research Record: Journal of the Transportation Research Board, No. 2457, Transportation Research Board of the National Academies, Washington, D.C., 2014, pp. 51–57.

Meyerhof, G.G. (1965): "Shallow foundations.", Journal of the Soil Mechanics and Foundations Division, ASCE, 1965(Vol. 91(2)) pp 21-31.

Moayed, R. Z. and Naeini S.A. (2006), "Evaluation of modulus of subgrade reaction (Ks) in gravely soils based on SPT results. ", International Association for Engineering Geology and the Environment 2006, Issue 505. PP. 1-6

Mohamed, F.M.O., and Vanapalli, S. K. (2012),” Estimation of Bearing Capacity of Saturated and Unsaturated Sands from the SPT and CPT Correlations”, Advances in Civil, Environmental, and Materials Research (ACEM’ 12) Seoul, Korea, August 26-30, 2012, pp. 1992-2005.

Naeini. S. A., and Taherabadi. E. (2015). "Numerical and Theoretical Study of Plate Load Test to Define Coefficient of Subgrade Reaction. ", Geotechnical and Transportation

Engineering: Journal of Geotechnical and Transportation Engineering - 2015 vol. 1 (2) Volume 1 | Issue 2

Nazarian, S., Ii, Kenneth, H. S. and Hudson, W R, (1983). "Use of Spectral Analysis of Surface Waves Method for Determination of Moduli and Thicknesses of Pavement Systems. ", Transportation Research Board, ISSN:1930. pp 38-45.

Nazzal, M., Abu-Farsakh, M., Alshibli, K., & Mohammad, L. (2007), "Evaluating the Light Falling Weight Deflectometer Device for in Situ Measurement of Elastic Modulus of Pavement Layers." Transportation Research Record: Journal of the Transportation Research Board, Vol. 2016, No.1, pp. 13-22.

Nazzal, M., Abu-Farsakh, M., Alshibli, K., & Mohammad, L. (2016). "Evaluating the Light Falling Weight Deflectometer Device for in Situ Measurement of Elastic Modulus of Pavement Layers." Transportation Research Record: Journal of the Transportation Research Board, 2016, 13–22.

Oh, W. T., and Vanapalli, S. K. (2013). "Scale Effect of Plate Load Tests in Unsaturated Soils." International Journal of Geomaterials, June, 2013, Vol. 4, No. Japan4(2), 585–594.

Ohio River Division. (1943). " Field bearing tests on natural subgrade and prepared subbase using different size bearing Plates. Cincinnati", OH: U.S. Army Corps of Engineers, Ohio River Division Engineers, Cincinnati Testing Laboratory

Palix, E. T. Willems, and S. Kay., (2011)., "Caisson capacity in clay: VHM resistance envelope – Part1: 3D FEM numerical study."

Peck, R. B. Hanson, W. E., and Thornburn T. H., (1997), "Foundation Engineering-Second Edition ", New York 1997.

Ping L. S. and Yang L. W., (1998) "Subgrade Reaction and Load-Settlement Characteristics of Gravelly Cobble Deposits by Plate-Load Tests," Canadian geotechnical Journal, Vol. 35, No. 5, 1998, pp. 801-810.

Ping, W., and Sheng, B. (2011). "Developing Correlation Relationship Between Modulus of Subgrade Reaction and Resilient Modulus for Florida Subgrade Soils. " Transportation Research Record: Journal of the Transportation Research Board, 2232(11), 95–107.

PLAXIS. (2013). "Finite Element Analyses - PLAXIS Reference Manual." 3D-PLAXIS, Version 1.5.

Rao, C., George, V., and Shiva Shankar, R. (2008). "PFWD, CBR and DCP Evaluation of Lateritic Subgrades of Dakshina Kannada, India." The 12th International Conference of International Association for Computer Methods and Advances in Geotechnics (IACMAG), National Institute of Technology Karnataka, Mangalore, India, Goa, India, 4417-4423.

Rao, S.S. (2011)., "The Finite Element Method in Engineering, Fifth Edition." Elsevier 2011, ISBN 978-1-85617-661-3, pp 726,

Razouki SS, Al-Omari RR, Nashat IH, Razouki HF, and Khalid S., (1994), "The problem of gypsiferous soils in Iraq. In: Proceedings of the sumposium on gypsiferous soils and their effect on structures.", NCCL, Baghdad; 1994. p. 7–33.

Razouki SS, and Ibrahim A.N. (2019), "Improving the resilient modulus of a gypsum sand roadbed soil by increased compaction." International Journal of Pavement Engineering, 20:4, pp. 432-438.

Razouki SS, and Kuttah DK. (2004), "Effect of soaking period and surcharge load on resilient modulus and California bearing ratio of gypsiferous soils.", Quarterly Journal of Engineering Geology and Hydrogeology, Vol. 37, pp.155–164.

Reza Z. M. and Masoud J. (2008), "Foundation Size Effect on Modulus of Subgrade Reaction in Clay Soil. ", the Electronic Journal of Geotechnical Engineering, Vol. 13, 2008, pp. 1-8

Roesset, J. M. (1998), "Nondestructive Dynamic Testing of Soils and Pavements. "Tamkang Journal of Science and Engineering, vol.1, No. 2, pp. 61-81.

Selvadurai, A.P.S. (1984).: "The flexure of an infinite strip of finite width embedded in an isotropic elastic medium of finite extent", Int. J. Numer. Anal. Meth. Geomech, 1984(Vol. 8) pp 157-166.

Setiadji B. H., and Fwa T. F., ASCE. M. (2009). "Examining k - E Relationship of Pavement Subgrade Based on Load-Deflection Consideration." Journal of Transportation Engineering, Vol. 135, No. 3, March 1, 2009. ©ASCE, ISSN.

Shaban, A. M. (2016), "Evaluation of Unbound Pavement Layers Moduli Using the Miniaturized Pressuremeter Test." PhD dissertation. Florida Institute of Technology, Melbourne, 2016.

Shaban, A., and Cosentino, P., (2016), " Comparative Analyses of Granular Pavement Moduli Measured from Lightweight Deflectometer and Miniaturized Pressuremeter Tests." Transportation Research Record: Journal of the Transportation Research Board, Vol. 2016, No.2579, pp. 48-58.

Siddiqi, Q. S. and Hudson, W. R. (1970). "Experimental Evaluation of Subgrade Modulus and Its Application in Small-Dimension Slab Studies.", Research Report Number 56-16, The Texas Highway Department Interagency Contract No. 4613-1007.

Teodoru, I. B, and TOMA, I. O. (2009). "Numerical Analyses of Plate Loading Test.", Journal: Bulletin of the Polytechnic Institute of Jessy, Constructions. Architecture Section, Vol. LV (LIX) 1, 2009, PP. 57-69

Terzaghi, K. (1943), "Theoretical Soil Mechanics", Wiley, New York

Terzaghi, K. (1955), "Evaluation of Coefficients of Subgrade Reaction,", Géotechnique, Vol. 5, No. 4, 1955, pp. 297-326.

Tuleubekov K., and D.R. Brill. (2014)."Correlation between Subgrade Reaction Modulus and CBR for Airport Pavement Subgrades." T&DI ©ASCE 2014.

Tuse B.B., Patil A. P., Parkhe, D.D**.** (2016). ‘‘Compilation of plate bearing test data’’. International Journal of Advances in Science Engineering and Technology, ISSN: 2321-9009, Vol-4, Iss-4, Spl. Issue-2 Dec.-2016.

Tuse, B.B., Patil, A. P., and Parkhe, D.D**.** (2016). " Compilation of Plate Bearing Test Data", International Journal of Advances in Science Engineering and Technology, ISSN: 2321-9009, Vol-4, Iss-4 Issue-2 Dec.-2016

U.S. Army Waterways Experiment Station. (1945). " Rigid plate bearing test investigation. ", Vicksburg, MS: U.S. Army Waterways Experiment Station.

Ullidtz, P. _1987_. *Pavement analysis*, Elsevier, Amsterdam, The Netherlands.

Unified Facilities Criteria (UFC). (2001). "Pavement design for airfields". UFC 3-260-02. Washington, DC: Departments of the Army, Air Force, and Navy.

Vennapusa K. R., and White J. (2013)."Comparison of Light Weight Deflectometer Measurements for Pavement Foundation Materials." Geotechnical Testing Journal, Vol. 32, No. 3. pp 1-13.

Vesic, A. B. (1961), "Beams on Elastic Subgrade and Winkler's Hypothesis, " Proceedings of the 5th of International conference on Soil Mechanics and Foundation Engineering, Paris, 1961, pp. 845-850.

Vesic, A. S., and K. Saxena. 1974. "Analysis of structural behavior of AASHO road test rigid pavements." NCHRP Report No. 97. Washington, D.C: Highway Research Board.

Zhang, J., (2010). "Evaluation of mechanistic-based compaction measurements for earthwork QC/QA", Iowa State University Capstones, Theses and Dissertations

Appendix A: LWD Testing Curves

A-1: A-1-b Soil Curves

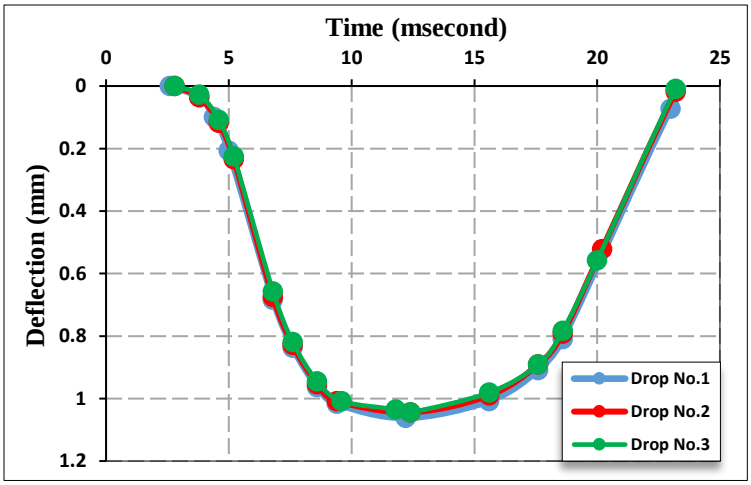

Figure (A.1.1): Point one time-deflection curve of LWD for A-1-b soil (No. of passing 8)

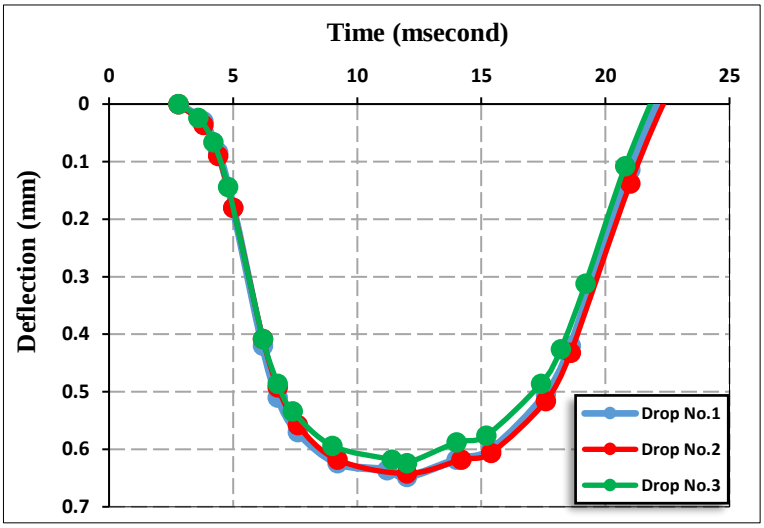

Figure (A.1.2): Point two time-deflection curve of LWD for A-1-b soil (No. of passing 8)

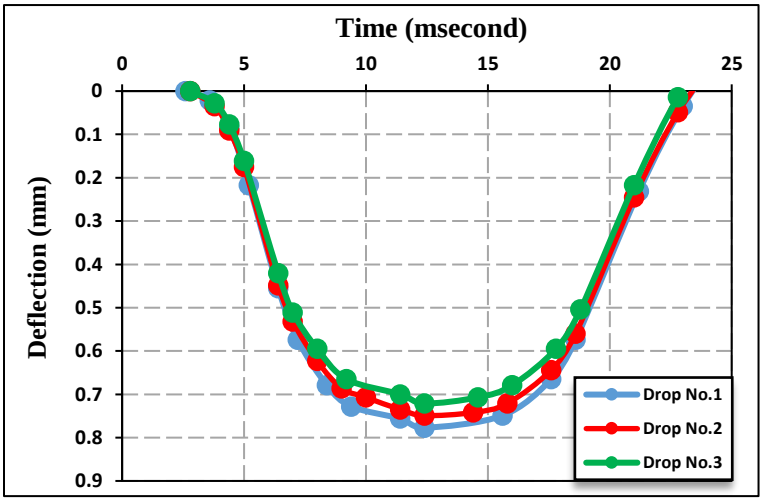

Figure (A.1.3): Point three time-deflection curve of LWD for A-1-b soil (No. of passing 8)

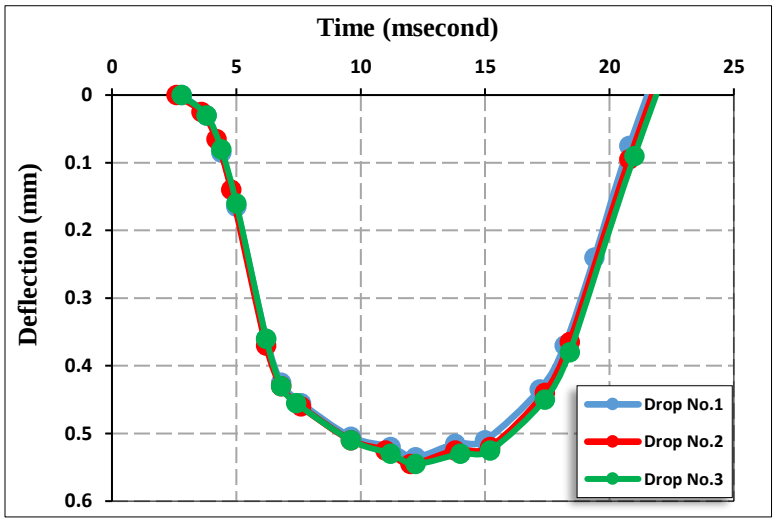

Figure (A.1.4): Point four time-deflection curve of LWD for A-1-b soil (No. of passing 8)

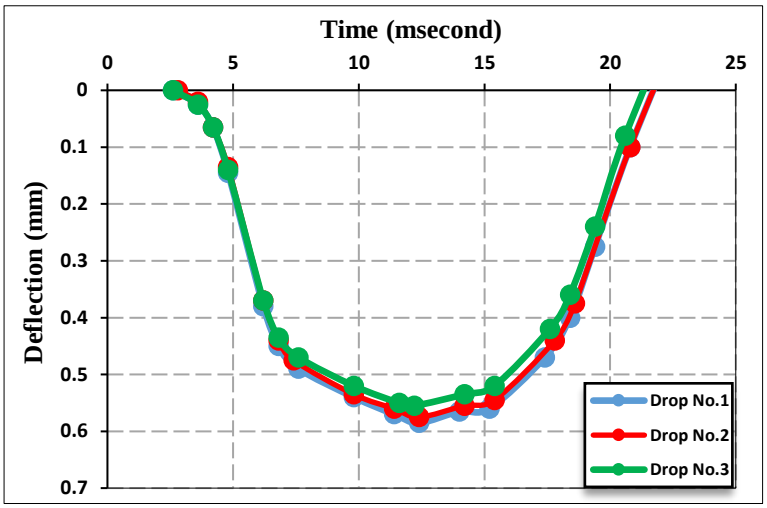

Figure (A.1.5): Point five time-deflection curve of LWD for A-1-b soil (No. of passing 8)

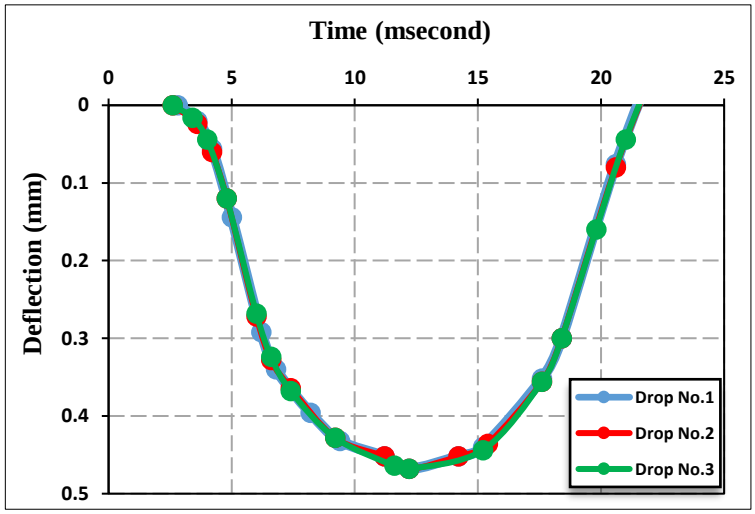

Figure (A.1.6): Point six time-deflection curve of LWD for A-1-b soil (No. of passing 8)

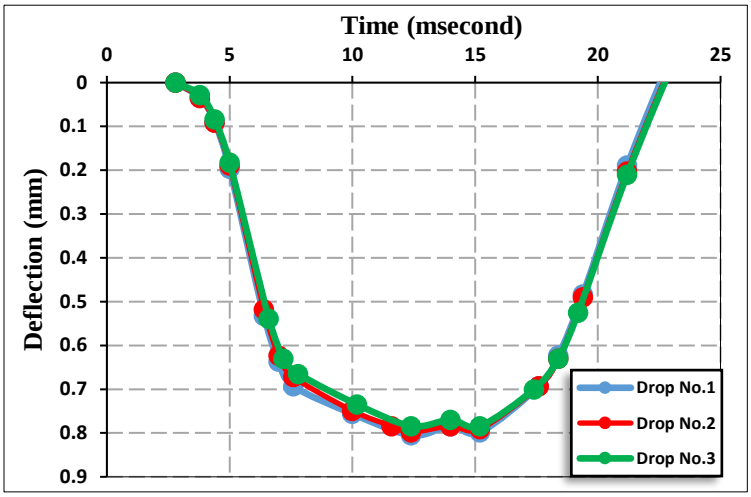

Figure (A.1.7): Point one time-deflection curve of LWD for A-1-b soil (No. of passing 12)

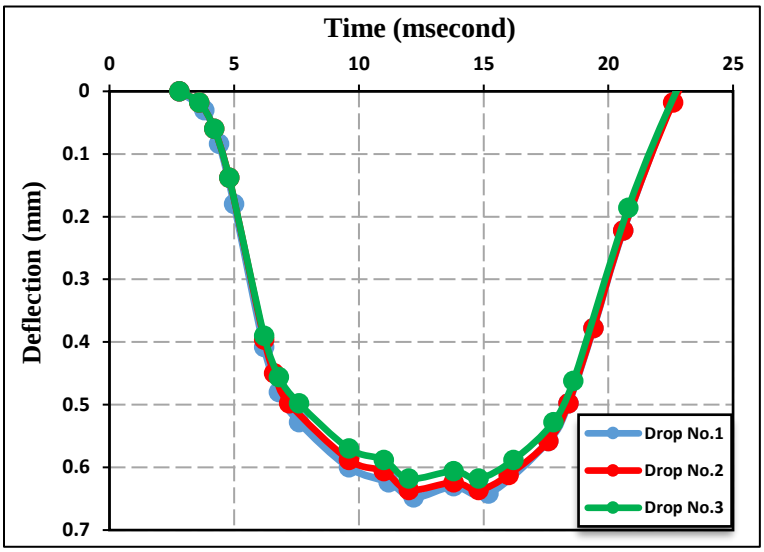

Figure (A.1.8): Point two time-deflection curve of LWD for A-1-b soil (No. of passing 12)

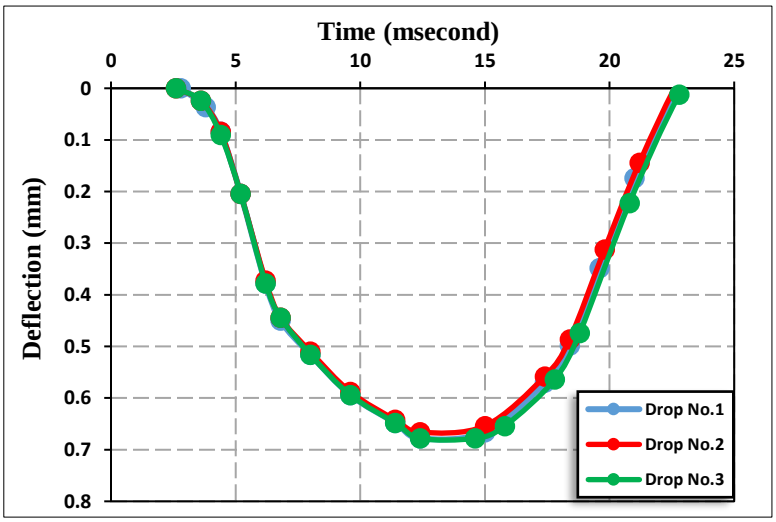

Figure (A.1.9): Point three time-deflection curve of LWD for A-1-b soil (No. of passing 16)

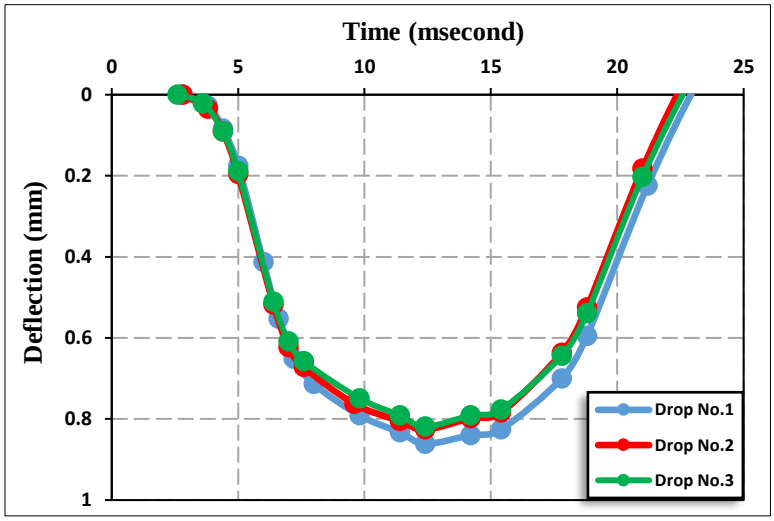

Figure (A.1.10): Point four time-deflection curve of LWD for A-1-b soil (No. of passing 12)

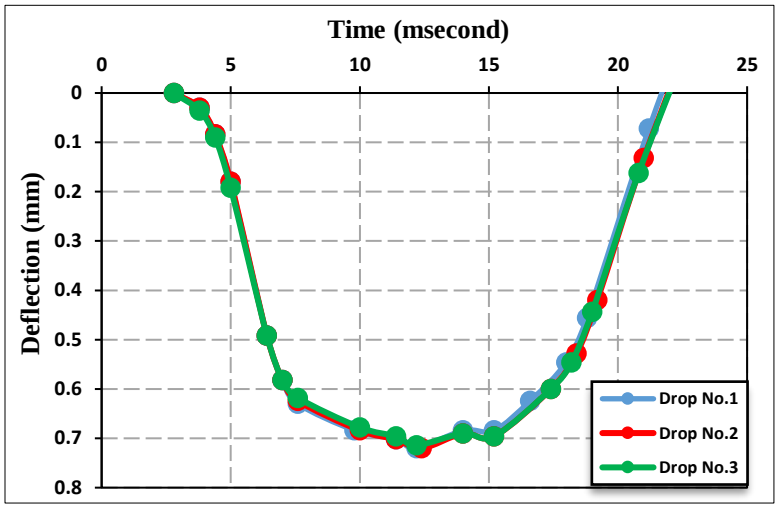

Figure (A.1.11): Point five time-deflection curve of LWD for A-1-b soil (No. of passing 12)

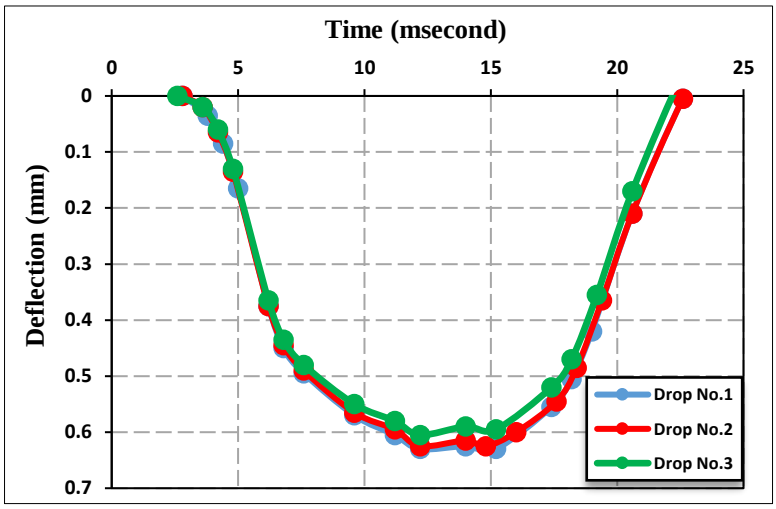

Figure (A.1.12): Point six time-deflection curve of LWD for A-1-b soil (No. of passing 12)

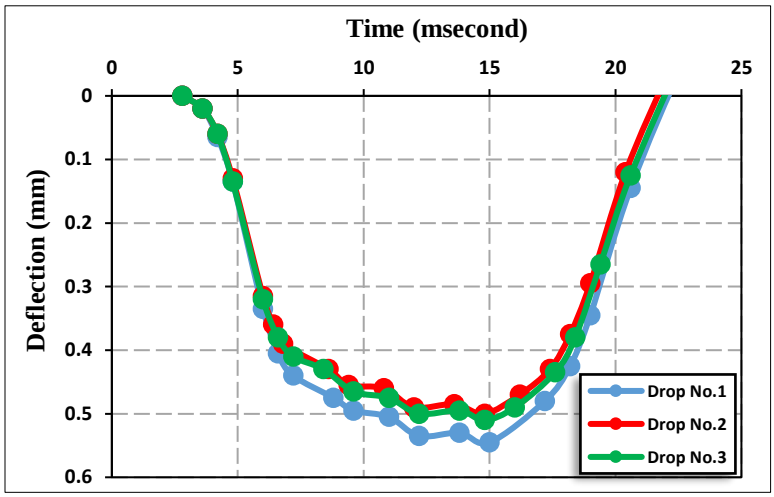

Figure (A.1.13): Point one time-deflection curve of LWD for A-1-b soil (No. of passing 16)

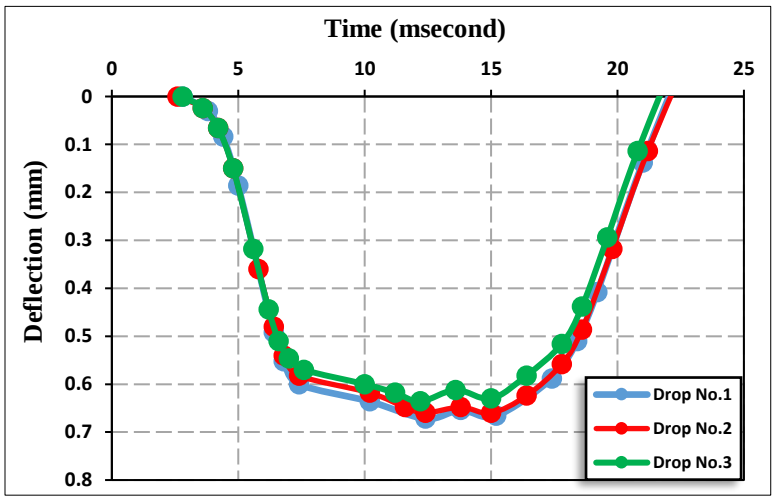

Figure (A.1.14): Point two time-deflection curve of LWD for A-1-b soil (No. of passing 16)

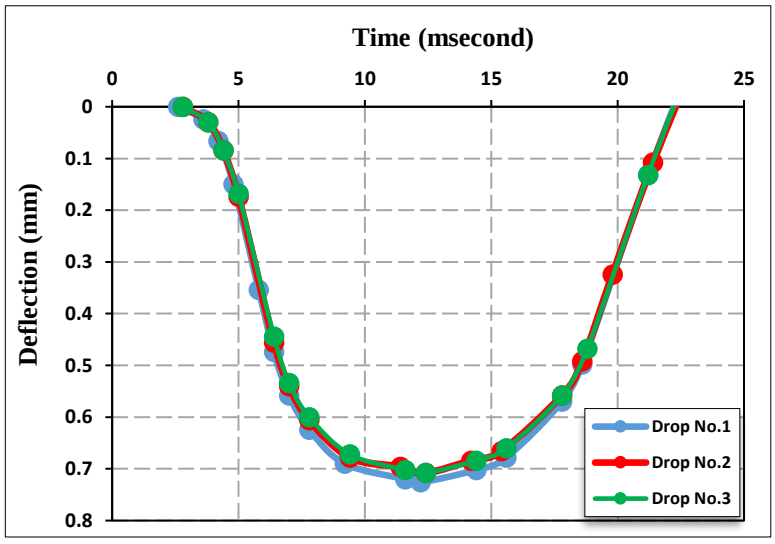

Figure (A.1.15): Point three time-deflection curve of LWD for A-1-b soil (No. of passing 16)

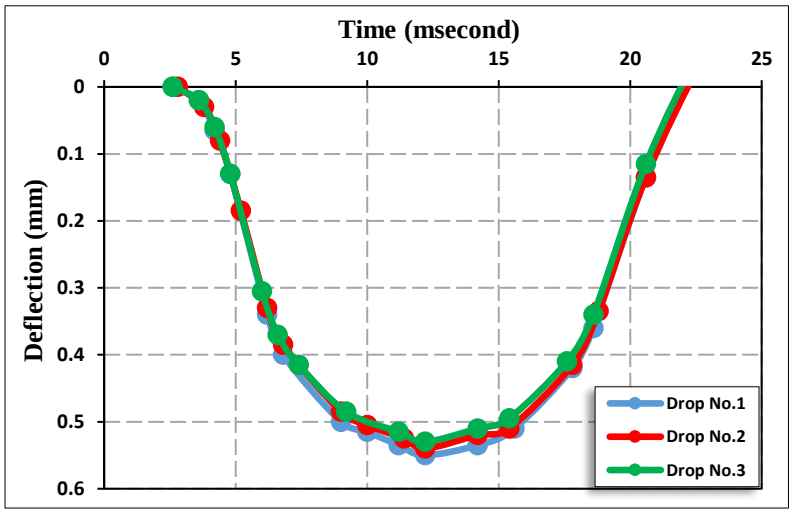

Figure (A.1.16): Point four time-deflection curve of LWD for A-1-b soil (No. of passing 16)

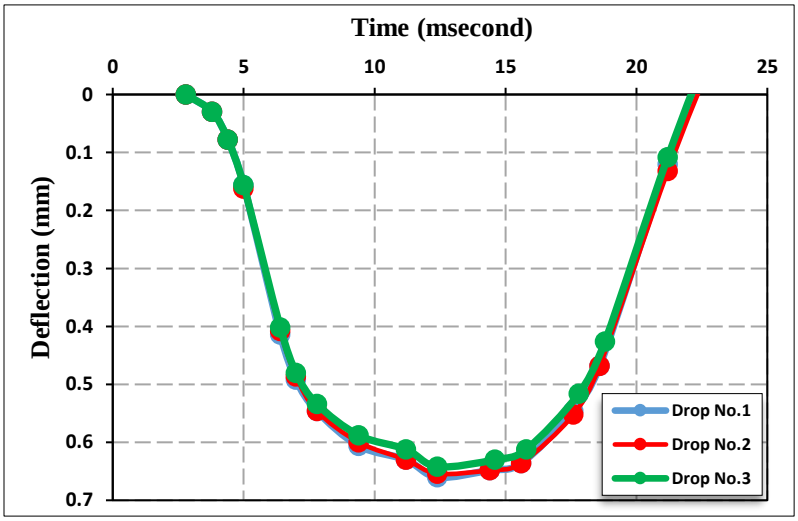

Figure (A.1.17): Point five time-deflection curve of LWD for A-1-b soil (No. of passing 16)

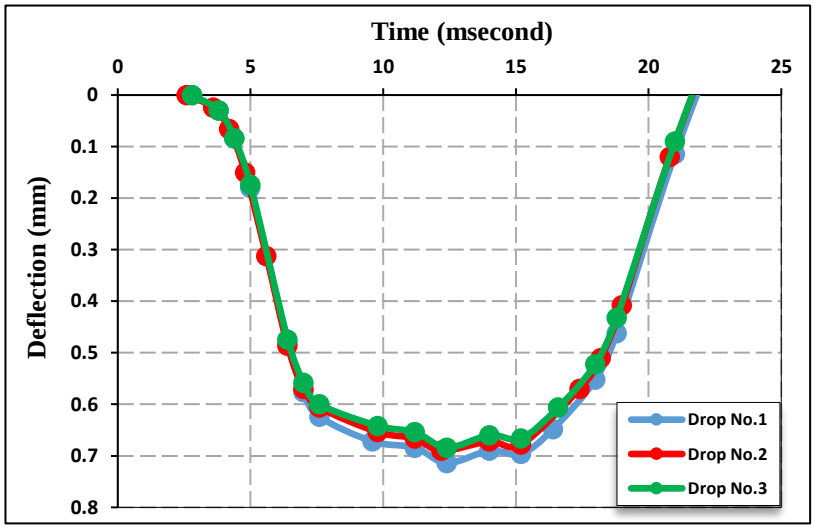

Figure (A.1.18): Point six time-deflection curve of LWD for A-1-b soil (No. of passing 16)

A-2: A-3 Soil Curves

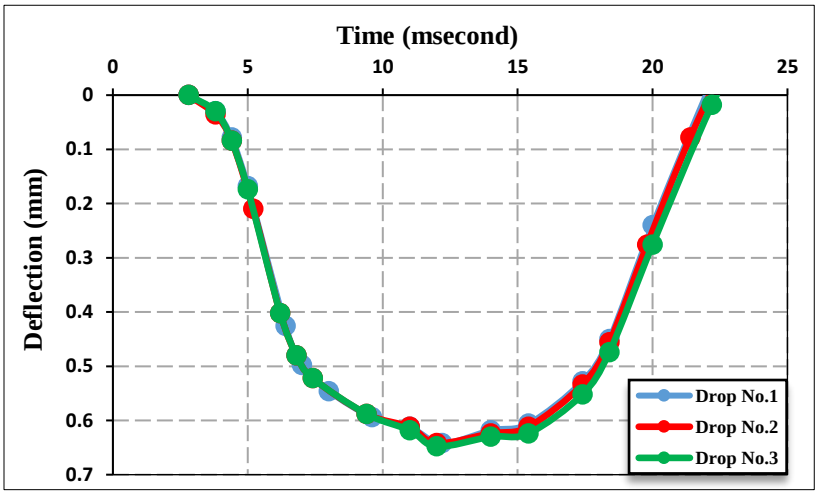

Figure (A.2.1): Point one time-deflection curve of LWD for A-3 soil (No. of passing 8)

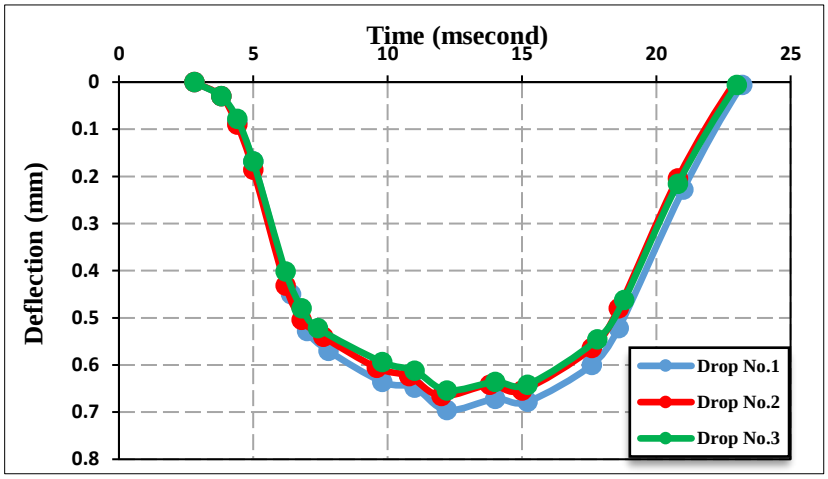

Figure (A.2.2): Point two time-deflection curve of LWD for A-3 soil (No. of passing 8)

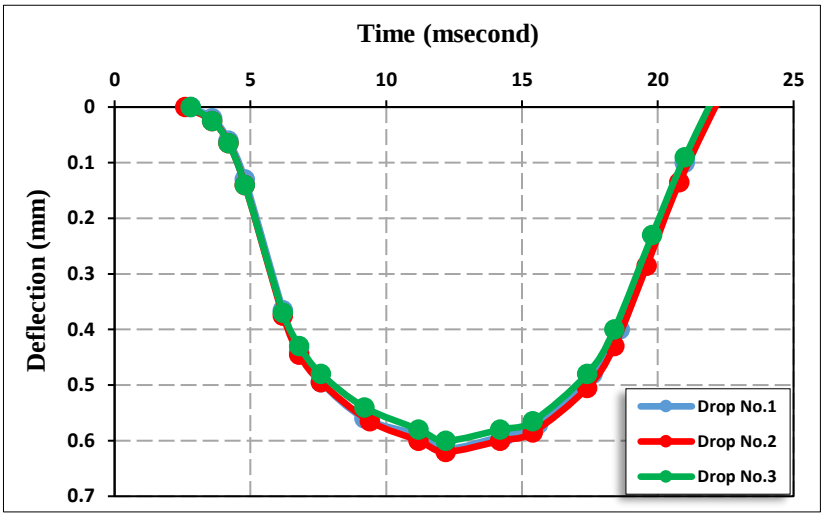

Figure (A.2.3): Point three time-deflection curve of LWD for A-3 soil (No. of passing 8)

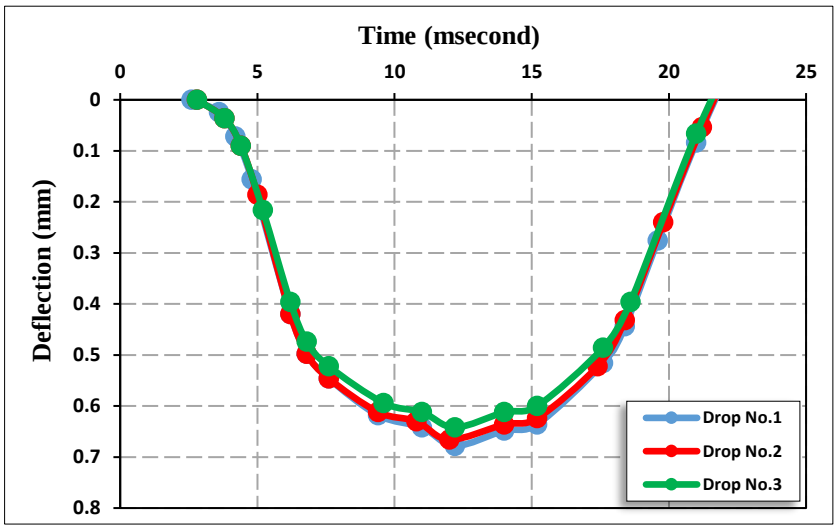

Figure (A.2.4): Point four time-deflection curve of LWD for A-3 soil (No. of passing 8)

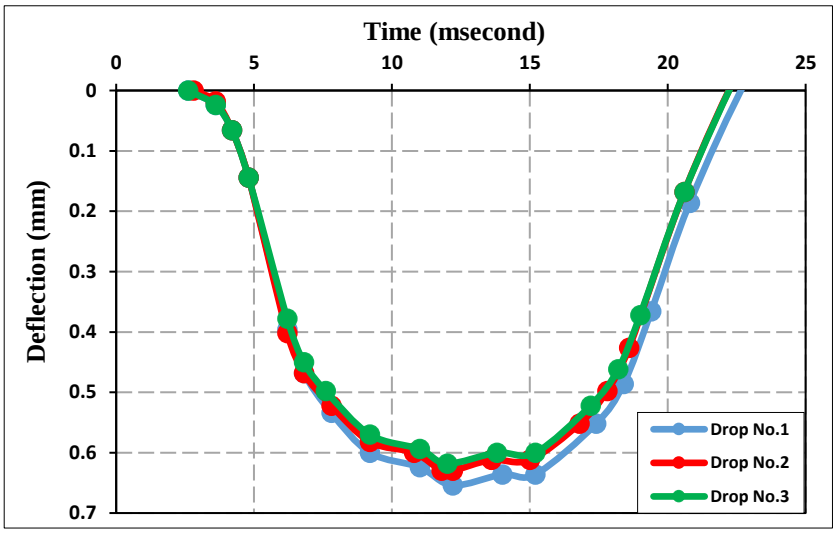

Figure (A.2.5): Point five time-deflection curve of LWD for A-3 soil (No. of passing 8)

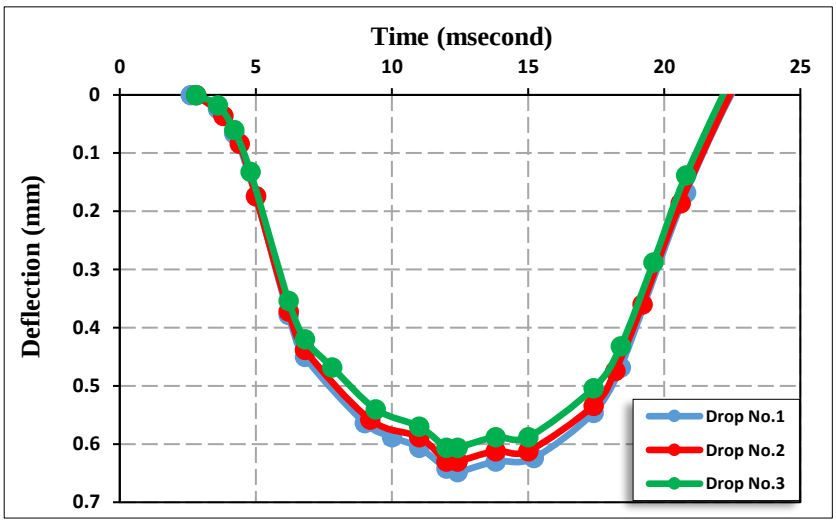

Figure (A.2.6): Point six time-deflection curve of LWD for A-3 soil (No. of passing 8)

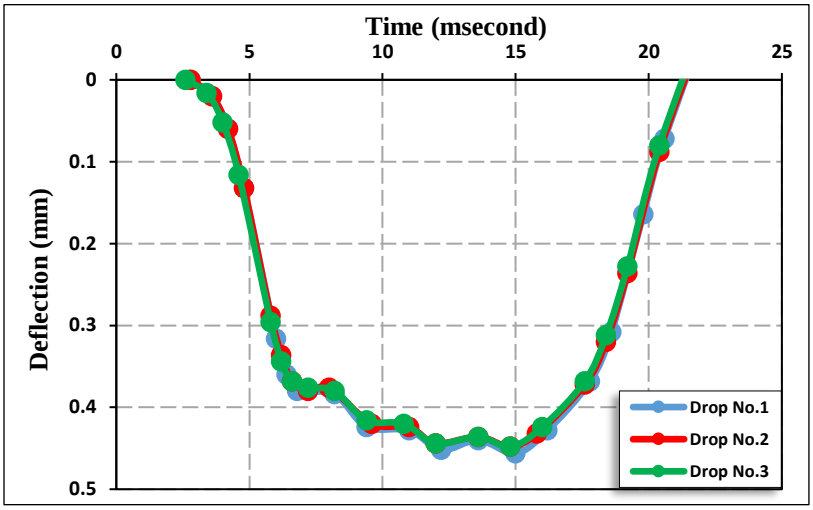

Figure (A.2.7): Point one time-deflection curve of LWD for A-3 soil (No. of passing 12)

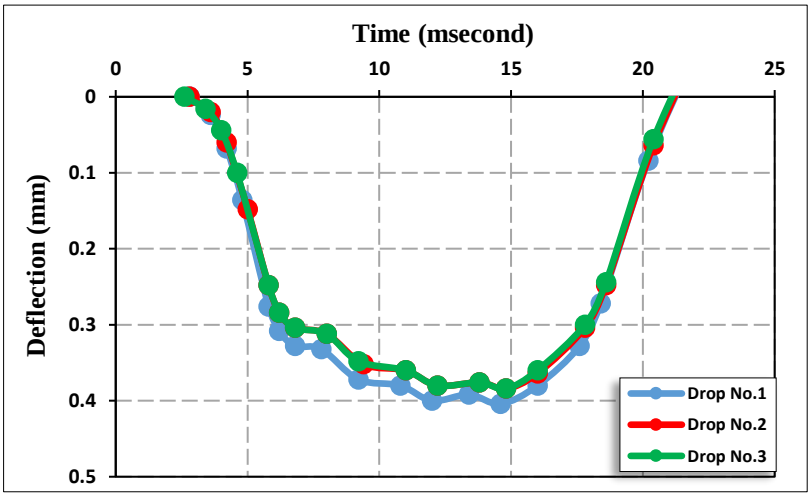

Figure (A.2.8): Point two time-deflection curve of LWD for A-3 soil (No. of passing 12)

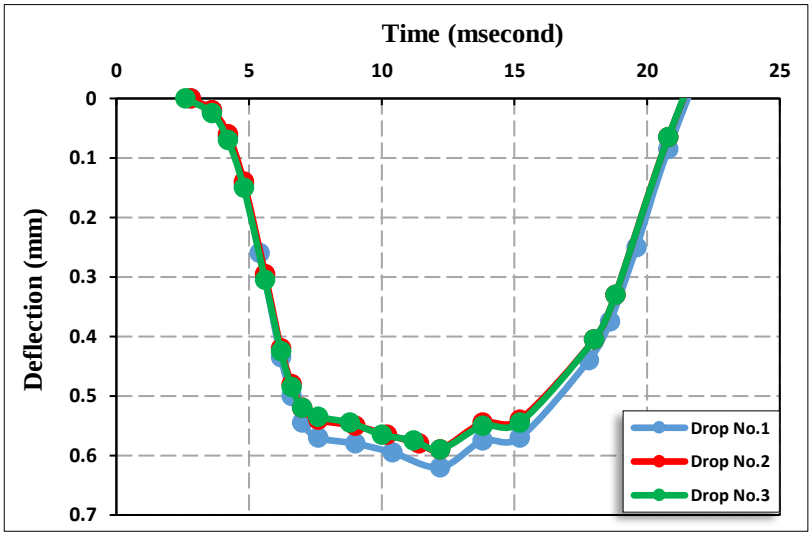

Figure (A.2.9): Point three time-deflection curve of LWD for A-3 soil (No. of passing 12)

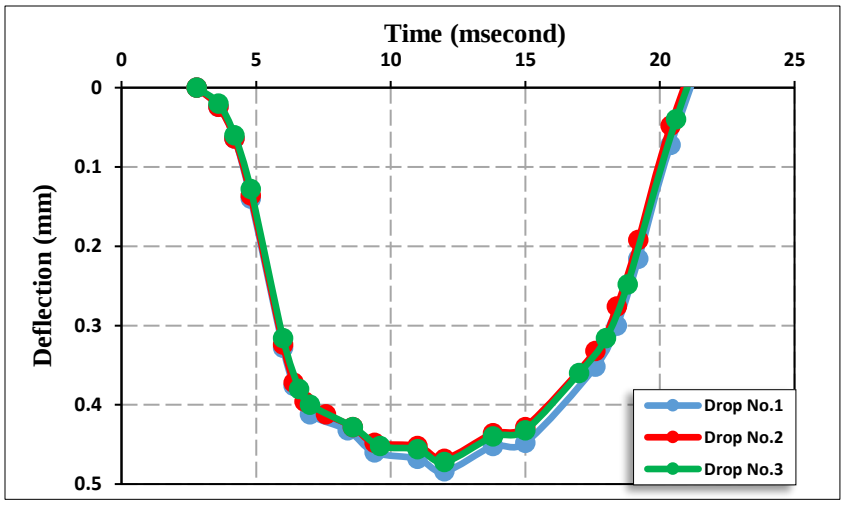

Figure (A.2.10): Point four time-deflection curve of LWD for A-3 soil (No. of passing 12)

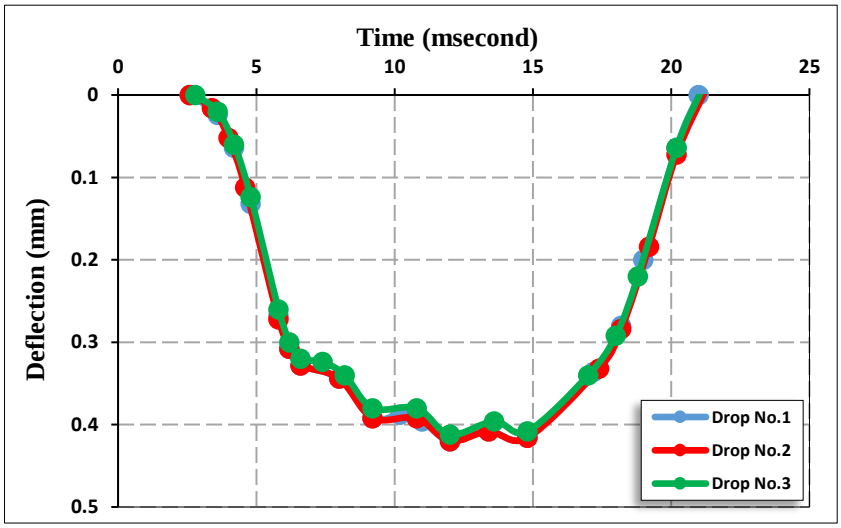

Figure (A.2.11): Point five time-deflection curve of LWD for A-3 soil (No. of passing 12)

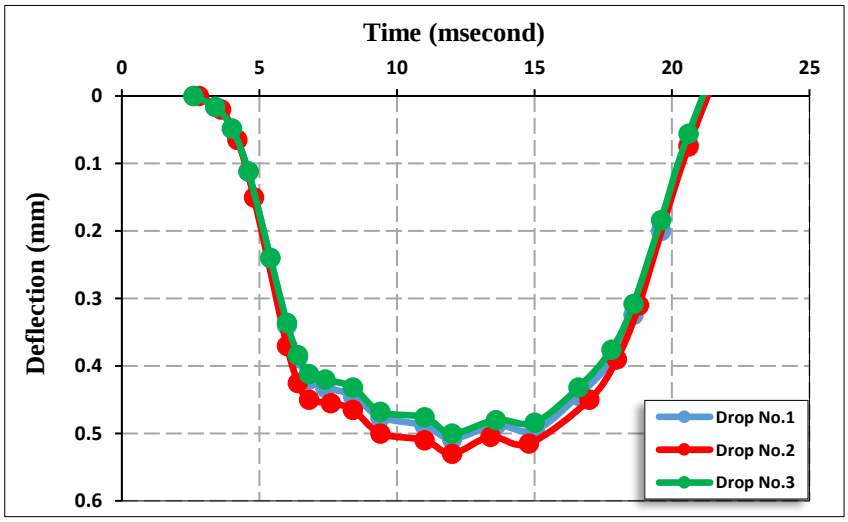

Figure (A.2.12): Point six time-deflection curve of LWD for A-3 soil (No. of passing 12)

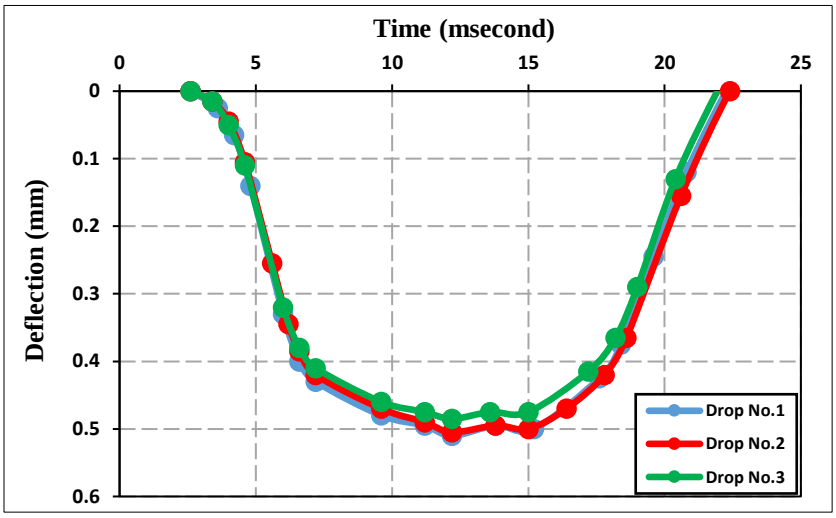

Figure (A.2.13): Point one time-deflection curve of LWD for A-3 soil (No. of passing 16)

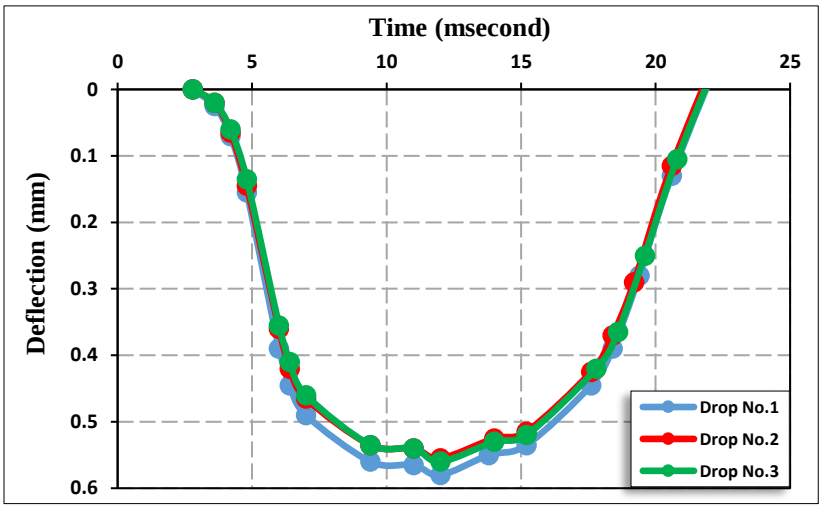

Figure (A.2.14): Point two time-deflection curve of LWD for A-3 soil (No. of passing 16)

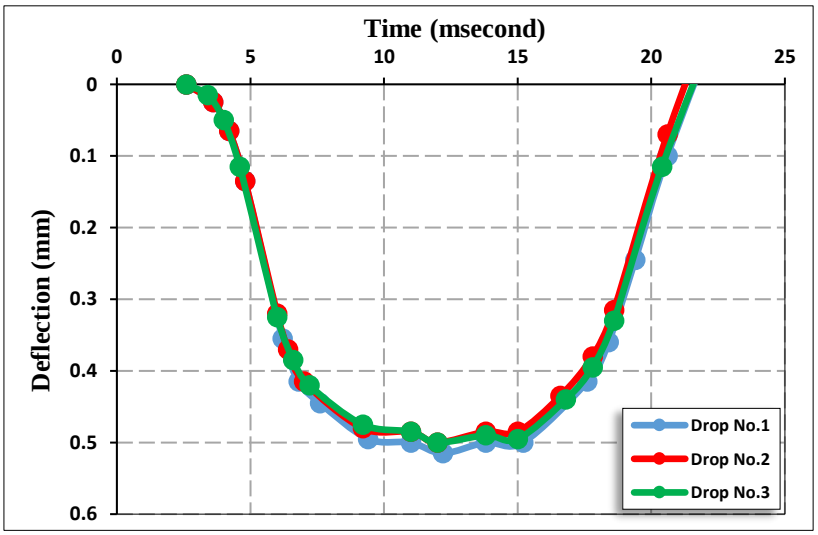

Figure (A.2.15): Point three time-deflection curve of LWD for A-3 soil (No. of passing 16)

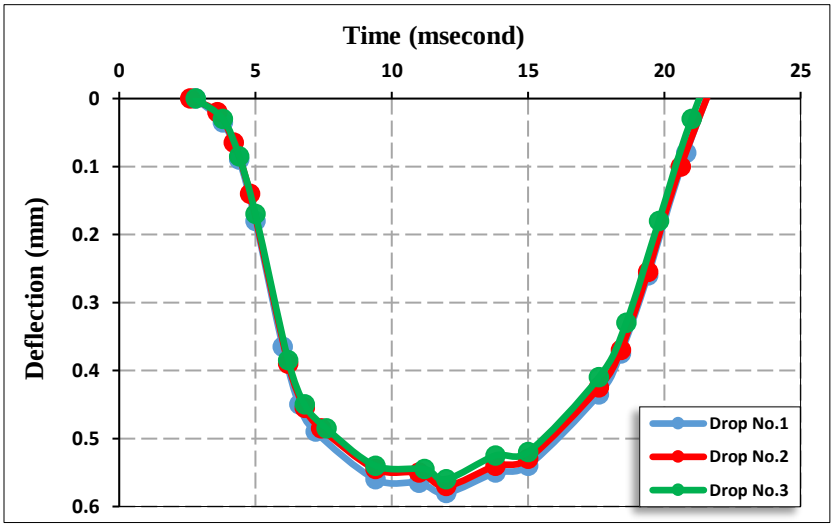

Figure (A.2.16): Point four time-deflection curve of LWD for A-3 soil (No. of passing 16)

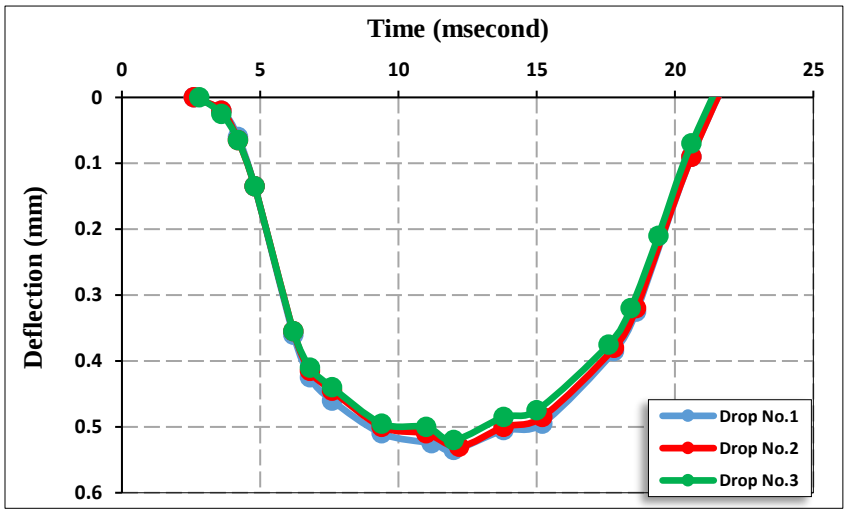

Figure (A.2.17): Point five time-deflection curve of LWD for A-3 soil (No. of passing 16)

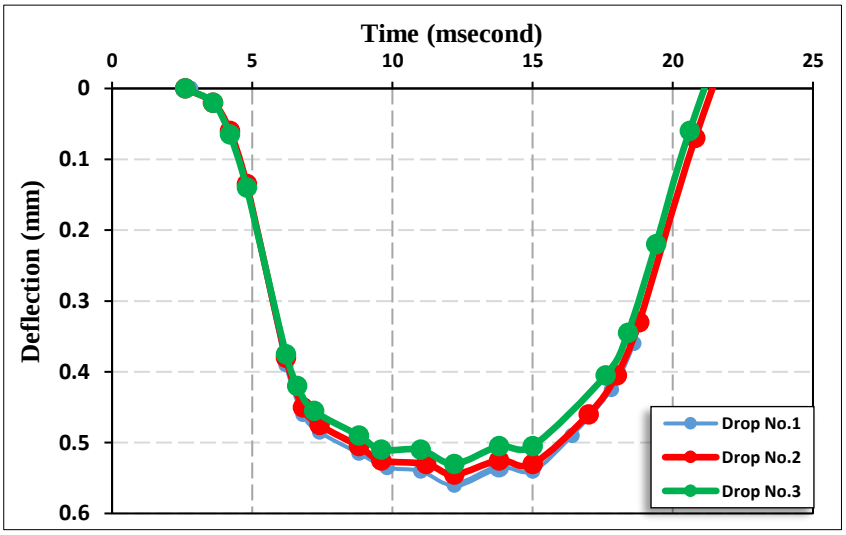

Figure (A.2.18): Point six time-deflection curve of LWD for A-3 soil (No. of passing 16)

A-3: A-7-6 Soil Curves

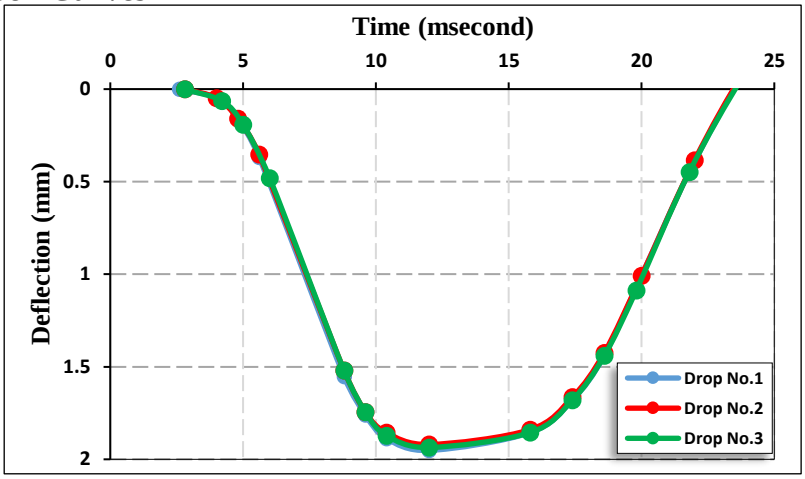

Figure (A.3.1): Point one time-deflection curve of LWD for A-7-6 soil (No. of passing 8)

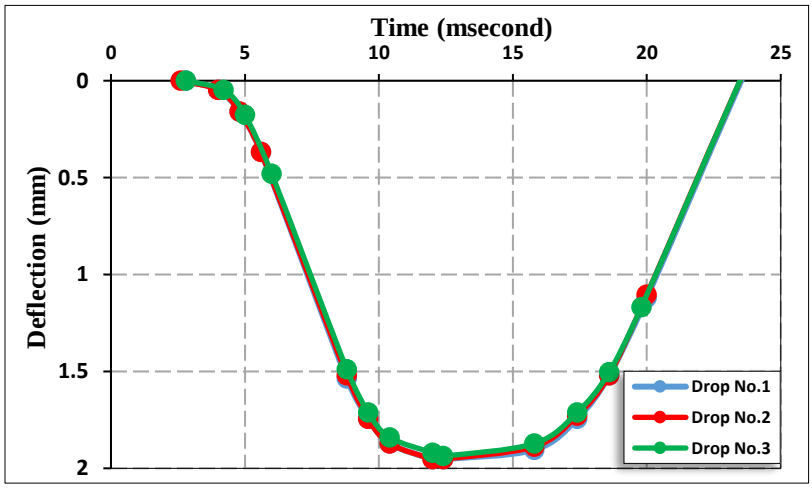

Figure (A.3.2): Point two time-deflection curve of LWD for A-7-6 soil (No. of passing 8)

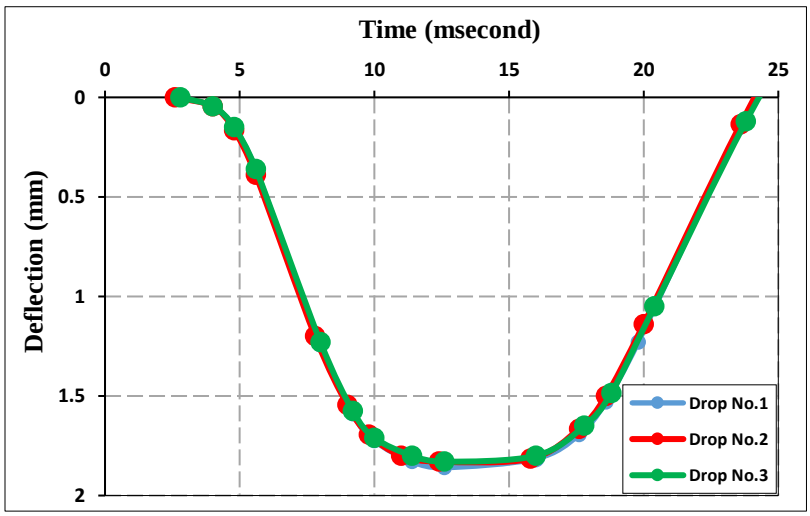

Figure (A.3.3): Point three time-deflection curve of LWD for A-7-6 soil (No. of passing 8)

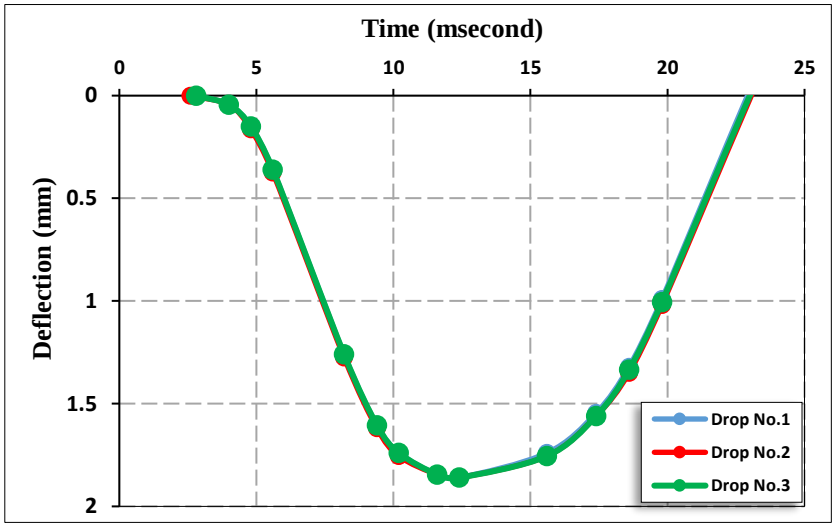

Figure (A.3.4): Point four time-deflection curve of LWD for A-7-6 soil (No. of passing 8)

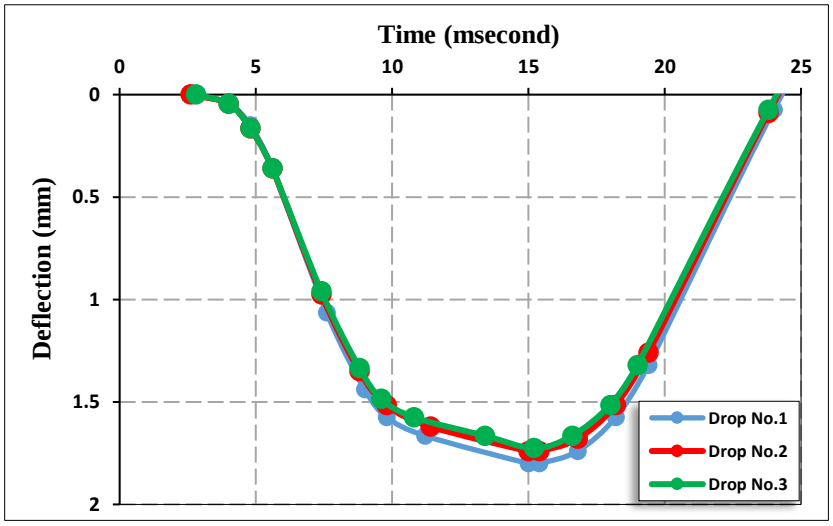

Figure (A.3.5): Point five time-deflection curve of LWD for A-7-6 soil (No. of passing 8)

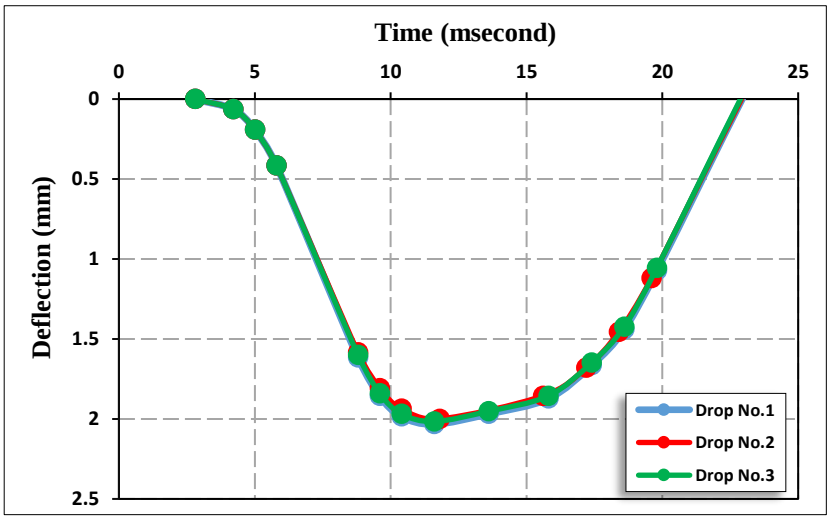

Figure (A.3.6): Point six time-deflection curve of LWD for A-7-6 soil (No. of passing 8)

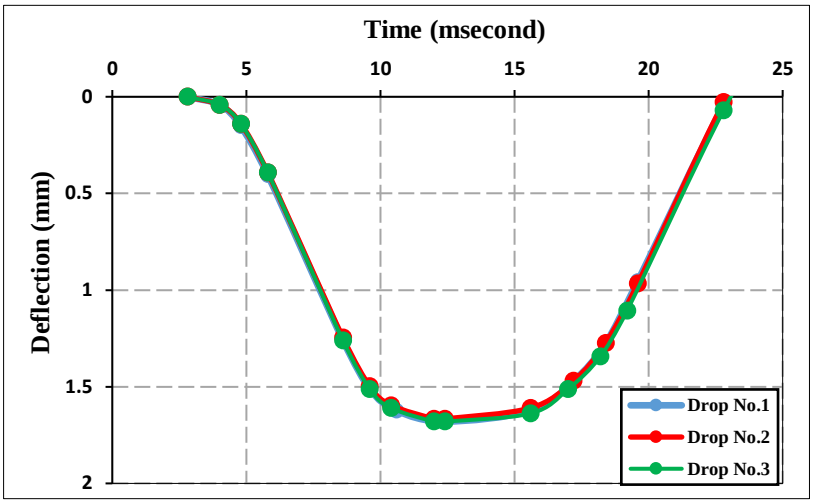

Figure (A.3.7): Point one time-deflection curve of LWD for A-7-6 soil (No. of passing 12)

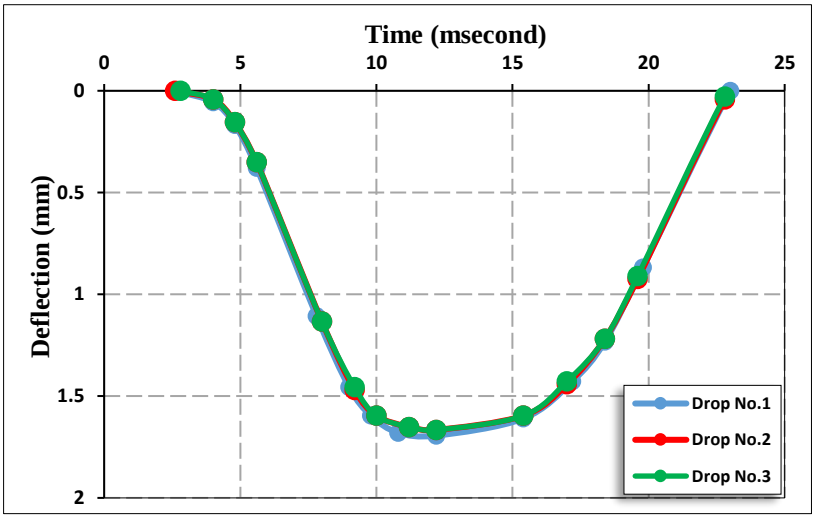

Figure (A.3.8): Point two time-deflection curve of LWD for A-7-6 soil (No. of passing 12)

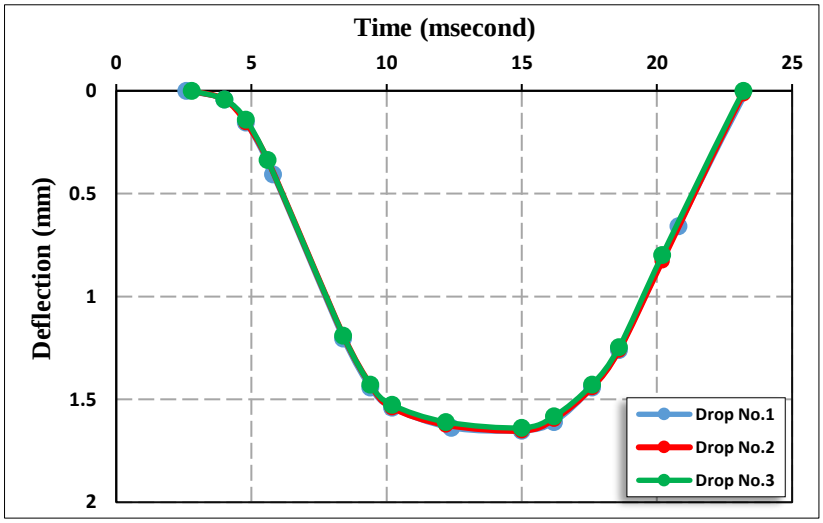

Figure (A.3.9): Point three time-deflection curve of LWD for A-7-6 soil (No. of passing 12)

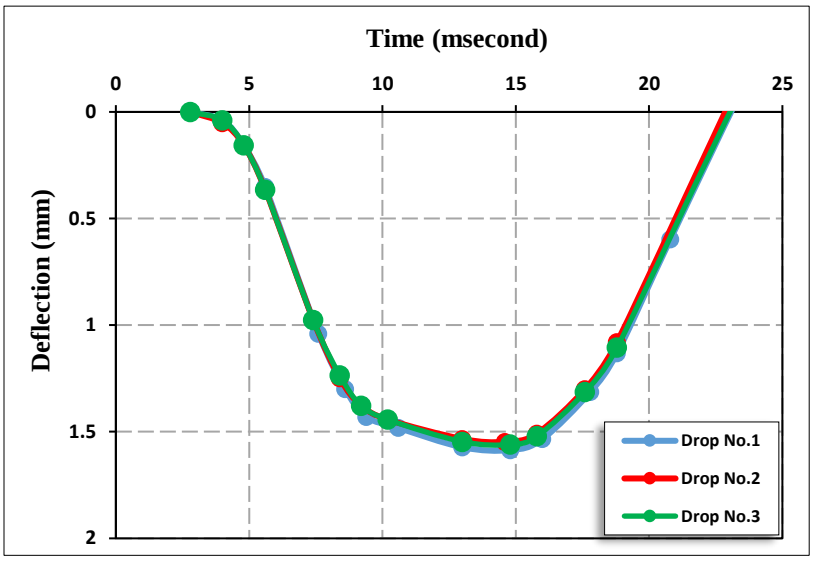

Figure (A.3.10): Point four time-deflection curve of LWD for A-7-6 soil (No. of passing 12)

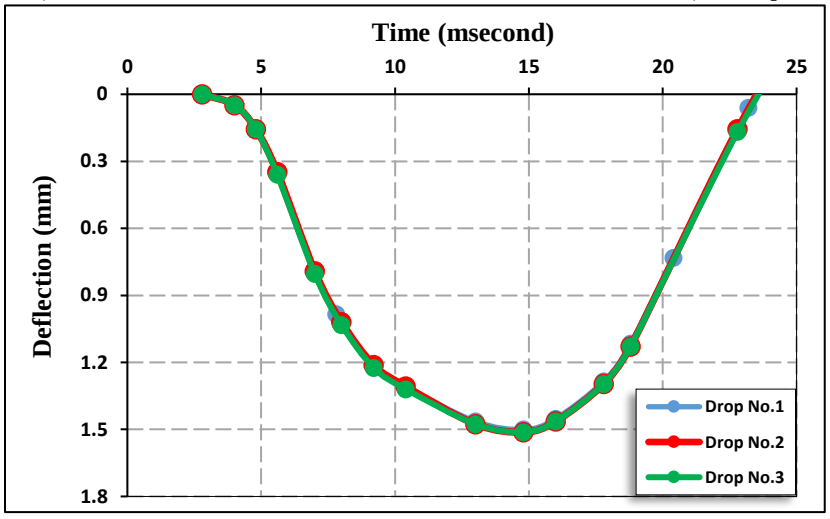

Figure (A.3.11): Point five time-deflection curve of LWD for A-7-6 soil (No. of passing 12)

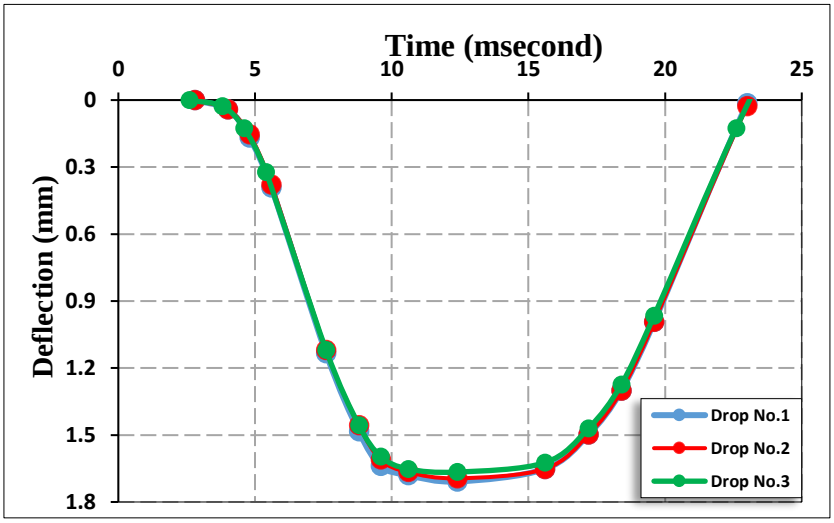

Figure (A.3.12): Point six time-deflection curve of LWD for A-7-6 soil (No. of passing 12)

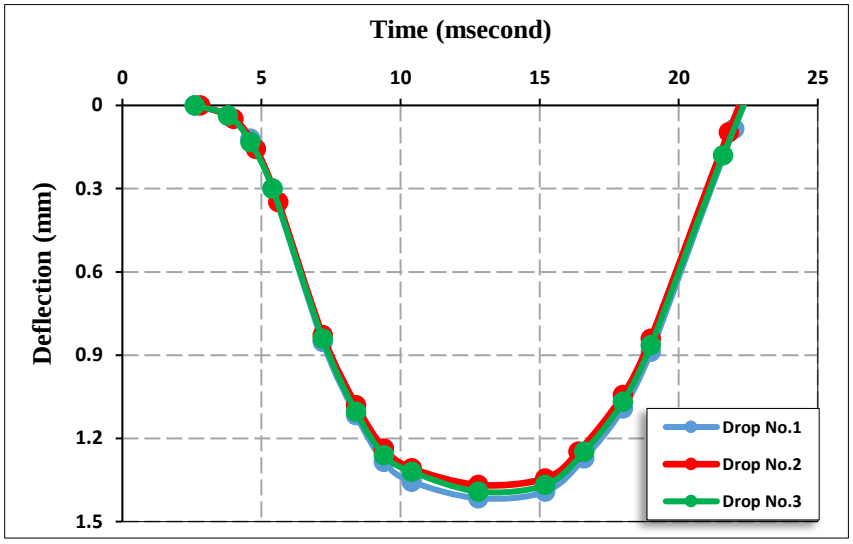

Figure (A.3.13): Point one time-deflection curve of LWD for A-7-6 soil (No. of passing 16)

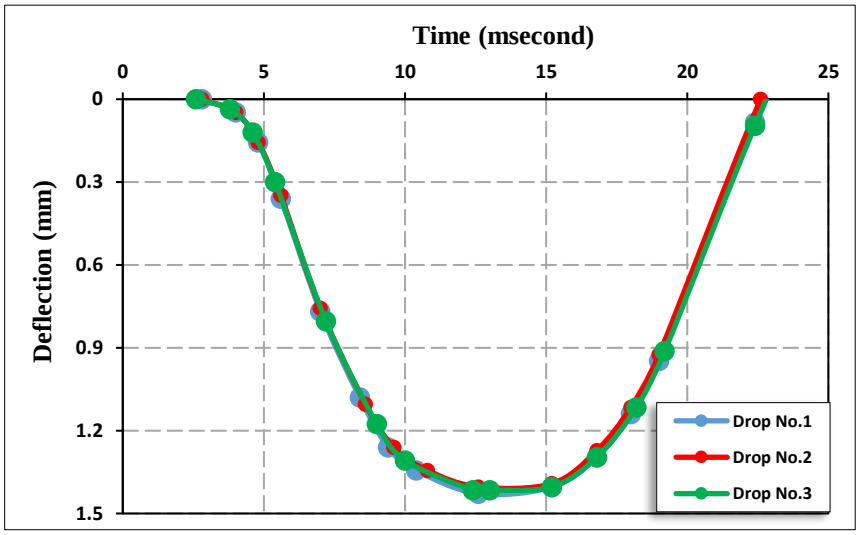

Figure (A.3.14): Point two time-deflection curve of LWD for A-7-6 soil (No. of passing 16)

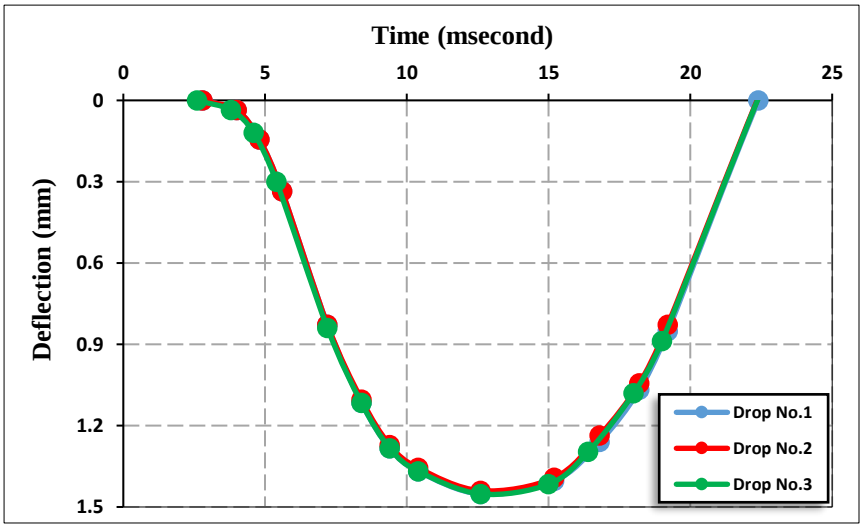

Figure (A.3.15): Point three time-deflection curve of LWD for A-7-6 soil (No. of passing 16)

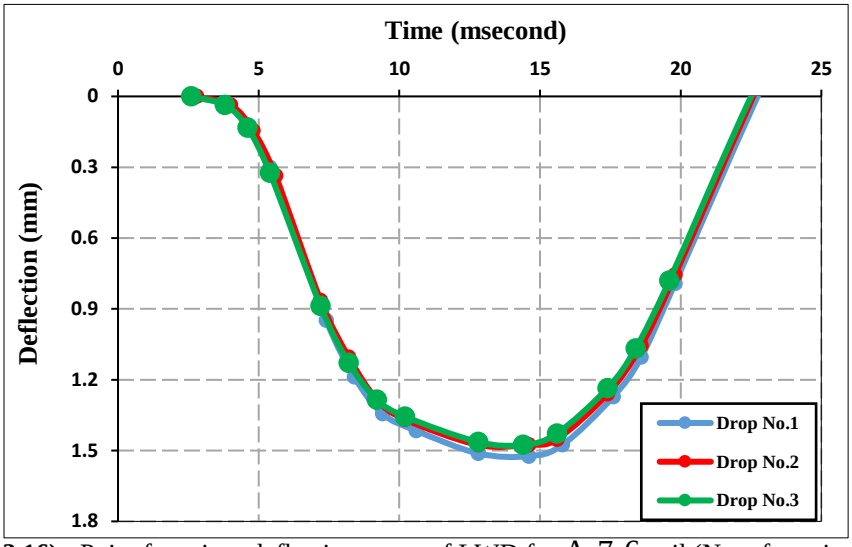

Figure (A.3.16): Point four time-deflection curve of LWD for A-7-6 soil (No. of passing 16)

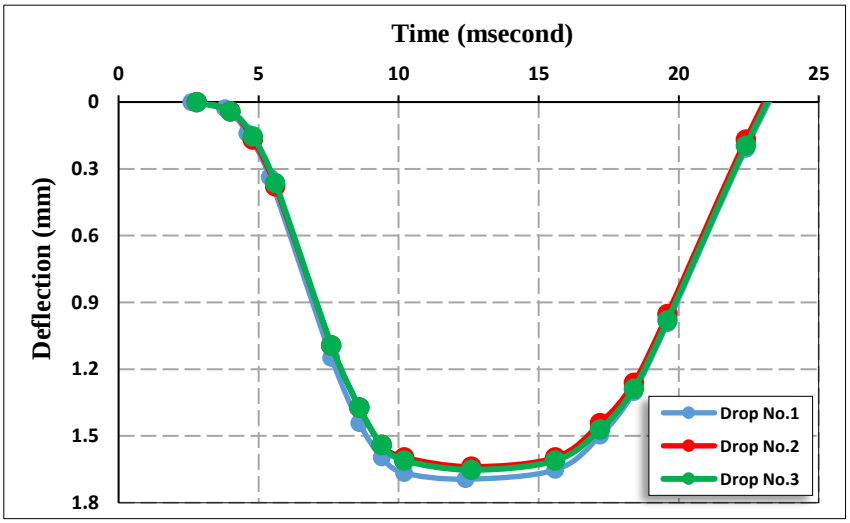

Figure (A.3.17): Point five time-deflection curve of LWD for A-7-6 soil (No. of passing 16)

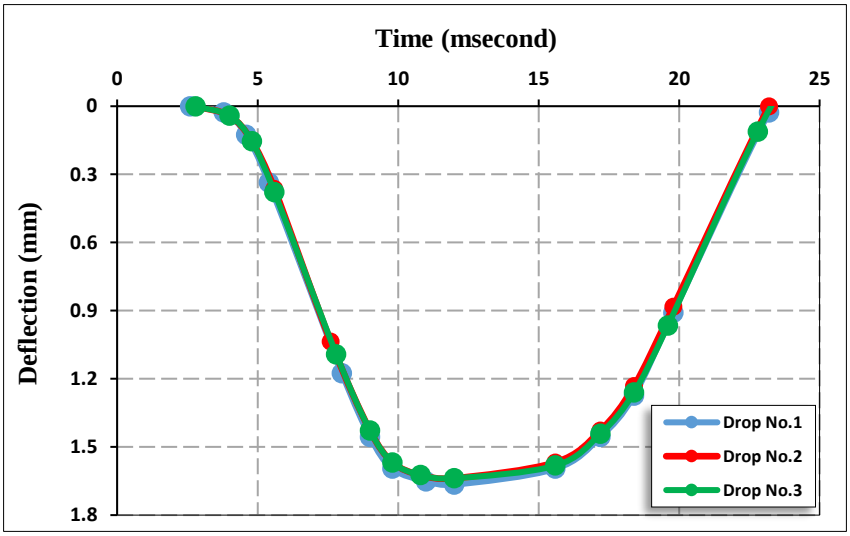

Figure (A.3.18): Point six time-deflection curve of LWD for A-7-6 soil (No. of passing 16)

Appendix B: Finite Element Curves

B-1: A-1-b Soil Curves

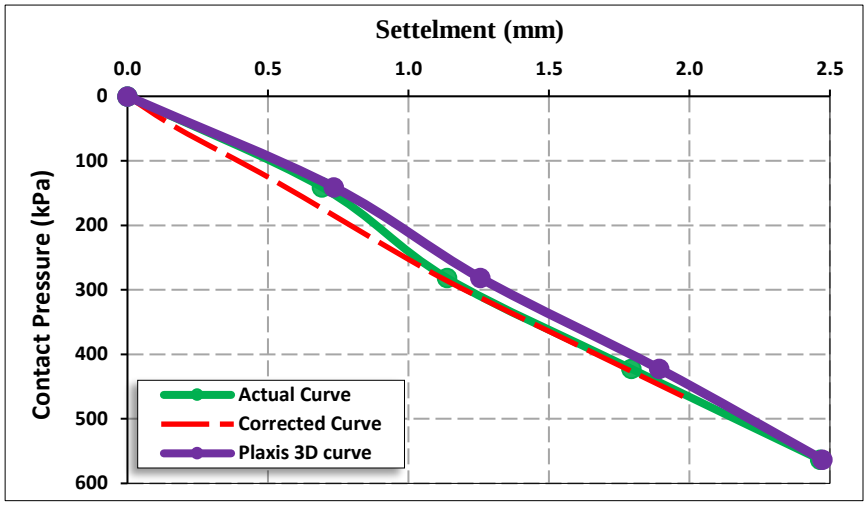

Figure (B.1.1): Point one simulated load – deformation curve for A-1-b soil (No. of passing 8)

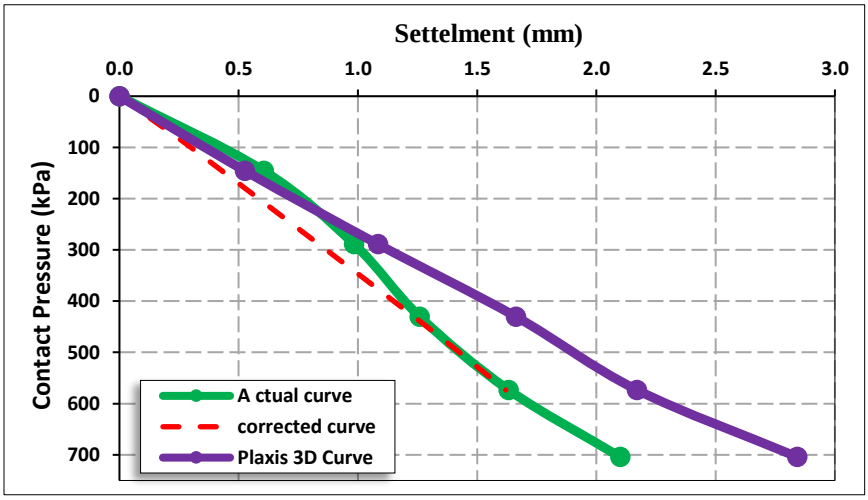

Figure (B.1.2): Point two simulated load – deformation curve for A-1-b soil (No. of passing 8)

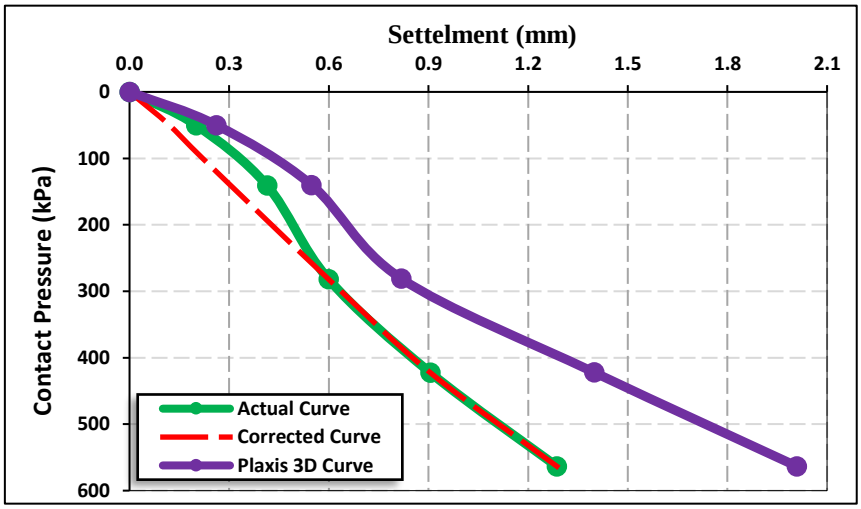

Figure (B.1.3): Point three simulated load – deformation curve for A-1-b soil (No. of passing 8)

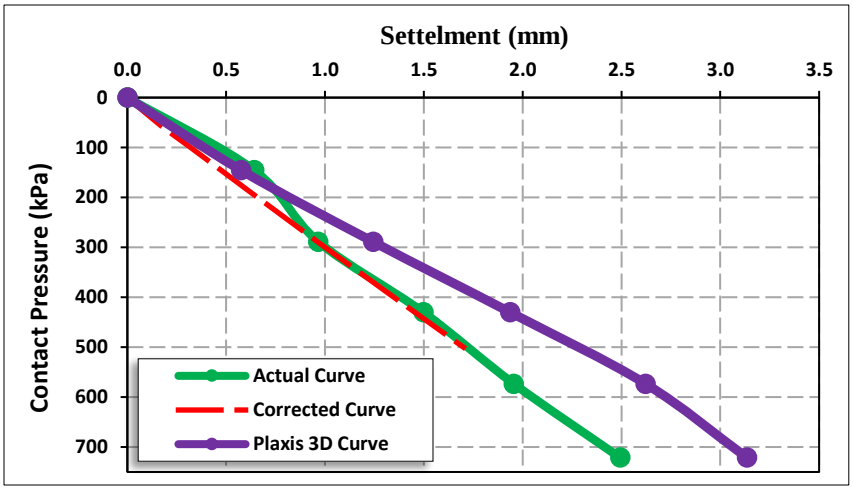

Figure (B.1.4): Point one simulated load – deformation curve for A-1-b soil (No. of passing 12)

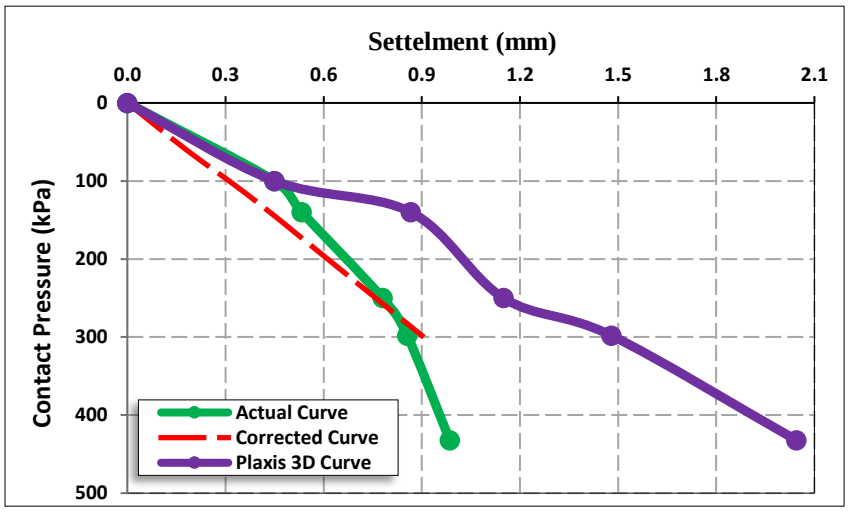

Figure (B.1.5): Point two simulated load – deformation curve for A-1-b soil (No. of passing 12)

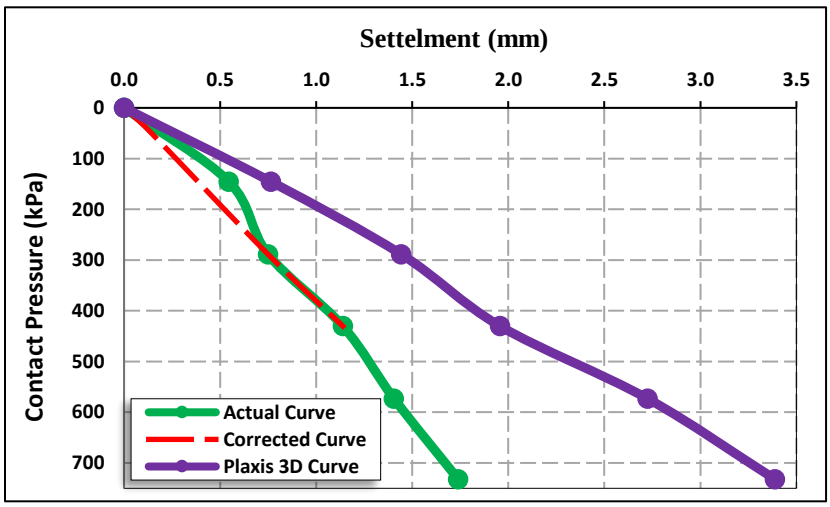

Figure (B.1.6): Point three simulated load – deformation curve for A-1-b soil (No. of passing 12)

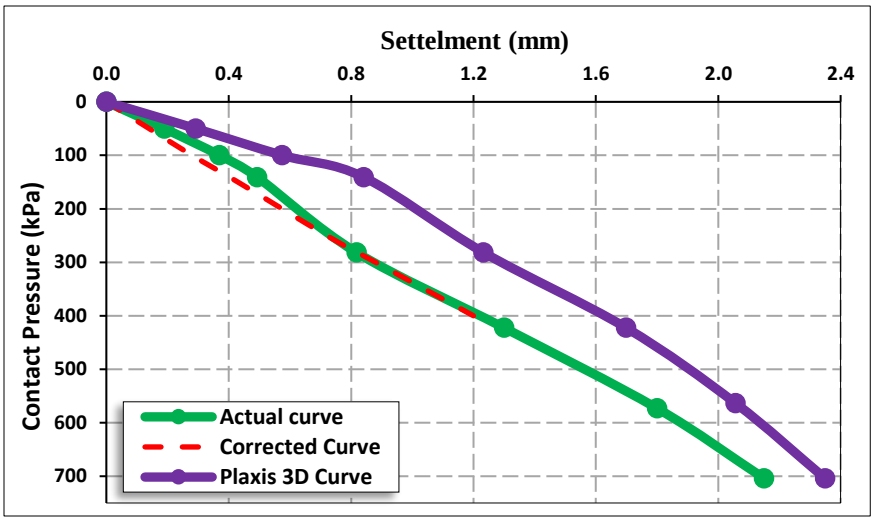

Figure (B.1.7): Point one simulated load – deformation curve for A-1-b soil (No. of passing 16)

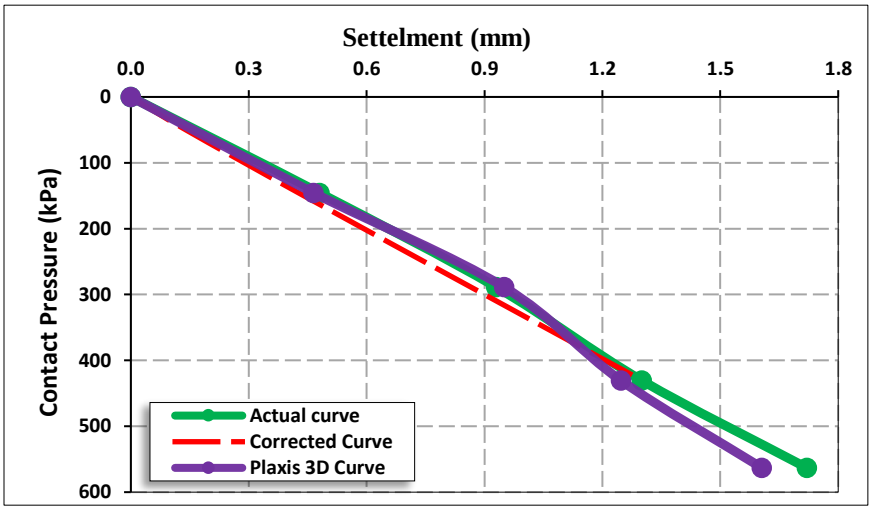

Figure (B.1.8): Point two simulated load – deformation curve for A-1-b soil (No. of passing 16)

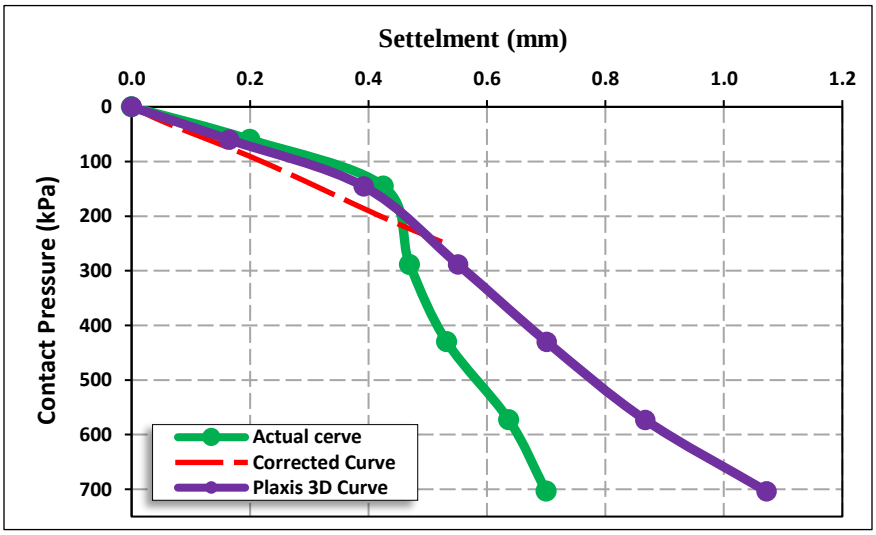

Figure (B.1.9): Point three simulated load – deformation curve for A-1-b soil (No. of passing 16)

B-2: A-3 Soil Curves

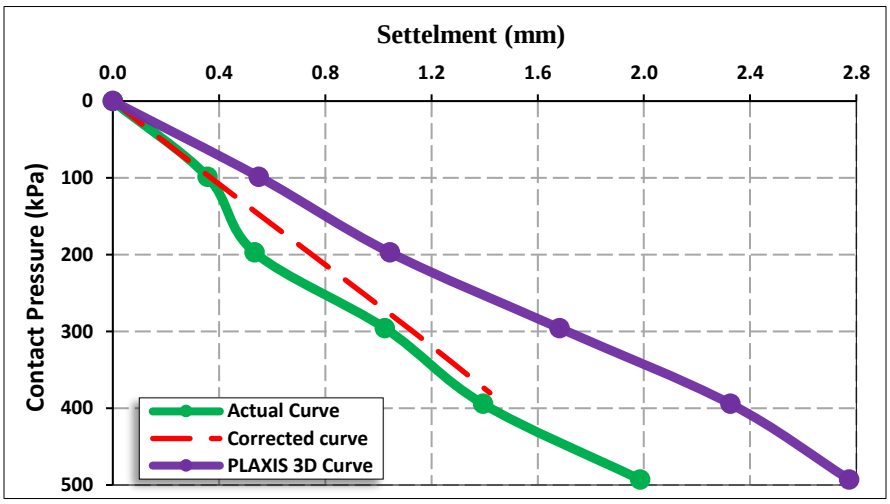

Figure (B.2.1): Point one simulated load – deformation curve for A-3 soil (No. of passing 8)

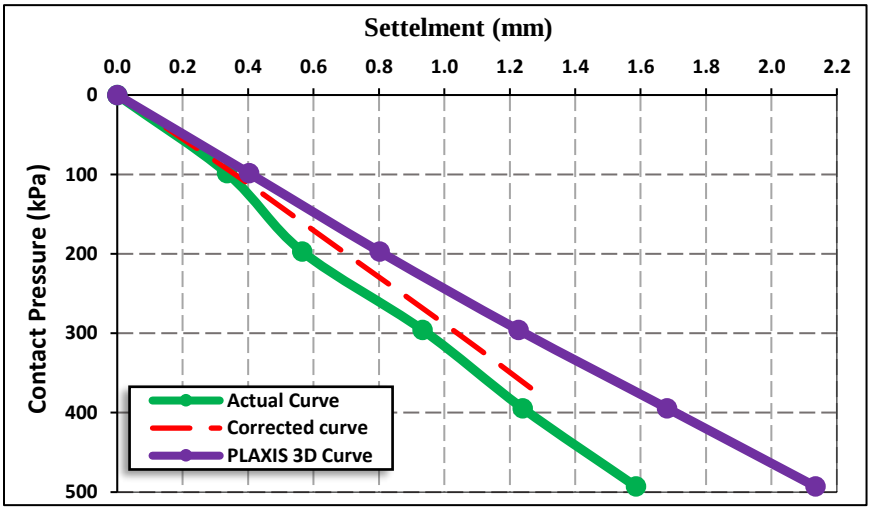

Figure (B.2.2): Point two simulated load – deformation curve for A-3 soil (No. of passing 8)

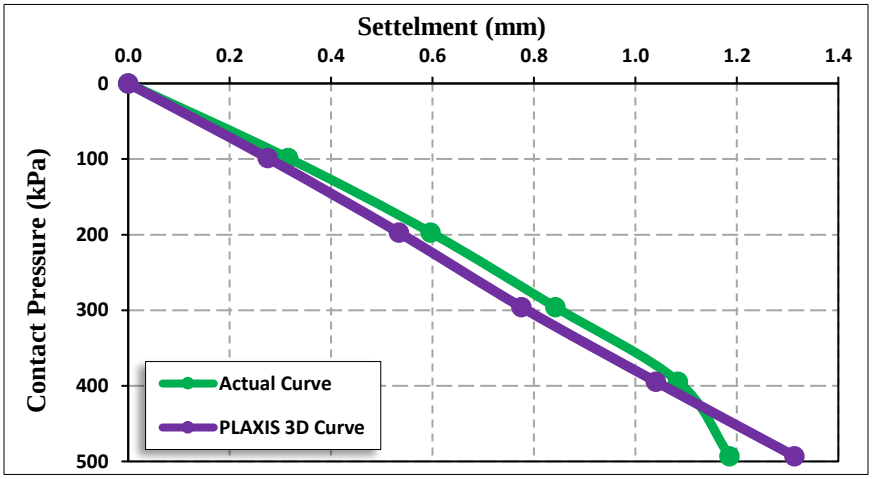

Figure (B.2.3): Point three simulated load – deformation curve for A-3 soil (No. of passing 8)

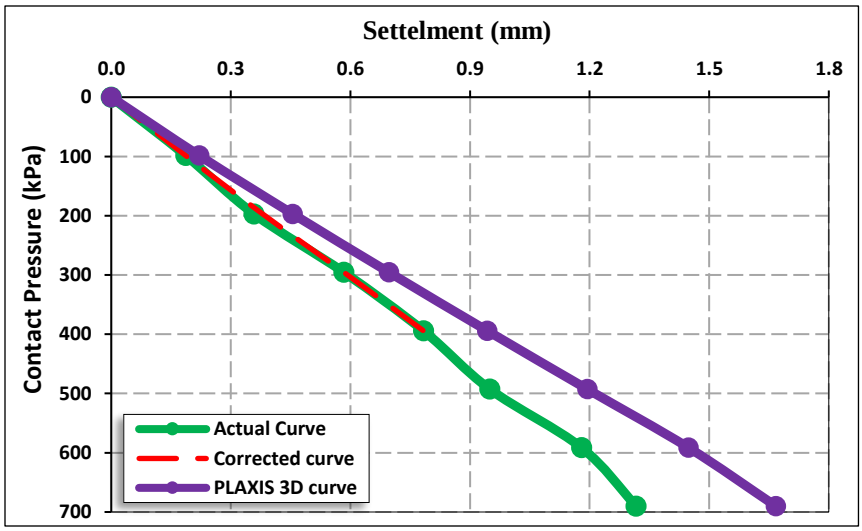

Figure (B.2.4): Point one simulated load – deformation curve for A-3 soil (No. of passing 12)

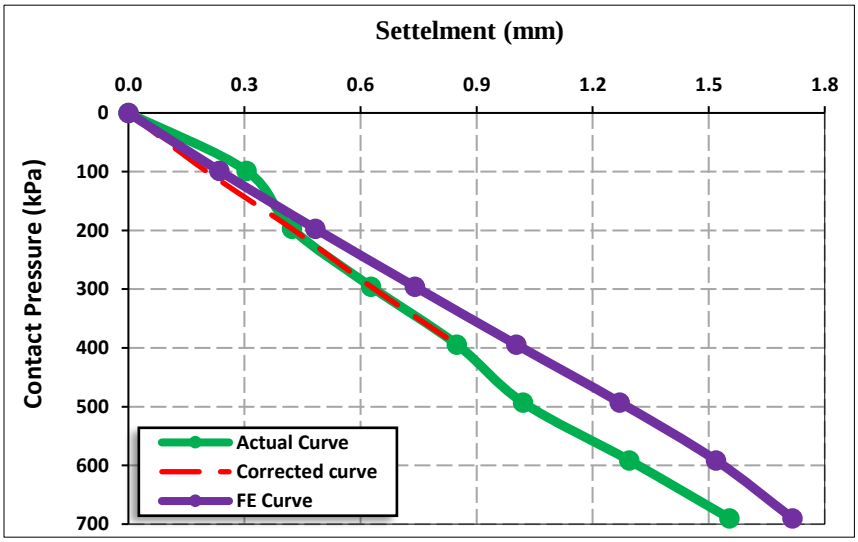

Figure (B.2.5): Point two simulated load – deformation curve for A-3 soil (No. of passing 12)

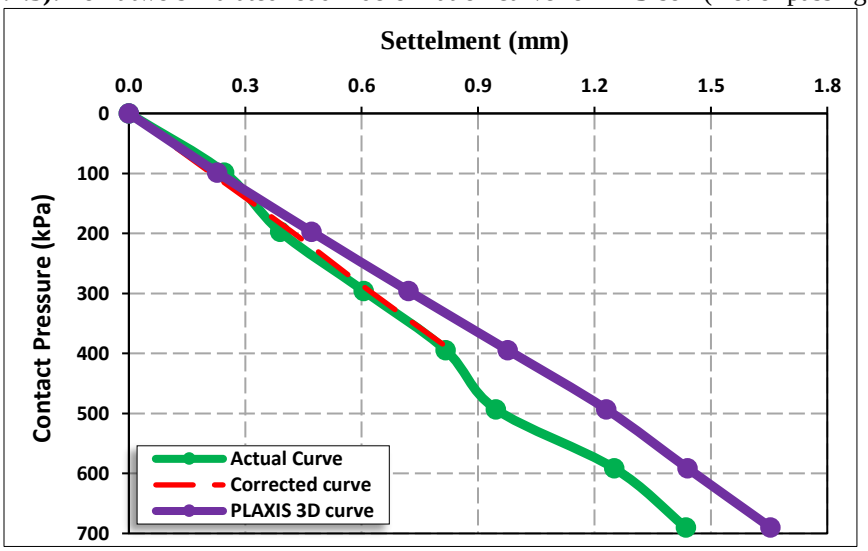

Figure (B.2.6): Point three simulated load – deformation curve for A-3 soil (No. of passing 12)

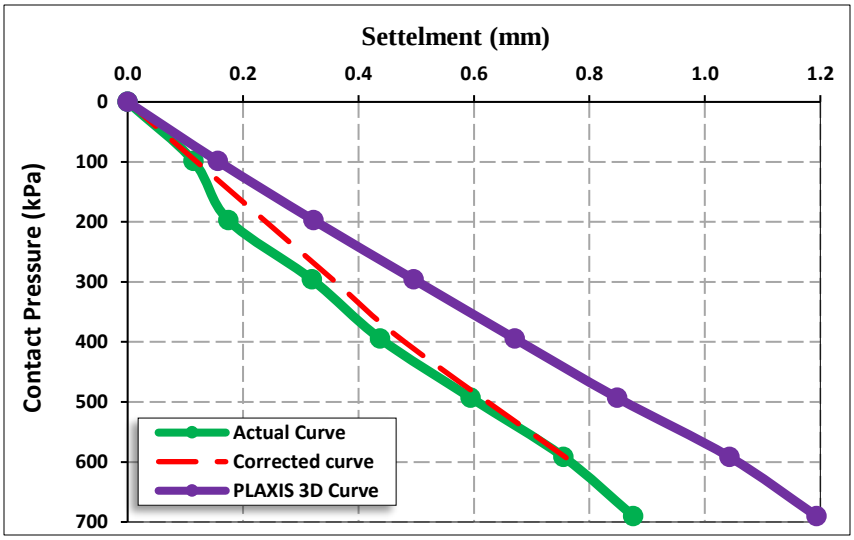

Figure (B.2.7): Point one simulated load – deformation curve for A-3 soil (No. of passing 16)

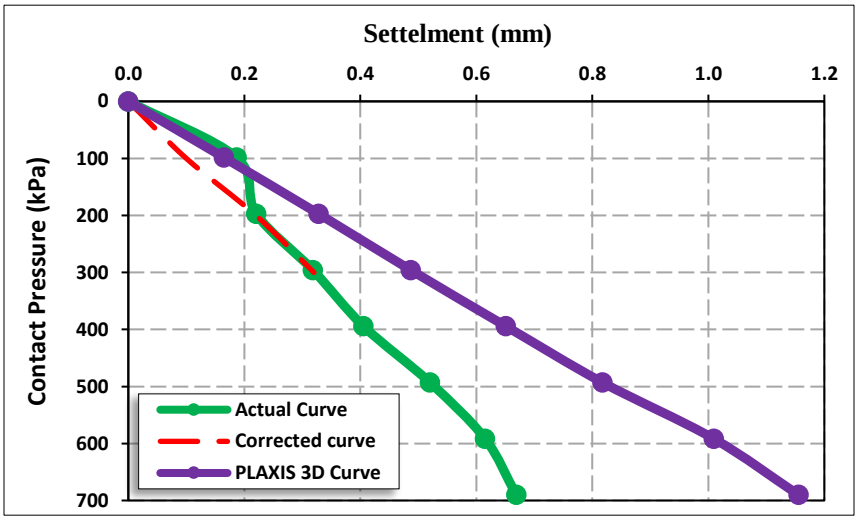

Figure (B.2.8): Point two simulated load – deformation curve for A-3 soil (No. of passing 16)

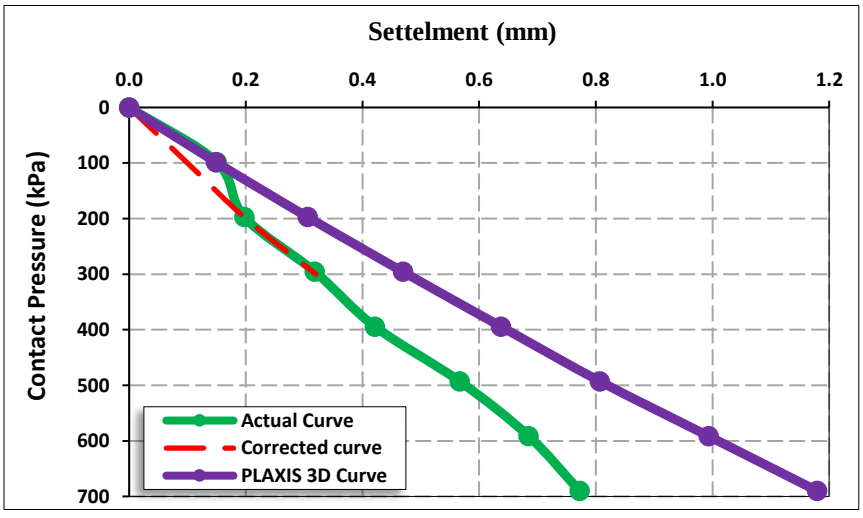

Figure (B.2.9): Point three simulated load – deformation curve for A-3 soil (No. of passing 16)

B-3: A-7-6 Soil Curves

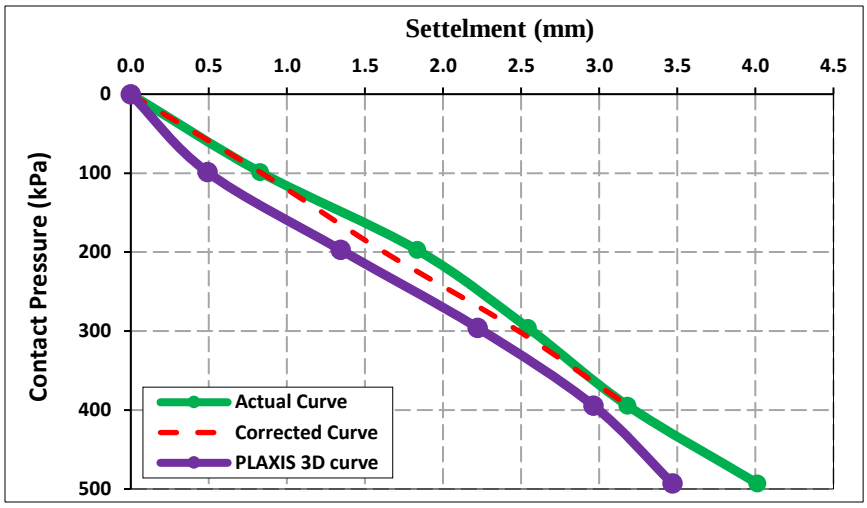

Figure (B.3.1): Point one simulated load – deformation curve for A-7-6 soil (No. of passing 8)

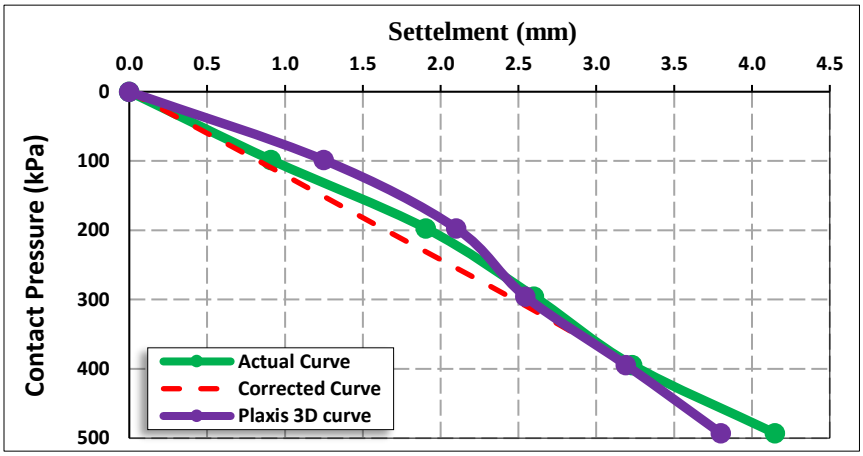

Figure (B.3.2): Point two simulated load – deformation curve for A-7-6 soil (No. of passing 8)

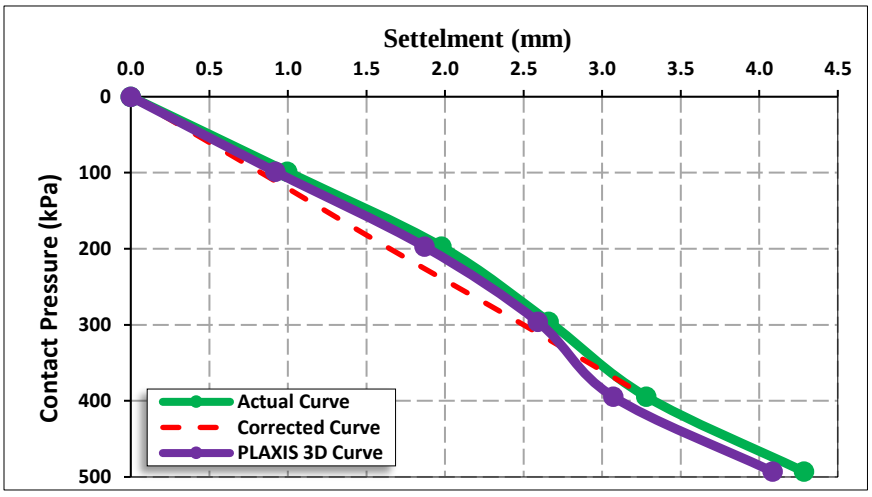

Figure (B.3.3): Point three simulated load – deformation curve for A-7-6 soil (No. of passing 8)

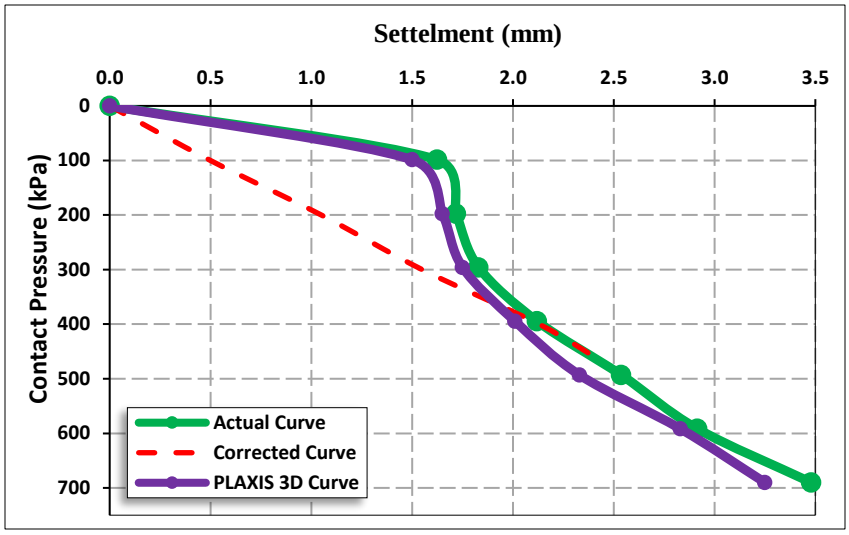

Figure (B.3.4): Point one simulated load – deformation curve for A-7-6 soil (No. of passing 12)

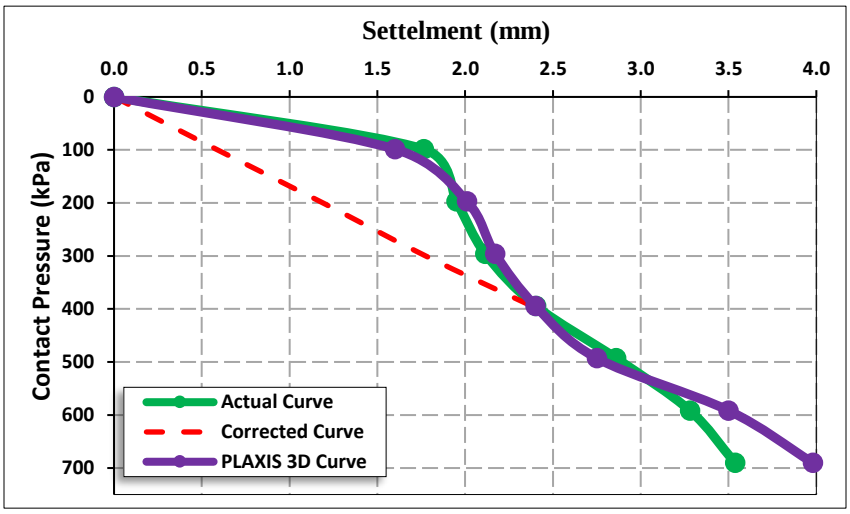

Figure (B.3.5): Point two simulated load – deformation curve for A-7-6 soil (No. of passing 12)

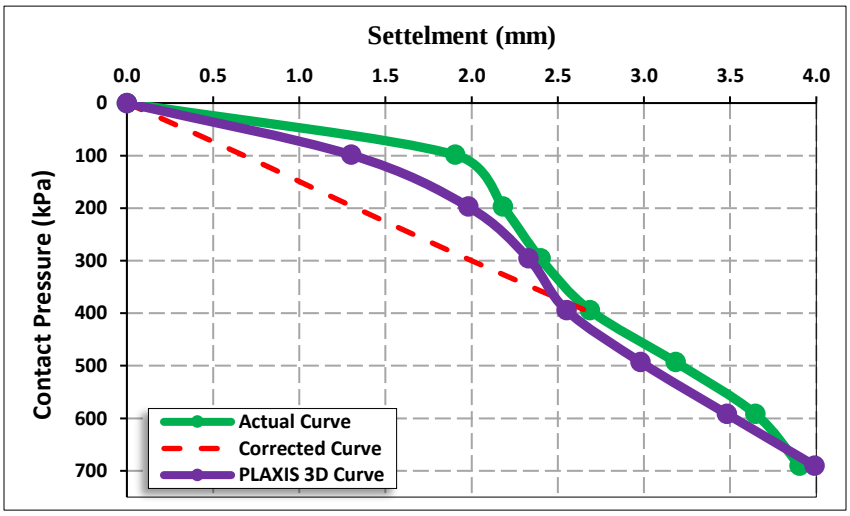

Figure (B.3.6): Point three simulated load – deformation curve for A-7-6 soil (No. of passing 12)

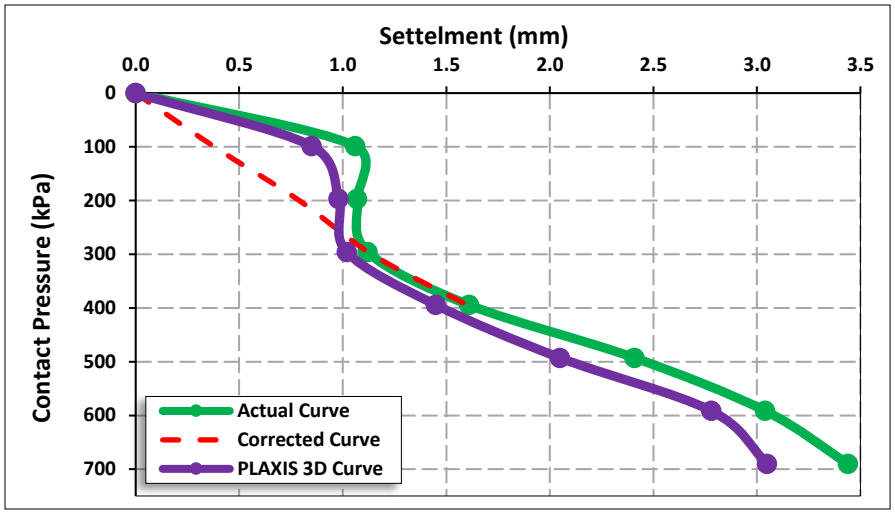

Figure (B.3.7): Point one simulated load – deformation curve for A-7-6 soil (No. of passing 16)

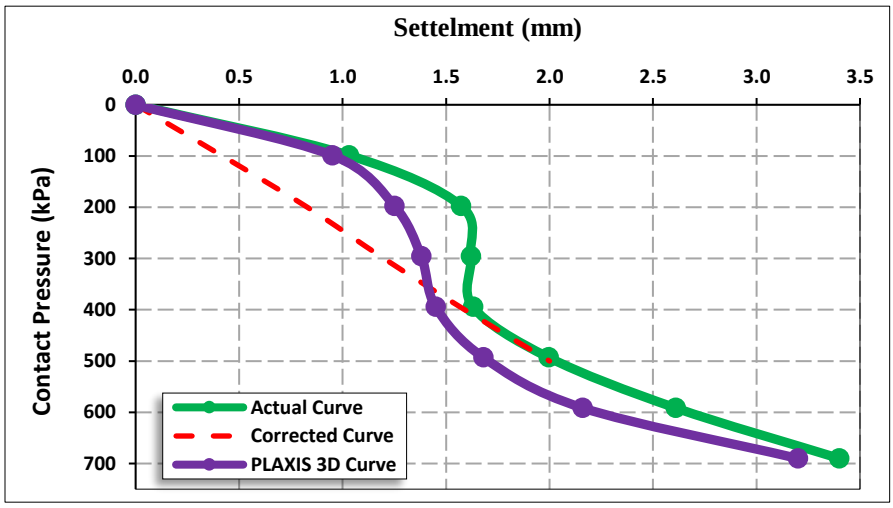

Figure (B.3.8): Point two simulated load – deformation curve for A-7-6 soil (No. of passing 16)

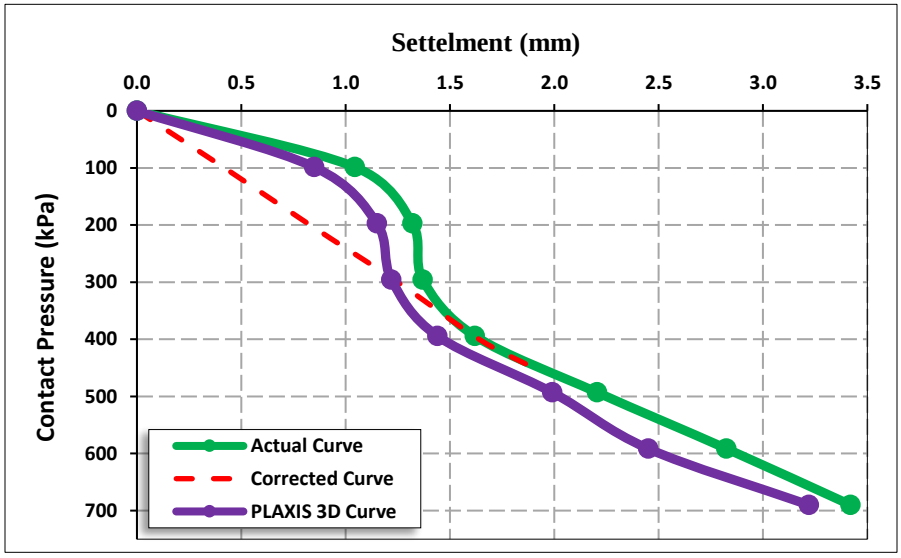

Figure (B.3.9): Point three simulated load – deformation curve for A-7-6 soil (No. of passing 16)

الخلاصه

الارض الطبيعيه هي طبقة التربة التي يوضع فوقها طبقات التبليط والطبقات الحبيبية الاخرى. وبالتالي فهي تعمل كأساس لدعم هيكل الطريق. المعامل التصميمي الجيوتكنيكي الاكثر اهمية واللذي يعطي العلاقة بين الاجهاد والهطول المصاحب له هو معامل رد فعل التربة (Ks). معامل رد فعل التربة يعتبر معامل رئيسي في تصميم وتحليل التبليط الجاسيئ . يمتلك تأثير مهم على السمك المطلوب لسطح التبليط, ويعطي تخمين لمقدار الاسناد للطبقات تحت سطح التبليط. يتم ايجاد هذا المعامل باستخدام فحص تحميل الصفيحة (PLT) حيث يعتبر هذا الفحص من الطرق المكلفة والمعقدة والتي تستغرق الكثير من الوقت . ولغرض التغلب على بعض من هذه الصعوبات من الضروري ايجاد تقنية اختبار بديلة يمكنها بسرعة وببساطة التنبؤ بهذا المعامل.

تهدف هذه الدراسة إلى تقييم فعالية استخدام جهاز فحص الهطول خفيف الوزن (LWD) و هو جهازفحص لا اتلافي محمول ويعرف ايضا باسم فحص صفيحة التحميل الديناميكية التي تستخدم لقياس خصائص التربه تحت تاثيرالاحمال الديناميكيه.

ولغرض تحقيق هدف هذه الدراسه, اجريت سلسله من الاختبارات على ثلاث انواع من التربه. تم تجميع نماذج التربه من مشاريع في مواقع مختلفه في مدينة كربلاء وهي (الميلاد, الفارس, والرفيع), تم تجميع التربه واختبارها في نموذج اختبار تم تصميمه وتصنيعه لمحاكاة الضروف الحقليه. تم فحص التربه وتحليل خصائصها تحت تثير الحمل من فحص تحميل الصفيحه الساكن (PLT) بالاقتران مع اختبار حمل اللوحه الديناميكي (LWD)

اجري تحليل احصائي لخصائص التربة المفحوصة بكلا الطريقتين الديناميكية والساكنة ولنوعين من الترب هي الحبيبية والتربه الطينية.

للتربة الحبيبية, تم تطوير ثلاث مجاميع من موديلات الانحدار بالاعتماد على المتغيرت المستقلة: (1) بيانات مقياس الهطول خفيف الوزن , (2) خصائص التربة الاساسية, (3) كلا البيانات في (1 و2). في هذه المجموعه اعلى قيمة R^2هي 0.93 لموديل ردفعل التربه – ونسبة الحدل

اللنربة الطينية, اجريت مجموعتان من موديلات الانحدار بالاعتماد على المتغيرات المستقلة, (1) بيانات مقياس الهطول خفيف الوزن (LWD), (2) خصائص التربة الاساسية. اضهرت النتائج علاقة جيدة بين الكثافة الجافة للتربة ومعامل رد فعل التربة. ايضا بينت النتائج وجود علاقة مقبولة بين معامل رد فعل التربة والمحتوى المائي.

بالاضافه الى ذلك تم التاكد من النتائج باستخدام برنامج PLAXIS 3D حيث تم استخدام موديلLinear elastic في محاكاة التربه لتمثيل فحص التحميل اللوحه الديناميكية. اما فحص تحميل الصفيحه الساكن فتم استخدام موديل Mohr-Coulomb.كما تمت المقارنه بين نتائج البرنامج ونتائج التجربه باستخدام فحص T. ففي التحميل الديناميكي كان مقدار الفرق في قيمة النزول بين القيمه العدديه والتجريبيه يتراوح بين 0.003 الى 0.242

اما الفرق في انحراف السطح تحت تاثير الحمل الساكن يتراوح بين 0.105 الى 0.15 .ومقدار الخطأ في رد الفعل يتراوح بين 3.088 اللى 25.125 .

واخيرا أظهرت نتائج هذه الدراسة كفاءة وإمكانية استخدام جهاز LWD لتنبؤ معامل رد فعل التربه بسرعه وسهوله.

جمهورية العراق
وزارة التعليم العالي والبحث العلمي
جامعة كربلاء
كلية الهندسة
قسم الهندسة المدنية

"ايجاد معامل رد فعل التربه لانواع مختلفه من الارض الطبيعيه باستخدام جهاز فحص تحميل الصفيحه الديناميكي خفيف الوزن "

رسالة مقدمة الى قسم الهندسة المدنية, جامعة كربلاء وهي جزء من متطلبات الحصول على درجة الماجستير في الهندسة المدنية (هندسة البنى التحتية)

من قبل :

أهله علاء جواد

بكلوريوس في علوم الهندسة المدنية لسنة 2015-2016

بأشراف

م-د. رائد رحمن المحنة

م-د. علاء محمد شعبان

1441 محرم

سبتمبر 2019